SOUTHEASTERN GEOLOGY

PUBLISHED AT DUKE UNIVERSITY DURHAM, NORTH CAROLINA

VOL.23 NO.1 MARCH, 1982

SOUTHEASTERN GEOLOGY

PUBLISHED QUARTERLY

AT

DUKE UNIVERSITY

This journal welcomes original papers on all phases of geology, geophysics, and geochemistry as related to the Southeast. Transmit manuscripts to S. DUNCAN HERON, JR., BOX 6665, COLLEGE STATION, DURHAM, NORTH CAROLINA 27708. Observe the following:

1) Type the manuscript with double space lines and submit in duplicate.
2) Cite references and prepare bibliographic lists in accordance with the method found within the pages of this journal.
3) Submit line drawings and complex tables as finished copy.
4) Make certain that all photographs are sharp, clear, and of good contrast.
5) Stratigraphic terminology should abide by the code of Stratigraphic Nomenclature (AAPG, v. 45, 1961).

Proofs will be sent authors.

Reprints must be ordered prior to publication; prices available upon request. Subscriptions to Southeastern Geology are $8.00 per volume (US and Canada) $10.00 per volume (foreign). Inquiries should be sent to: SOUTHEASTERN GEOLOGY, BOX 6665, COLLEGE STATION, DURHAM, NORTH CAROLINA 27708. Make checks payable to: Southeastern Geology.

SOUTHEASTERN GEOLOGY

Table of Contents

Vol. 23, No. 1

March, 1982

THE PALEOECOLOGIC HISTORY OF LATE PLEISTOCENE ESTUARINE AND MARINE FOSSIL DEPOSITS IN DARE COUNTY, NORTH CAROLINA

By

William Miller, III
Earth Sciences Department
Tulane University
New Orleans, Louisiana 70118

ABSTRACT

Exposures of late Pleistocene backbarrier lagoonal deposits at the Stetson borrow pit, in north-central mainland Dare County, North Carolina, afforded an excellent opportunity to study stratigraphic relationships, physical and biogenic sedimentary structures, and fossils within their enveloping lithofacies in an area devoid of natural surface outcrops. Bulk samples were collected for paleoecological analysis from the exposures and from a shallow power-auger boring in the floor of the borrow pit. A total of 4 m of backbarrier deposits was exposed in the borrow pit walls; the boring penetrated an additional 2 m of backbarrier material conformably overlying more than 9 m of nearshore marine sediments. Fossil associations (each derived from a single original benthic community) and assemblages (derived from more than one original community) were identified in the samples and consisted primarily of mollusk shells. These ecologic units, in ascending stratigraphic order, were: 1) inner shelf marine associations, 2) a transitional assemblage with both marine and estuarine shells, 3) a transported (?) estuarine association, 4) shoal flank associations, 5) an oyster biostrome association, 6) sand shoal (tidal delta?) associations, and 7) mixed assemblages containing elements from a variety of estuarine associations. These associations and assemblages were derived from at least five original communities: 1) inner shelf marine, 2) lagoonal shoal flank, 3) oyster bank, 4) lagoonal sand shoal, and 5) tidal (?) channel. The succession of ecologic units recognized at the Stetson borrow pit is the result of community replacement, reflecting the partitioning of a coastal compartment by a barrier island and the subsequent filling of a backbarrier lagoon in the vicinity of mainland Dare County during late Pleistocene time.

INTRODUCTION

The mainland portion of Dare County, located in the Outer Coastal Plain of northeastern North Carolina, is a broad, flat peninsula of swampland, surrounded on three sides by estuaries. Because surface elevations average only about + 1 m, no natural exposures of the fossiliferous Pleistocene sands and muds that underlie the area occur, so information on shallow subsurface stratigraphy must be obtained from artificial exposures in borrow pits or by drillling.

The purposes of this paper are to describe the excellent exposures of sediments and fossils at the Stetson borrow pit (Figures 1, 2), to interpret the paleoenvironments represented by lithofacies identified in surface exposures and in an auger boring, and to use the fossils together with lithostratigraphic information to develop a paleoenvironmental history of the borrow pit section. Because the emphasis here will be largely focused on the sequence of fossil associations and assemblages contained within the local stratigraphic framework, what I will actually develop will be a *paleoecologic history* of the section. Interpreting the paleoecologic history of Atlantic Coastal Plain stratigraphic frameworks from sequences of ecologic units offers a means of cross-checking paleoenvironmental reconstructions, which traditionally have been based on lithostratigraphic evidence and on a few conspicuous fossil species used merely as corroborative environmental indices.

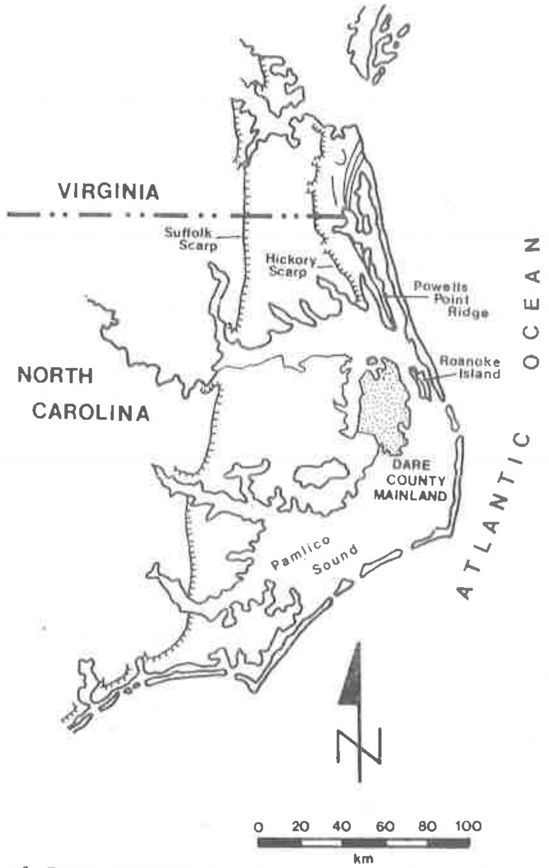

Figure 1. Location of Dare County mainland (stippled area), and major geomorphic features of the region.

STRATIGRAPHY

Regional Framework

Early investigators placed the deposits exposed in shallow excavations in Dare County within the late Pleistocene Pamlico Formation owing to location in the lowest and presumably youngest coastal terrace-formation (Stephenson, 1912; Stephenson and Johnson, 1912). Richards (1936, 1950) also placed the uppermost beds in the county within the Pamlico Formation because of location directly beneath the Pamlico Terrace, presence of marine fossils, and predominance of *extant taxa* among the fossil shells that he collected.

More recently, a group of investigators based at East Carolina University has investigated the dynamic stratigraphy of eastern Dare County using paleoenvironmental interpretations, radiocarbon dating techniques, and foraminiferal biostratigraphy, completely deferring the use of formational nomenclature (see O'Connor and Riggs, 1971, 1974; O'Connor and others, 1972; Riggs and O'Connor, 1974; Byrum, 1978, 1979). They interpreted the stratigraphy of the mainland as consisting of a lower, moderate energy marine unit of Pleistocene age (below about - 6 m), a middle lagoonal unit also of Pleistocene age (from about -3 to - 6 m), and an upper "filled mainland lagoon" of Holocene age (above - 3 m) (Riggs and O'Connor, 1974; Byrum, 1978, Fig. 9). They reported radiocarbon dates of 24,560$\pm$ to > 40,000 yrs. B.P. from the middle and lower units, and decided on a Wisconsinan age for these deposits.

My observations in Dare County, based on subsurface sampling in the region (see North Carolina Department of Transportation unpublished reports of projects 8.11225 and 6.804138) and on a detailed field study of the Stetson pit, allow me to confirm the

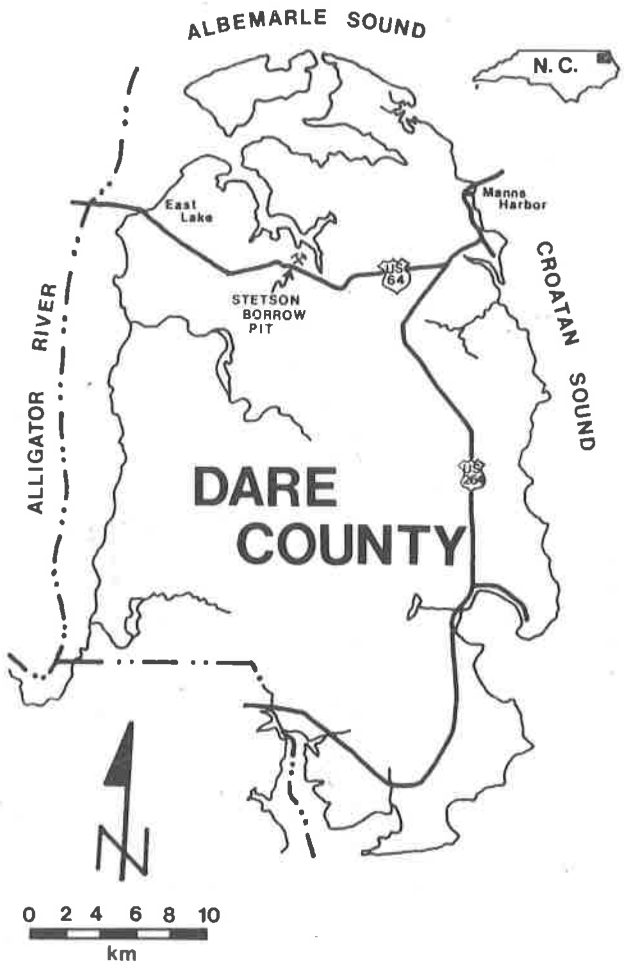

Figure 2. Map of Dare County mainland showing location of Stetson borrow pit.

general three-part division recognized by the East Carolina University group. In power-auger borings the lower and middle units are indistinguishable using lithologic criteria alone; both are largely muddy sands that are most easily differentiated using the change in fossils occurring at an elevation of about - 4 m at the borrow pit (Figure 3). Based on the change in abundance of two conspicuous fossil mollusks, the late Pleistocene section locally can be divided into two easily recognized biofacies: a lower *Mulinia lateralis* biofacies and an upper *Crassostrea virginica* biofacies.

Many difficulties hamper correlation of the Dare County deposits with Pleistocene stratigraphic units recognized in more thoroughly studied areas (e.g., correlation with units in southeastern Virginia; see Oaks and Coch, 1973; Oaks and others, 1974). All fossils recovered in this study have long geologic ranges and little utility in temporal correlations. Although the radiocarbon dates reported by the East Carolina University group appear to indicate a mid-Wisconsinan age for at least the upper portion of the Pleistocene section in Dare County, an amino acid racemization date on a single specimen of *Mercenaria mercenaria* from the upper part of the *Mulinia lateralis* biofacies at the Stetson pit suggests a Sangamonian age (~ 120,000 yrs. B.P.; Daniel F. Belknap, person. comm.). I could discern no unconformities at the borrow pit, and the only division of the total section was based on an environmentally controlled change in fossils. So, because of the great distance of the study area from stratigraphically well known areas in Virginia (60 km) and central coastal North Carolina (120 km), and because geochronometric dates appear to be conflicting, correlations with units recognized to the north and south are deferred. The problem

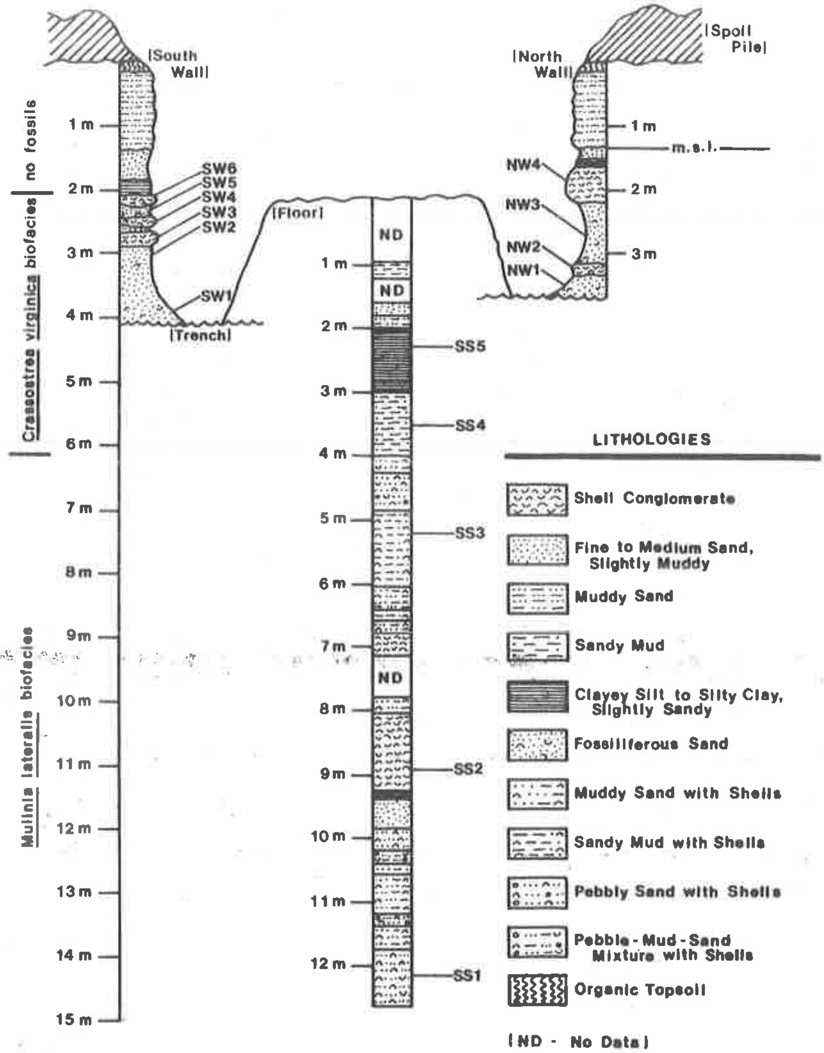

Figure 3. Stratigraphic section at the Stetson borrow pit showing exposures in the walls of the pit, the bored section, and bulk sample locations (indicated by SW's, NW's, and SS's).

of establishing positive correlations will be resolved by connecting Dare County with better known areas by a network of closely spaced surface and subsurface control points, by dating more material, and by identifying the relationships of stratigraphic units to ancient shorelines in the region (see Cronin, 1980).

Stetson Borrow Pit

In 1978, the only outcrops of late Pleistocene sediments in Dare County were at the Stetson pit, on the north side of U.S. Highway 64 between Croatan Sound and Alligator River (Figure 2). The Stetson pit section is shown in Figure 3.

Beds of the *Mulinia lateralis* biofacies were encountered at an elevation of -4 m, or about 3 m beneath the floor of the pit. These deposits consist of an interbedded sequence of sparingly to extremely fossiliferous muddy sand with occasional sandy mud, pebbly sand, and clay layers. Fossils recovered included marine mollusks, an ahermatypic coral, cap-shaped bryozoan colonies, echinoid fragments, a scaphopod, and miliolid foraminifera, indicating nearshore marine sedimentary environments. Frequent environmental disturbances are suggested by numerical dominance of valves and fragments of *M. lateralis*, a small, opportunistic mactrid bivalve (Levinton, 1970; Rhoads and others, 1978), in all samples examined. This sequence of beds was probably deposited in moderate to low energy, inner shelf environments that included lower shoreface, shoal, and inter-shoal areas. Contact with superjacent estuarine beds appears to be gradational at the Stetson pit.

Only the *Crassostrea virginica* biofacies is exposed in the walls of the pit (Figure 3). These deposits comprise a regressive sequence of lagoonal beds capped by pedogenically altered river-estuary deposits. The sequence begins just beneath the floor of the borrow pit with a shelly, sandy mud containing a mixture of marine and estuarine mollusks, and is succeeded by a bed of very sparsely fossiliferous clay with a few estuarine shells. The deposits document the initiation of estuarine conditions in the area, and possibly could record the partitioning of a coastal compartment landward of an accreting barrier shoal or island (Powells Point Ridge, Figure 1) to form a lagoon (see Fisher, 1968; Field and Duane, 1976). The clay layer grades upward into muddy fine sand that crops out in the lowest levels of the borrow pit. This bed contains a low diversity estuarine fauna and represents a transition from a lagoonal basin to a shoal flank environment. Enclosed within the muddy sand are oyster biostromes consisting of patches of *C. virginica* in life positions. Shoal flank deposits grade in turn upward into clean, cross-laminated, fine to medium sand with wavy clay laminations, bivalve burrows, elasmobranch feeding traces (see Howard and others, 1977), and a moderately diverse estuarine fauna dominated numerically by Gemma gemma. The sand layer contains lenticular shell beds packed with cross-bedded and imbricated valves of *C. virginica*, indicating deposition in current-swept channels. The sand with shell lenses was deposited in either intertidal or very shallow subtidal shoal and channel environments (flood-tidal delta?).

Above the shelly beds in the walls of the Stetson pit is a silty clay layer containing load structures that probably accumulated in mainland embayments similar to embayments or "lakes" that presently surround mainland Dare County. A bed of cross-laminated fine sand with wavy clay laminations succeeds the clay unit, and may represent a nearshore, river-estuary depositional environment. The highest bed at the pit is a muddy fine sand with abundant roots. This layer appears to be a relict soil zone that is buried to the east and west of the borrow pit beneath locally thick accumulations of Holocene peat and muck (unpubl. N.C. Dept. Trans. reports 8.11225 and 6.804138).

FAUNAL ANALYSIS

Methods

Fifteen bulk samples ranging in volume from 0.5 to 4.0 litres were taken from surface and subsurface intervals for paleoecologic analyses (see sample locations, Figure 3). Samples were soaked in Calgon solution and washed through a series of sieves to separate all fossils larger than 1 mm in smallest dimension. (Smaller subsamples were set aside for foraminiferal analyses which were used to cross-check the paleoenvironmental interpretations.) Fossil specimens were dried, counted, and carefully examined for physical and biogenic damage. Gastropods occurring as fragments with apical or apertural areas intact were counted as individual shells; for bivalves, the beak area had to be preserved for tabulation as one valve. A total of 26,642 identifiable fossils representing eight animal phyla, but mostly Mollusca, were recovered from samples (see complete inventory in Miller, 1978). Although only the megascopic fossils were used in this study, it is important to note that the Pleistocene deposits in Dare County contain a rich microflora and microfauna (Byrum, 1978; Thomas M. Cronin, person. comm.).

Fossil associations and assemblages were recognized by means of: 1) empirically determined recurrence, 2) by identifying original spatial co-occurrences of taxa, 3) by assessing the degree of post-mortem damage to shells, 4) by evaluating ecologic compatibility (i.e., whether or not skeletons represented organisms that existed

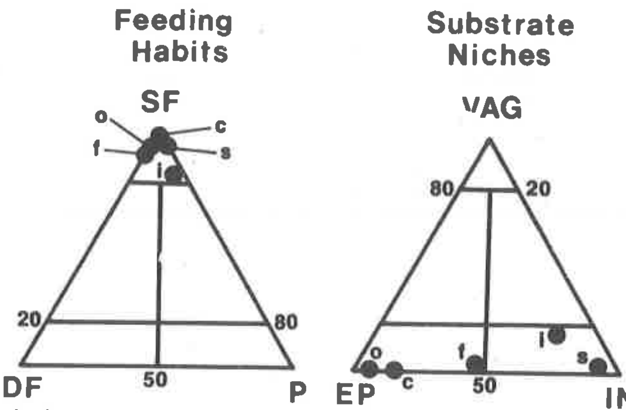

Figure 4. Descriptive trophic structure of in-place and disturbed-neighborhood fossil associations. The method of constructing and interpreting ternary feeding habit and substrate niche diagrams is described by Scott (1976, 1978); relative abundances of taxa in the different feeding/substrate niche categories were used to plot points. (SF = suspension feeding, DF = detritus feeding, P = predator, VAG = vagrant, EP = epifaunal, IN = infaunal; i = inner shelf, f = shoal flank, o = oyster biostrome, s = sand shoal, c = channel bottom).

together in life either due to similar environmental requirements or to obligatory biological associations; evaluated by comparison with modern faunas), and 5) by correlation with ancient substrates (Johnson, 1960, 1971, 1972; Shotwell, 1964; Scott, 1970, 1974; Kauffman, 1974; Walker, 1974; Kauffman and Scott, 1976; Hanley, 1976). Empirically recognized fossil associations and assemblages are probably valid ecologic units if component taxa are derived from original communities that inhabited patchy, stressful environments where species diversity was relatively low, degree of correlation with specific substrates was moderately high, and the spatial intermingling of continguous communities was minimal. Ecologic compatibility was emphasized in the analysis of samples because all mollusks identified belong to extant taxa and a large literature exists on the geographic ranges, habitats, and functional morphologies of Western Atlantic Mollusca (see Abbott, 1968, 1974; Stanley, 1970; Gosner, 1971; Porter and Tyler, 1976; Van Dover and Kirby-Smith, 1979).

Associations and Assemblages

Seven well-defined fossil associations (ecologically compatible remnants derived from one original community) and assemblages (mixtures of elements from more than one original community) were recognized. These units are disucssed in the order of their occurrence in the stratigraphic section at the pit, beginning with the oldest unit. In-place and disturbed-neighborhood associations (ecologic units that have undergone the least amount of damage by transport and mixing; terminology of Scott, 1970) are classified according to feeding and substrate niche categories (Figure 4), using the descriptive trophic classification described and employed by Scott (1976, 1978). The most abundant taxa in these associations are listed in Table 1.

Inner Shelf Associations (samples SS1, SS2, SS3; Figure 3). Samples from the ***Mulinia lateralis*** biofacies contained species-rich (68 species), high-dominance, marine fossil associations. Valves and fragments of ***M. lateralis*** were numerically dominant; other characteristic taxa were ***Discoporella sp.*** (a cheilostome bryozoan), ***Retusa canaliculata*** and ***Olivella mutica*** (small, predatory gastropods), and indeterminate mactrid bivalves. Abundance of shells in the samples was moderate to high, and the enveloping lithofacies was muddy fine to medium sand. Mode of origin for the association was probably disturbed-neighborhood.

Transitional Assemblage (SS4; Figure 3). Succeeding the inner shelf associations was a species-poor (18 species) mixed assemblage of marine and estuarine fossils

Table 1. Major taxonomic components[1] of the in-place and disturbed-neighborhood fossil assocations from the Stetson pit.

Species	Animal Type[2]	Feeding/Substrate Niche Category[3]	Relative Abundance	Rank
INNER SHELF ASSOCIATION				
Mulinia lateralis (Say)	Bi	SF/IN	46.50%	1
Discoporella sp.	Br	SF/EP	12.99	2
Retusa canaliculata (Say)	G	P/VAG	4.88	3
Mactridae indet.	Bi	SF/IN	4.22	4
Olivella mutica (Say)	G	P/VAG	4.00	5
Polydora sp.	An	SF/IN	2.77	6
Balanus sp.	Ar	SF/EP	2.55	7
Turbonilla interrupta (Totten)	G	P/VAG	2.44	8
Electra sp.	Br	SF/IN	2.11	9
Pleuromeris tridentata (Say)	Bi	SF/IN	1.89	10
Crassinella lunulata (Conrad)	Bi	SF/IN	1.78	11
Ensis directus Conrad	Bi	SF/IN	1.33	12
Nassarius trivittatus (Say)	G	DF/VAG	1.33	12
Spisula solidissima (Dillwyn)	Bi	SF/IN	1.00	13
Anadara transversa (Say)	Bi	SF/IN	1.00	13
Tellina agilis Stimpson	Bi	DF/IN	1.00	13
Mercenaria mercenaria (Linné)	Bi	SF/IN	0.89	14
Veneridae indet.	Bi	SF/IN	0.67	15
Macrocallista sp.	Bi	SF/IN	0.55	16
Polinices duplicatus (Say)	G	P/VAG	0.55	16
Mitrella lunata (Say)	G	P/VAG	0.55	16
Nassarius acutus (Say)	G	DF/VAG	0.55	16
			95.55%	
SHOAL FLANK ASSOCIATION				
Balanus sp.	Ar	SF/EP	45.55%	1
Polydora sp.	An	SF/IN	34.65	2
Crassostrea virginica (Gmelin)	Bi	SF/EP	5.94	3
Mulinia lateralis (Say)	Bi	SF/IN	2.97	4
Electra sp.	Br	SF/IN	2.97	4
Nassarius obsoletus (Say)	G	DF/VAG	1.98	5
?Bryozoa indet. (brown, branching trace on shells)	Br?	SF?/EP	1.98	5
			95.04%	
OYSTER BIOSTROME ASSOCIATION				
Crassostrea virginica (Gmelin)	Bi	SF/EP	52.42%	1
Balanus sp.	Ar	SF/EP	39.95	2
Mulinia lateralis (Say)	Bi	SF/IN	1.39	3
Macoma balthica (Linné)	Bi	DF/IN	1.27	4
			95.03%	
SAND SHOAL ASSOCIATION				
Gemma gemma (Totten)	Bi	SF/IN	85.05%	1
Crassostrea virginica (Gmelin)	Bi	SF/EP	2.59	2
Mulinia lateralis (Say)	Bi	SF/IN	2.08	3
Petricola pholadiformis (Lamarck)	Bi	SF/IN	1.97	4
Balanus sp.	Ar	SF/EP	1.70	5
Polydora sp.	An	SF/IN	0.99	6
Mitrella lunata (Say)	G	P/VAG	0.92	7
			95.30%	
TIDAL (?) CHANNEL ASSOCIATION				
Balanus sp.	Ar	SF/EP	~60.00%	1
Crassostrea virginica (Gmelin)	Bi	SF/EP	~30.00	2
Gemma gemma (Totten)	Bi	SF/IN	~10.00	3
			~100.00%	

1 - Numerically minor components of associations are listed in Miller, 1978.

2 - Animal types: An = Annelida; Br = Bryozoa; Ar = Arthropoda; Bi = Bivalvia (Mollusca): G = Gastropoda (Mollusca).

3 - Feeding and substrate niche category symbols: P = predators (including parasites); DF = detritus feeders; SF = suspension feeders; VAG = vagrant; EP = epifaunal sedentary; IN = infaunal sedentary.

representing a transition from open marine to backbarrier benthic communities. Marine taxa in the assemblage included *Discoporella sp.*, and the infaunal suspension-feeding bivalves *Pleuromeris tridentata* and *Crassinella lunulata*; estuarine taxa included *Crassostrea virginica*, the infaunal suspension-feeding clam *Gemma gemma*, and the ectoparasitic snail *Odostomia impressa*. An unknown number of original communities contributed material to this assemblage and transportation of some elements cannot be ruled out. Fossil abundance in the sample was low, and the matrix lithology was muddy fine sand.

Transported (?) Estuarine Association (SS5; Figure 3). A very sparsely fossiliferous, species-poor (6 species) association of fragmental shells occurred stratigraphically above the transitional assemblage. The association contained typical estuarine mollusks, including *Crassostrea virginica*, *Gemma gemma*, and *Nassarius obsoletus*, heavily bored by *Cliona sp.* These shallow-water taxa may be ecologically incompatible with the soft-bottom, lagoonal basin depositional environment suggested by the clay matrix and stratigraphic position, and the shells could have been transported from shallower areas as a result of storms.

Shoal Flank Associations (NW1, SW1; Figure 3). Samples from the lowest bed exposed in the borrow pit contained species-poor (13 species), shallow subtidal, in-place estuarine associations. The balanid *Balanus sp.*, a boring polychaete *Polydora sp.*, and their host organism *Crassostrea virginica* were the most abundant components. Fossil abundance was low, most of the bivalves occurred with articulated valves, and the enveloping lithofacies was sandy mud grading upward into muddy fine sand.

Oyster Biostrome Association (NW2; Figure 3). A discontinuous shelly layer, containing abundant Crassostrea virginica preserved in life positions, was exposed in the north wall of the pit. This shelly layer contained the remains of an in-place, oyster biostrome buried by muddy shoal flank deposits. Fossil abundance was high, and the matrix was shelly, muddy fine sand. Oyster biostrome and shoal flank fossil associations appeared to intergrade, indicating that the original, patchy oyster bank community graded into the surrounding intershoal communities.

Sand Shoal Associations (NW3, SW2, SW5; Figure 3). The shoal flank associations passed gradually upward into moderately species-rich (35 species), intertidal to shallow subtidal, sand shoal associations. Sand shoal fossils were associated with a variety of sedimentary structures including cross-laminations, wavy clay laminations, the feeding traces of rays, vertically-oriented cylindrical burrows containing *Mya arenaria* shells, and curved, cylindrical burrows with Ensis directus shells. Valves and articulated shells of *Gemma gemma* averaged about 2000 specimens/litre o sample and were numerically dominant components in the associations. Other characteristic taxa were the suspension-feeding bivalves *Crassostrea virginica*, *Mulinia lateralis*, and *Petricola pholadiformis*. Fossil abundance in samples was low to moderate, and the enveloping lithofacies was fine to medium sand with clay interlaminations. Mode of origin appears to have been in-place or possibly disturbed-neighborhood.

Mixed Estuarine Assemblages (NW4, SW3, SW4, SW6; Figure 3). Lenticular shell beds within the sand shoal lithofacies contained faunal elements belonging to at least three original communities: oyster biostrome, sand shoal,and channel bottom. Species richness of the mixed assemblages was moderate (30 species). Abundance of fossils in samples as very high, and the lithology was sandy shell conglomerate with valves and fragments of *Crassostrea virginica* as the dominant components. Some specimens of *C. virginica*, *Balanus sp.*, and *Gemma gemma* appear to comprise a species poor, in-place channel association. Transported taxa from originally contiguous oyster banks and sand shoal areas made up the remainder of the fossils recovered.

COMMUNITY RECONSTRUCTIONS

Taxa that possess hard, protective skeletons and either exploit a seasonally variable planktic tropic resource or have evolved the ability to avoid physiological stress (e.g., by deeply burrowing) are the ecologically best suited organisms for successful occupation of niche space on or within environmentally variable, sandy substrates of lagoonal and nearshore marine seas (Schopf, 1978; Scott, 1978; Rhoads and others, 1978; Vermeij, 1978). Recurrent groups (communities) of such organisms are expected to be "physically accommodated" and loosely organized, with biological interactions being less significant than organism-environment interactions (Johnson, 1972). Benthic communities that inhabited late Pleistocene estuaries and inner shelf marine waters in the area of mainland Dare County were mainly of this type.

Inner shelf associations were derived from a moderately species-rich, high-dominance, nearshore marine community that may have been composed mainly of bivalves and gastropods. *Mulinia lateralis*, the most abundant fossil in samples, saturated the fossil record of this community through numerous explosive invasions. M. lateralis populations were an "unstable fringe:" in ecosystem structure that took advantage of frequent degradational events in the successional history of the marine community, but dominated primary consumer trophic levels probably for only short periods of time (Levington, 1970; Valentine, 1972). This small mactrid bivalve is presently saturating the sediments of Long Island Sound with its skeletons, and its role in secondary succession was recently described by Rhoads and others (1978). Another important faunal component was the bryozoan ***Discoporella sp.*** with lunulitiform (cap-shaped) zoaria. This type of colonial growth habit is an adaptation to life on sandy, current-swept substrates (Stach, 1936; Schopf, 1969). The community also contained many predatory gastropods, sparse miliolid foraminifera, a coral, echinoids, a scaphopod, and a large number of infaunal suspension-feeding bivalves. The marine community appears to have been the most complex organization of organism populations represented among the fossil associations, even though it was subject to repeated episodes of degradation in successional stage and invasion by opportunists.

The shoal flank association was derived from a low diversity, muddy bottom, estuarine community. Preserved portions of the original community were mainly ***Crassostrea virginica*** and its epilithic and endolithic associates. Only a few deposit feeders, such as ***Nassarius obsoletus***, ***Macoma balthica***, and ***Tagelus plebeius***, were represented as fossils. It is possible that many soft-bodied deposit feeders (e.g., polychaete worms) belonged to this community and that they may have been numerically dominant within the muddy substrate. The homogenized appearance of shoal flank deposits at the Stetson pit lends support to this idea. The presence of abundant oysters and their associates indicates spillover of organism populations that were centered on nearby oyster banks into surrounding muddy substrates between sand shoal areas.

The same sediments that enveloped shoal flank associations also contained concentrations of Crassotrea virginica in life positions. The picture emerges of patches of oyster reefs surrounded by muddy, subtidal, intershoal areas within a coastal lagoon.

Second only to the inner shelf associations in species richness were the backbarrier sand shoal associations. The sand shoal fossils were derived from a community that was possibly mollusk-dominated but may have contained large numbers of burrowing polychaete worms (see descriptions of modern sand shoal communities in Morris and Rollins, 1977). Sediments of the sand shoal environment contained millions of shells of ***Gemma gemma***. Sanders and others (1962) reported population densities of ***G. gemma*** up to $331,000/m^2$ in Barnstable Harbor. Population explosions may have locally crowded out other suspension-feeders in the sand shoal environment during periods of seasonally abundant phytoplankton, resulting in discontinuous shelly laminations or "streaks" composed primarily of this small venerid clam visible in the walls of the borrow pit. ***G. gemma*** shell concentrations are potentially useful indicators of poorly drained, intertidal sand flats in late Cenozoic lagoonal deposits. Other important organisms in the sand shoal community were suspension-feeding bivalves, and predatory and ectoparasitic gastropods.

The structurally simplest community recognized is represented by the channel associations contained in mixed asemblages in the lenticular shell beds at the pit. The channel associations were derived from a very low diversity, channel-bottom community that could have been subaerially exposed during low tides, and was composed of organisms that either cemented themselves to the shelly substrate for stability (***Crassostrea virginica*** and ***Balanus sp.***) or nestled into wet, sandy interstices in the shell rubble for protection (***Gemma gemma***).

COMMUNITY REPLACEMENT AND PALEOECOLOGIC HISTORY

When fossil associations and assemblages identified in this study were arranged in the stratigraphic framework of the Stetson borrow pit area, a sequence of ecologic units emerged that allowed an interpretation of the late Pleistocene history of the study area primarily in terms of the paleoecologic aspects of deposits at the pit. The vertical sequence of units is the result of community replacement during the time span represented by the stratigraphic section at the borrow pit and records significant changes in nearshore environmental configurations in the Dare County area (see Rollins

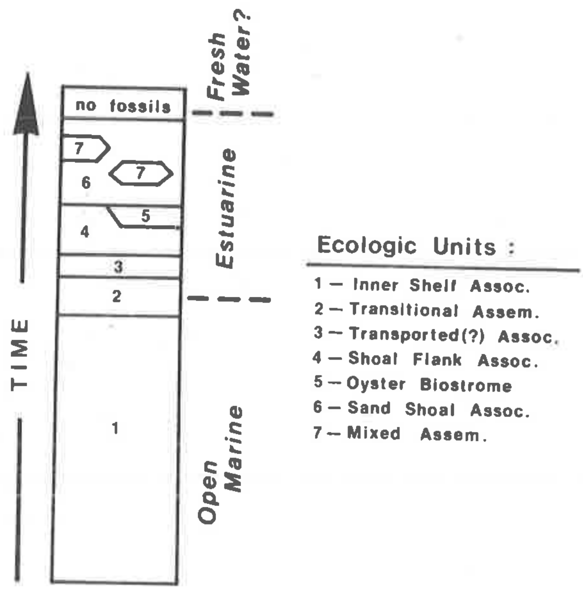

Figure 5. Schematic paleoecologic history of late Pleistocene fossil deposits in the Stetson borrow pit area.

and others, 1979). Bailey (1977) used a similar approach in interpreting shelly deposits within the Pliocene Yorktown Formation in North Carolina, and Rollins and Donahue (1975) employed the same sort of method to describe the history of Upper Pennsylvanian deposits in the Appalachian Basin. The paleoecologic history of the Stetson pit area is shown schematically in Figure 5.

CONCLUSIONS

1. Late Pleistocene paleoenvironments identified at the Stetson pit, in surface exposures and in a bored section, included in ascending order: marine inner shelf areas, lagoonal basin, lagoonal intershoal areas, shoals and channels (tidal delta complex?), lagoon margin embayments, and river-estuary. The regressive sequence of nearshore marine to estuarine deposits records the partitioning of a coastal compartment by a barrier shoal or island, and the subsequent filling of a backbarrier lagoon in the area of mainland Dare County.

2. The fossil record of these deposits is made up primarily of shelled, opportunistic and stress-tolerant suspension-feeding mollusks that were uniquely suited for existence in unstable, unpredictable, sandy-bottom nearshore environments.

3. Ecologic units identified in bulk samples from the borrow pit included: disturbed-neighborhood, inner shelf marine associations; a transitional assemblage composed of both marine and estuarine fossils; a transported (?) estuarine association; in-place shoal flank associations; an in-place oyster biostrome; in-place or disturbed-neighborhood sand shoal associations; and mixed assemblages in channel deposits containing taxa from a variety of backbarrier communities.

4. Associations and assemblages were derived from at least five original communities. The inner shelf associations represent the remains of a single marine community, whereas the estuarine associations and assemblages represent an intergradational patchwork of backbarrier communities (shoal flank, oyster bank, sand shoal, and tidal (?) channel-bottom communities).

5. Ecologically compatible fossil associations and mixed assemblages were arranged stratigraphically to produce a sequence of ecologic units, which allowed the interpretation of the history of Pleistocene deposits in mainland Dare County primarily in paleoecologic terms (Figure 5). Paleoecologic histories delineate the history of stratigraphic sections based primarily on the remains of communities preserved in

layers of sediment, and both confirm and add significant detail to paleoenvironmental interpretations.

ACKNOWLEDGMENTS

The constructive criticisms of earlier versions of this paper by B.W. Blackwelder, T.M. Cronin, M.F. Miller, and R.D.K. Thomas are gratefully acknowledged. J. Baldwins, N.A. Brown, S.I. Fuerst, and especially J.R. Herbert provided valuable assistance in the field. Identifications of foraminifers were provided by N.J. Whitcomb. This report is based on a M.S. thesis completed at Duke University under the supervision of G.W. Lynts, with grant support from Duke University and the North Carolina Department of Natural and Economic Resources.

REFERENCES CITED

Abbott, R.T., 1968, Seashells of North America:Golden Press, New York, 280p.

Abbott, R.T. 1974, American Seashells:Van Nostrand Reinhold, New York, 663 p.

Bailey, R.H., 1977, Neogene molluscan assemblages along the Chowan River, North Carolina: Southeastern Geol., v. 8, p. 173-189.

Byrum, S.R., 1978, Foraminiferal biostratigraphy and upper Pleistocene sediments from the Outer Banks of North Carolina:M. S. Thesis East Carolina University, 57 p.

Byrum, S.R., 1979, Paleoecology of an upper Pleistocene regressive sequence in coastal North Carolina:Geol. Soc. Am. Abstracts with Programs, v. 11, no. 4, p. 173.

Cronin, T. M., 1980, Biostratigraphic correlation of Pleistocene marine deposits and sea levels, Atlantic Coastal Plain of the southeastern United States:Quat. Research, v. 13, p. 213-229.

Field, M. E. and Duane, D. B., 1976, Post-Pleistocene history of the United States inner continental shelf:significance to origin of barrier islands:Geol. Soc. Am. Bulletin, v. 87, p. 691-702.

Fisher, J. J., 1968, Barrier island formation:discussion:Geol. Soc. Am. Bulletin, v. 79, p. 1421-1425.

Gosner, K.L., 1971, Guide to identification of marine and estuarine invertebrates:John Wiley and Sons, New York, 693 p.

Hanley, J. H., 1976, Paleosynecology of nonmarine Mollusca from the Green River and Wasatch Formations (Eocene), southwestern Wyoming and northwestern Colorado, *in* Scott, R. W. and West, R.R., eds., Structure and classification of paleocommunities:Dowden, Hutchinson and Ross, Stroudsburg, Penn., p. 235-261.

Howard, J. D., Mayon, T. V., and Heard, R. W., 1977, Biogenic sedimentary structures formed by rays:Jour. Sed. Petrology, v. 47, p. 339-346.

Johnson, R. G., 1960, Models and methods of analysis of the mode of formation of fossil assemblages:Geol. Soc. Am. Bulletin, v. 71, p. 1075-1086.

Johnson, R. G., 1971, Animal-sediment relations in shallow water benthic communities:Marine Geol., v. 11, p. 93-104.

Johnson, R. G., 1972, Conceptual models of benthic marine communities, in, Schopf, T. J. M., ed., Models in paleobiology:Freeman, Cooper, and Co., San Francisco, p. 148-159.

Kauffman, E. G., 1974, Cretaceous assemblages, communities, and associations: Western Interior United States and Caribbean Islands, *in* Ziegler, A. M., and others. Principles of benthic community analysis:Sedimenta IV, Univ. of Miami, p. 12.1-12.27.

Kauffman, E. G. and Scott, R. W., 1976, Basic concepts of community ecology and paleoecology, *in* Scott, R. W. and West, R. R., eds., Structure and classification of paleocommunities:Dowden, Hutchinson and Ross, Stroudsburg, Penn., p. 1-28.

Levinton, J. S., 1970, The paleoecological significance of opportunistic species: Lethaia, v. 3, p. 69-78.

Miller, W., III, 1978, Ecological units, paleocommunity structure, and ecological history of late Pleistocene deposits in Dare County, North Carolina:M.S. thesis Duke University, 135 p.
Morris, R. W. and Rollins, H. B., 1977, Observations on intertidal organism associations of St. Catherines Island, Georgia. I. General description and paleoecological implications:Bull. Am. Museum Nat. Hist., v. 159, p. 89-128.
Oaks, R. Q. and Coch, N. K., 1973, Post-Miocene stratigraphy and morphology, southeastern Virginia:Virginia Div. Min. Res., Bulletin 82, 135 p.
Oaks, R. Q., Coch, N. K., Sanders, J. E., and Flint, R. F., 1974, Post-Miocene shorelines and sea levels, southeastern Virginia, *in* Oaks, R. Q. and and DuBar, J. R., eds., Post-Miocene stratigraphy--central and southern Atlantic Coastal Plain:Utah State Univ. Press, Logan, p. 53-87.
O'Connor, M. P. and Riggs, S. R., 1971, Relict sediments within a transgressive barrier island-estuarine system, North Carolina Atlantic Coast (abstract):International Sedimentological Congress VIII, Heidelberg, Germany, p. 74.
O'Connor, M. P. and Riggs, S. R., 1974, Mid-Wisconsin to Recent sea level fluctuation and time-stratigraphy of the northern Outer Banks of North Carolina:Geol. Soc. Am. Abstracts with Programs, v. 6, no. 7, p. 894.
O'Connor, M. P., Riggs, S. R., and Winston, D., 1972, Recent estuarine sediment history of the Roanoke Island area, North Carolina, *in* Nelson, B. W., ed., Environmental framework of coastal plain estuaries:Geol. Soc. Am. Memoir 133, p. 453-463.
Porter, H. J. and Tyler, J., 1976, Seashells common to North Carolina:Sea Grant Publication UNC-SG-72-09, 36 p.
Rhoads, D. C., McCall, P. L., and Yingst, J. Y., 1978, Disturbance and production on the estuarine seafloor: Am. Scientist, v. 66, p. 577-586.
Richards, H. G., 1936, Fauna fo the Pleistocene Pamlico formation of the southern Atlantic Coastal Plain:Geol. Soc. Am. Bulletin, v. 47, p. 1611-1656.
Richards, H. G., 1950, Geology of the Coastal Plain of North Carolina:Trans. Am. Philosoph. Soc., new series--v. 40, part 1, 83p.
Riggs, S. R. and O'Connor, M. P., 1974, Relict sediment deposits in a major transgressive coastal system:Sea Grant Publication UNC-SG-74-04, p. 1-20.
Rollins, H. B. and Donahue, J., 1975, Towards a theoretical basis of paleoecology: concepts of community dynamics:Lethaia, v. 8, p. 255-270.
Rollins, H. B., Carothers, M., and Donahue, J., 1979, Transgression, regression and fossil community succession:Lethaia, v. 12, p. 89-104.
Sanders, H. L. Goudsmit, E. M., Mills, E. L., and Hampson, G. E., 1962, A study of the intertidal fauna of Barnstable Harbor, Massachusetts:Limnol. Ocean., v. 7, 63-79.
Schopf, T. J. M., 1969, Paleoecology of ectoprocts (bryozoans):Jour. Paleontol., v. 43, p. 234-244.
Schopf, T. J. M., 1978, Fossilization potential of an intertidal fauna:Friday Harbor, Washington:Paleobiology, v. 4, p. 261-270.
Scott, R. W., 1970, Paleoecology and paleontology of the Lower Cretaceous Kiowa Formation, Kansas:Univ. Kansas Paleontol. Contrib., Article 52 (Cretaceous 1), 94 p.
Scott, R. W., 1974, Bay and shoreface benthic communities in the Lower Cretaceous:Lethaia, v. 7, p. 315-330.
Scott, R. W., 1976, Trophic classification of benthic communities, *in* Scott, R. W. and West, R. R., eds., Structure and classification of paleocommunities:Dowden, Hutchinson, and Ross, Stroudsburg, Penn., p. 29-66.
Scott, R. W., 1978, Approaches to trophic analysis of paleocommunities:Lethaia, v. 11, p. 1-14.
Shotwell, J. A., 1964, Community succession in mammals of the Late Tertiary, *in* Imbrie, J. and Newell, N., eds., Approaches to paleoecology:John Wiley and Sons, New York, p. 135-150.
Stach, L. W., 1936, Correlation of zoarial form with habitat:Jour. Geology, v. 44, p. 60-65.
Stanley, S. M., 1970, Relation of shell form to life habits of the Bivalvia (Mollusca): Geol. Soc. Am. Memoir 125, 296 p.

Stephenson, L.W., 1912, The Quaternary formations, *in* Clark, W. B. and others, The Coastal Plain of North Carolina:N. C. Geol. and Econ. Survey, v. 3, p. 266-290.
Stephenson, L. W. and Johnson, B. L., 1912, The water resources of the Coastal Plain of North Carolina:N. C. Geol. and Econ. Survey, v. 3, p. 333-483.
Valentine, J. W., 1972, Conceptual models of ecosystem evolution, *in* Schopf, T. J. M., ed., Models in paleobiology:Freeman, Cooper and Co., San Francisco, p. 192-215.
Van Dover, C. and Kirby-Smith, W. W., 1979, Field guide to common marine invertebrates of Beaufort, N. C.:Duke Univ. Marine Lab., Beaufort, 78 p.
Vermeij, G. J., 1978, Biogeography and adaptation; patterns of marine life:Harvard Univ. Press, Cambridge, Mass., 332 p.
Walker, K. R., 1974, Community patterns:Middle Ordovician of Tennessee, *in* Ziegler, A. M. and others, Principles of benthic community analysis:Sedimenta IV, Univ of Miami, p. 9.1-9.9

SANTA ROSA ISLAND, FLORIDA PANHANDLE,

ORIGINS OF A COMPOSITE BARRIER ISLAND

By

Ervin G. Otvos
Geology Section
Gulf Coast Reasearch Laboratory
Ocean Springs, Mississippi 39564

ABSTRACT

The narrow core area, under eastern Santa Rosa Island, from which the island subsequently developed, had been topographically a relatively high ground in early Holocene times. This island core is composed of Late Pleistocene barrier deposits, in turn underlain by open nearshore and brackish water deposits of the late Pleistocene Biloxi Formation. With the onset of the Holocene transgression, encroaching sea waters around 9,200 yrs B.P. reached a deeply incised river channel in present Pensacola Bay at -22.5 m below present mean sea level. This sea level value is in surprisingly good agreement with approximately contemporaneous sea level positions as far as Texas, Delaware and the Bermuda Islands. Further sea level rise transformed the narrow shore-parallel valley, located between the island core and the mainland Pleistocene barrier area, into a brackish lagoon. Foreshore and dune deposits veneered the core area as it became an island. Open nearshore sediments were deposited seaward of the Pleistocene barrier complex along the new mainland shore, east and west of the new island. Westward littoral drift, guided by the position of the new Gulf shoreline at Destin (Fig. 1) and along the new island, gradually increased island length through lateral accretion and possibly also by aggradation of adjacent shoal areas. As the island grew, Santa Rosa Sound gradually extended itself westward.

Although the Pleistocene core does not rise above present mean sea level, genetically the island is still classified as a composite (secondary) barrier island. This island category contains a shallow pre-Holocene (usually Pleistocene) core that extends near or above present sea level and is veneered by Holocene beach and dune deposits. Known composite barrier islands in which the Pleistocene core reaches above recent sea level include eastern Dauphin Island, Alabama, certain South Carolina-Georgia-north Florida barrier islands and Texel on the North Sea.

INTRODUCTION

Area Description and Hydrologic Conditions

Santa Rosa Island on the Florida Panhandle is the second longest (84 km) barrier island on the Gulf Coast. It averages only 300-500 m wide and the maximum width barely exceeds 1 km (Fig. 1). Sparsely vegetated dunes cover the interior. The highest dunes (12 m) occur on the more wooded, western island tip where denser vegetation has been better established. Wide Gulf beaches and narrow Sound beaches fringe Santa Rosa. Because of the cross-island migration of wind-blown sand, the textural distinction between Gulf and Sound beaches (Otvos, 1975b) did not develop as on Mississippi-Alabama barrier islands. The dilution effect of overwhelming volumes of eolian sand from the Gulf beaches prevented sand differentiation on the narrow Sound and bay beaches that are characterized by very low wave energy and insignificant littoral drift transport. The island is separated from the mainland by the 0.4-3.3 km wide, 0.4-7.5 m deep Santa Rosa Sound; on the east by Choctawhatchee Bay, on the west by Pensacola Bay. Only minor creeks enter the Sound from the mainland, but the bays receive fresh water from sizable streams. Throughout most of the year, low wave energy conditions prevail on this low microtidal coast (tidal range: 0.5-0.8 m). As the

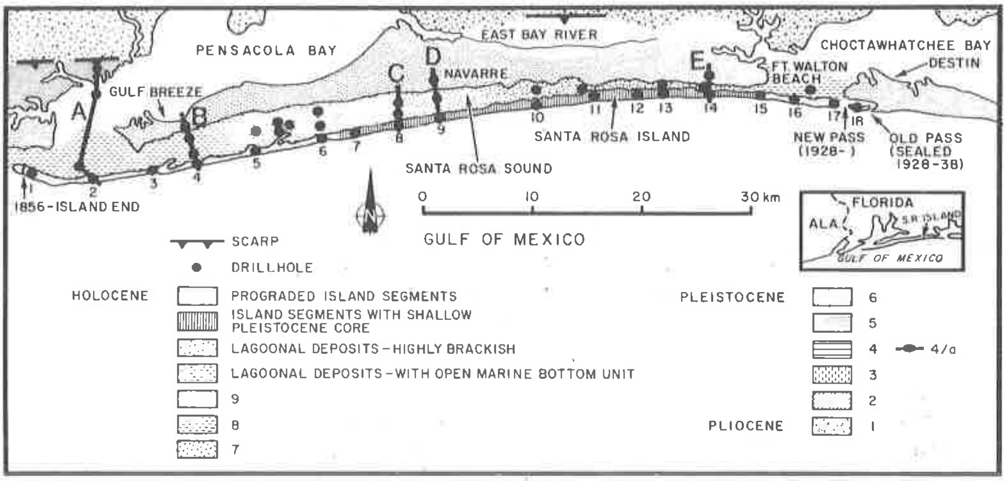

Figure 1. Surface geology, genetic island units and Holocene lagoonal sequence types, for the Santa Rosa Island area. Key for figs. 1, 2 and 3: Pliocene: 1-Citronelle Fm; fluvial silty-sands, gravelly sands; late Pleistocene: 2-Prairie Fm; fluvial silty sands, sands; 3-Biloxi Fm, non-leached estuarine-brackish silty sands, sands, sandy clays; 4-Biloxi Fm; only locally leached, open marine nearshore sands, silty sands, sandy clays; 4/a-microfauna location in leached unit; 5-Biloxi Fm, only locally leached, open marine nearshore sands, silty sands, sandy clays; 6-Gulfport Fm; regressive, sandy, sandy-silt, clayey-sand, mainland barrier, deposited in intertidal beach and dune environments; Holocene: 7- siltysand, clayey-sand brackish lagoon deposits; 8-nearshore open marine sands, silty sands, clayey sands; 9-sandy beach foreshore and dune deposits.

result of the dominant wave approach from the southeast, net littoral drift is westward.

Due to the high tidal current velocities and great depth, the Pensacola Bay entrance channel, at the western island tip, greatly slowed down the westward migration of the island. Historical changes also include the 1928 storm cut through the eastern island end (Stapor, 1975). The storm channel became permanent and subsequently this new eastern pass laterally migrated somewhat eastward. Lobate features that extend from the island's north shore into the Sound, indicate occasional hurricane washovers. A number of artificial islands occur in the eastern Sound between drillholes #11 and #14 (Fig. 1). Historical charts prove that they resulted from dredging activities.

The deep Pensacola Bay entrance channel often creates high salinities in the Bay proper and in adjacent areas of the Sound (G.A. Moshiri, written comm.; Gallagher, 1971; Cooley, 1978). Salinities in the Sound usually range between 4.0-25.0 ppt; higher in and near the Bay. Reduced salinity conditions in the Sound and Choctawhatchee Bay are reflected by the foraminifer fauna, dominated by *Ammotium salsum*, *Ammobaculites exiguus*; to a lesser extent by *Ammonia beccarii* and a few other species.

On the mainland side of the Sound, the land surface, underlain by the Pleistocene Gulfport Formation, slowly rises from the shore to the southern limits of the Pliocene Citronelle Formation at 7.5-22.5 m elevations. North of this border, land elevations quickly reach 35 m.

RESEARCH METHODS

Prior to our work in 1978-79, practically no geological information has been available on the shallow subsurface conditions of Santa Rosa Island, Santa Rosa sound and adjacent mainland coastal areas. Gulf Coast Research Laboratory drilled fifteen rotary core holes along the entire length of the island, in addition to 13 rotary-drilled core holes in the Sound and the two bays (Fig. 1). Three rotary holes were drilled on the mainland side of the Sound. Rotary-drilled cores from four earlier completed holes were provided by Pensacola engineering companies. In rotary drilling, 45-cm long, 3.8

cm diameter split-spoon cores were taken continuously to 3 m depth, and at 105 cm intervals thereafter. Recovery rates in sand averaged 50-75% in silty clayey units, 100%. The deepest rotary-drilled hole penetrated to 26.5 m. A dozen 3-4.5 m long, 9 cm-internal diameter vibracores from Santa Rosa Sound were provided by the U.S. Corps of Engineers.

Grain size analyses. statistical sediment texture calculations and microfauna preparation have been performed at the Sedimentation Laboratory, Gulf Coast Research Laboratory. W.D. Bock analyzed the foraminifer fauna. Radiocarbon age dating was performed at the Center for Applied Isotope Studies, University of Georgia.

PREVIOUS WORK, ISLAND STRATIGRAPHY

Publications, dealing with coastal changes in the Santa Rosa area, have been summarized by Stapor(1975). Subsurface exploration of barrier island and adjacent lagoonal areas, usually limited in extent and scope, were first reported from the Texas Gulf coast by Shephard and Moore (1955), Fisk and others (1959), Bernard and others (1959) and from the Florida Gulf Coast, by Schnable (1966) and Riggs and O'Connor (1974). The importance of the Pleistocene substrate under islands in certain types of barrier island development has been emphasized by numerous writers, including Zeigler (1959), Tanner (1960), Oertel (1979) and others. As intensive subsurface study of northeastern Gulf barrier islands was initiated in 1973 and included Mississippi, Alabama and Florida Panhandle islands (Otvos, 1979; 1981a).

STRATIGRAPHY

Citronelle Formation (Pliocene)

This fluvial unit, not recognized in the present drillholes under Santa Rosa Island, underlies the upland surfaces a few kilometers north of the present coastline. Light yellowish-brown to reddish-orange silty-to-sandy deposits and light-gray, gravelly-to-sandy layers are characteristic. At shallow depths, the Formation overlies detrital late Miocene sediments with an unconformity (Marsh, 1966). Relatively steep (fault?) escarpments often form its coastward limit (Otvos, 1981b).

Prairie Formation (Pleistocene)

Fluvial deposits, contemporaneous with Late Pleistocene (Sangamon Interglacial) estuarine and marine unit, deposited seaward of them, are widespread on the Gulf coast, including Mississippi and Alabama (Otvos, 1981b). These light yellowish-gray, yellowish-brown, silty-sandy and sandy deposits lie seaward of the Citronelle and upland in the Pensacola area (Figs. 1-3). Some of the nonfossiliferous Pleistocene silty-muddy sands, found in drillholes #2 and #3 under the western end of Santa Rosa Island (Figs. 1 and 2) and interpreted in this study as part of "leached" Biloxi Formation units, may actually belong to the Prairie Formation.

Biloxi Formation (Pleistocene)

This unit formed during the transgressive-regressive cycle of the Sangamon Interglacial and can be traced in the subsurface along the entire northern Gulf Coast (Otvos, 1975a). In the Santa Rosa area also it was deposited in open nearshore marine and estuarine-lagoonal brackish environments. In contrast with the Santa Rosa region, the formation has a much more muddy (silty-clayey) composition in Mississippi and Alabama, with lesser sand content.

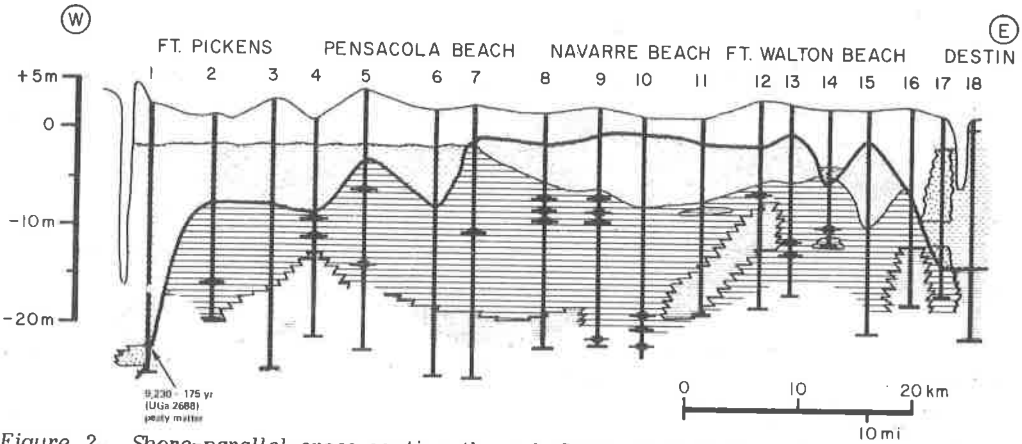

Figure 2. Shore-parallel cross section through Santa Rosa Island. Key: as in Figure 1.

(a) open nearshore marine sands

Medium- to fine-grained, white and light-gray, grayish-green, poorly sorted sands with at least 90% sand content are prominent. Brownish-gray, olive-gray, grayish-green, greenish-gray, clayey and silty medium sands, fine sandy clays with occasional, moderately-sorted, fine-grained sand layers form the rest of the unit. Sedimentary structures were difficult to identify in the sandy, unconsolidated core material. In a Gulf Breeze drillhole (W-2339, USGS; Fig. 3B), on the mainland, a sizeable molluscan fauna in this unit has mistakenly been described as part of the Pliocene Citronelle Formation (Marsh, 1966, p. 85). Large, calcareous foraminifer faunas with 10-50 species are present in this facies. The dominant taxa (4-40%) included ***Elphidium incertum mexicanum*, *E. gunteri*, *E. galvestonensis*, *Nonion depressulum matagordanum*, *Cribroelphidium poeyanum*, *Rosalina columbiensis*, *Hanzawaia strattoni*, *Ammonia beccarii*** and ***Guttulina laevis***. In the Santa Rosa Sound corehole immediately north of drillhole No. 14 (Fig. 3E), between -5.8 - 6.7 m, an unusual fauna was found in humate-impregnated beds. Black, matted wood fragments above this unit yielded a Pleistocene date. Most species ***(Articulina mexicana*, *A. mucronata*, *Archaias angulatus*, *Peneroplis carinatus*, *P. proteus*, *Quinqueloculina* and *Triloculina* species)** were absent from all other drillholes. This fauna alone consisted of identifiable black (humate-filled) internal foraminifer casts.

(b) Estuarine sands-clayey sands

Deposited in reduced salinity environments, these sediments had the same range of sedimentary characteristics (color, texture, etc.), as did the previous unit. Scarcity of microfossils was typical. The samples contained chitinous linings of tests of only three foraminifer species (***Ammonia beccarii*, *Ammotium salsum*** and, rarely ***Ammobaculites exiguus***, with very few (1-13) individuals. Occasional siliceous sponge spicules and rare diatoms were also found. All these were indicative of intensive syn- and/or postdepositional leaching of calcareous tests and shells, due to lowered pH values. These conditions may result from poor circulation of bottom waters and/or from the presence of decaying vegetation and other organic matter (W.D. Bock, written comm.). Fast burial resulted in the collapsed state of many chitinous foraminifer tests.

The brackish unit interfingers with open marine Biloxi beds (Figs. 2, 3) and possibly indicates the influence of brackish estuaries along certain shore segments of the open marine shoreline during the Sangamon Interglacial.

(c) "Leached" Biloxi unit (dominantly estuarine)

The open marine and brackish units laterally interfinger with fossil-free sands,

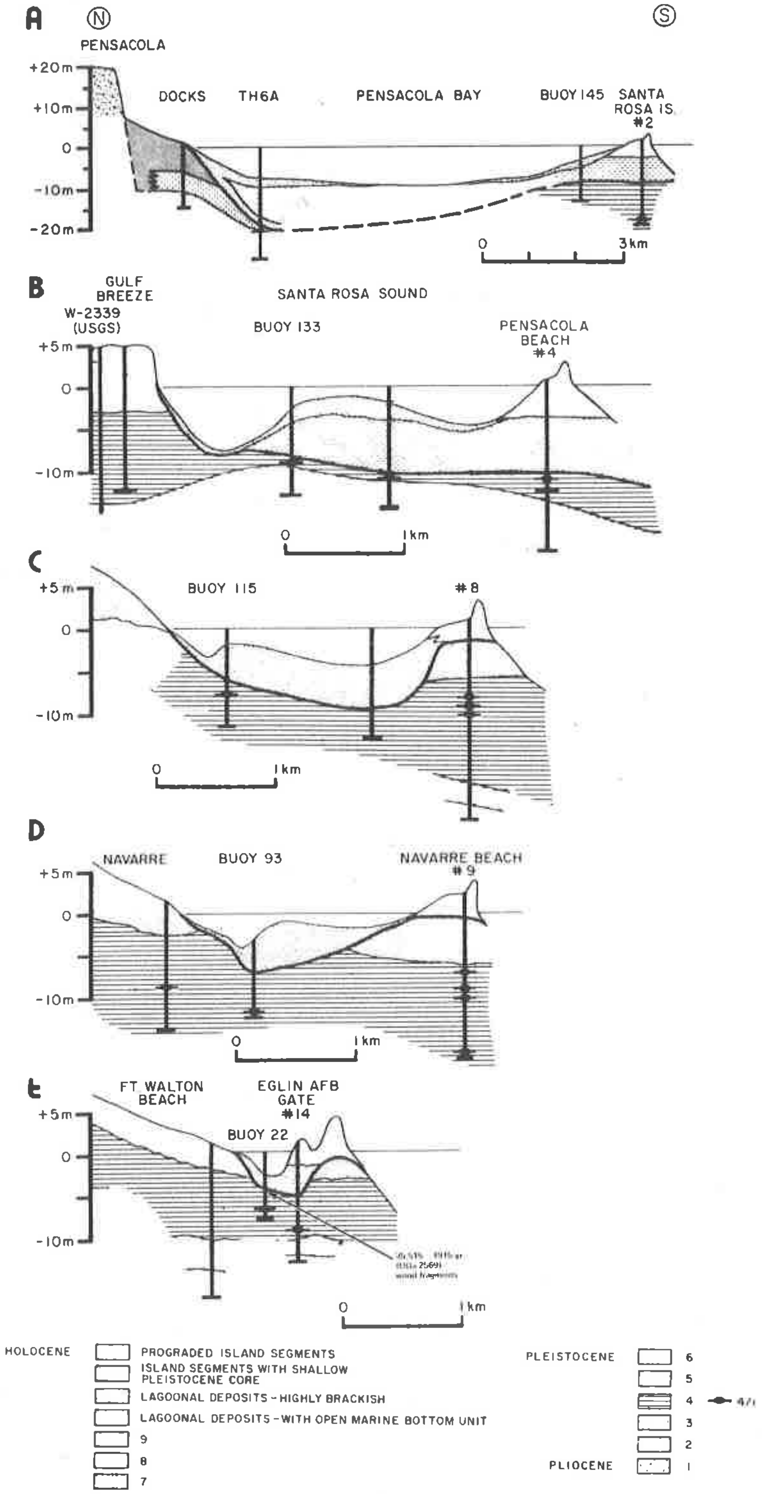

Figure 3. Mainland-island cross sections A-E. Locations: Fig. 1. Key: as in Figure 1.

silty and clayey sands and occasionally include lenses of the lithologically more resistant microfossils, that lived mostly in reduced-salinity environments (Figs. 2 and 3). Delineation of this unit from overlying Holocene deposits was not always clear-cut. Sediment colors were often dark brown, grayish and dusky yellowish-brown, caused by staining from organic compounds, including humate and iron hydroxides. Dark greenish-gray colors were among the most typical indicators of the Pleistocene age, used in distinguishing from overlying Holocene sediments. However, light tan and white colors, common in Holocene sands were also widespread.

As in the brackish Biloxi unit, syn- and/or postdepositional leaching is believed to have eliminated the calcareous tests and molluscan shells from these deposits. Non-deposition of calcareous tests around the soft foram body may be another reason for their absence. Where burial of the chitinous tests proceeded slowly, the tests were completely digested. Humate-impregnation of Biloxi beds, and enclosed foraminifer internal casts of humate matter in drillholes, is also indicative of postdepositional leaching and precipitation processes in these units. Dark-brown and black, humate-impregnated Gulfport sands are very common along the whole Gulf Coast (Otvos, 1972).

Gulfport Formation (Pleistocene)

Sandy units of this late Pleistocene barrier formation are considered correlative with the Live Oak-Ingleside barrier segments of Texas (Otvos, 1972). Segments of the barrier trend are found along the whole northern Gulf and they represent the peak and regressive phases of the Sangamon transgression following deposition of Biloxi beds. The Formation consists of light brown, light yellow- to reddish-brown and light-gray, 3-10 m thick, moderately-to very well-sorted, beach, offshore, foreshore and dune sands. Soil-forming processes and weathering in general are believed responsible for a postdepositional addition of the finer grain size fractions in the unit. As the result, sorting values were poorer here than in correlative barrier units on the Mississippi-Alabama coast (my unpublished data, on file). The sand fraction in Santa Rosa area Gulfport Formation samples usually was well sorted and reflected the sediment characteristics of the original beach and dune deposits before diagenetic changes occurred. Under Santa Rosa Island where the sand commonly is light tan or white, the Gulfport Formation can not readily be distinguished from directly overlying Holocene dune sands.

On the mainland shore the Gulfport belt is 4-6 km wide (Fig. 1) and reaches 12 m above sea level. The well-defined strandplain character of the Gulfport barrier, composed of numerous ridges with intervening swales, while common elsewhere, is absent in parts of the western Florida Panhandle. Syn- or postdepositional erosion may have destroyed such ridges or the vegetative cover was unfavorable for dune ridge accretion. Landward of the active beach ridges, the wind-blown sand was deposited in featureless sand sheets. This process may have resulted in the present, gently undulating plain that extends to East Bay River and the Citronelle area (Fig. 1).

Yellowish-brown sands that overlie Citronelle beds at 22-30 m elevations above sea level north of the Gulfport barrier zone, are also believed to be of late Pleistocene age and of eolian origins. The unconformity between better compacted, dark yellowish-orange, red, gravelly Citronelle sands and an overlying, 1-2 m thick sheet of moderately loose, pale yellowish-orange sand with 8-9% silt content, was conspicuous on the Citronelle slope north of East Bay River. Due probably to syn-depositional slopewash from Citronelle sediments, the upper unit is slightly granular. The upper sand appears to be correlative with the eolian Gulfport beds.

The top Pleistocene units in drillholes #8, 9, 10, 13 and 15 of Santa Rosa Island (Figs. 1, 2) are interpreted as part of the Gulfport Formation. A 0.4-1.5 km wide zone (Figs. 1, 3C, D, E,) separates today this Gulfport segment from the Gulfport barrier along the present mainland shore. The original dimensions of this swale are unknown but after the early Wisconsin regression the swale probably was widened and deepened by lateral migration and down-cutting of a stream that may have occupied it. The returning Holocene sea turned the shallow subaerial valley into the eastern segment of the Santa Rosa Sound. Parallel alignment of the central Sound with East Bay River (Fig. 1) and with certain Citronelle escarpments, suggests that the position of the original swale may have also been structurally influenced.

HOLOCENE ISLAND EVOLUTION

The sequence of sedimentary units encountered in the lowermost 12 m of drillhole #1 (Figs. 1, 2), Santa Rosa Island, represents a continuous transgression that filled a pre-existing major stream channel, incised during the Wisconsin glacial stage. This stream drained the present Pensacola Bay region. A single date from compressed plant matter: 9,230+175 yr B.P. (UGa-2688) from -22.5 m below mean sea level coincides almost perfectly with the depth-age plot of a dated peat on the sea-level curve from the east Texas shelf (Sample No. 78; Nelson and Bray, 1970, p. 76). Also, there is close agreement with sea level positions, derived from salt marsh peat dates in Delaware (Kraft, 1976) and the Bermuda Islands (Redfield, 1967) and from a *Rangia* date in the Apalachicola Delta (Schnable, 1966). A brackish basal unit that included the dated peat under Santa Rosa Island contained only numerous chitinous linings of *Ammotium salsum* tests. The foram fauna, transitional between highly brackish and marine species, found in the overlying clays and sandy clays (Fig. 2) was dominated by *Ammonia beccarii* (66%) and *Elphidium galvestonense* (10-21%). Further salinity increase upward in the sequence was demonstrated by the dominance (4-44%) of *Nonion depressulum matagordanum, Rosalina columbiensis, Cribroelphidium poeyanum, Buliminella elegantissima, Cibicides floridanus, Hanzawaia strattoni* and other foraminifer species in the greenish-gray sandy muds, silty sands and sand units. The number of species in some samples reached 45, also reflecting full-salinity nearshore conditions. Above -14 m (Fig. 2), the sediments consisted of poorly-to-moderately sorted white, light-tan nearshore sands and silty sands, that included few species. In drillhole #15 on the eastern island tip (Figs. 1, 2), *Remaneica* sp., a species that favors sandy bottoms, is also predominant in this horizon. It was accomplished by single individuals of *Ammonia beccarii, Elphidium incertum mexicanum, Hanzawaia strattoni*, and *Nonionella atlantica* species.

Judging from sand sorting values, sediment color and the absence or presence of very small numbers of microfaunal elements, the sand units that cap the transgressive early-mid Holocene sequence were deposited in beach and dune environments. These sediments are identical in appearance with the modern beach deposits that directly overlie them (Figs. 2, 3).

As the Holocene transgression reached its landward limits, open marine sediments were also deposited over the Pleistocene land surface, specifically in front of the high Gulfport barrier ridge, in the area of present-day western Santa Rosa Sound (Figs. 1, 3). The narrow subaerial swale, on the other hand, behind the isolated island core became a lagoon, protected from the full impact of high-salinity Gulf waters by the Pleistocene barrier core (Figs. 1, 3C, D, E). The entire Holocene sequence under eastern Santa Rosa Sound and the recent bottom sediments everywhere in the Sound are olive-brown, grayish-brown and light-gray sands and muddy sands. The deposits contained agglutinated *Ammotium salsum, Miliammina fusca, Ammobaculites exiguus*, a few *Arenoparrella mexicana, Trochammina inflata* and other species, typical of highly brackish conditions. Occasional siliceous diatom tests and sponge spicules also occurred. The faunal assemblage is also typical of recent deposits in the central Sound. Closer to Pensacola Bay, higher salinities resulted in greater proportions of calcareous forms (mostly *Ammonia beccarii, Elphidium* species, *Nonion depressulum matagordanum*, and others in the most recent lagoonal sediments. The western Sound, much wider than the rest, evolved as Santa Rosa Island grew westward by spit accretion through littoral drift from its eastern core area. A shallow infilled valley, located under the western Sound and extending toward present Pensacola Bay, was inherited from the pre-transgression land surface (Fig. 3B). High tidal current velocities in the gradually narrowing Pensacola Bay entrance-channel slowed down lateral island accretion. On the eastern side of the island, drift from the mainland shores of Destin shoaled the broad mouth of Choctawhatchee Bay, immediately east of the island core area (Fig. 1). Possible aggradation of these sandy shoals to supratidal elevations adjacent to the core area and westward spit accretion added an approximately 9 km long island segment to eastern Santa Rosa Island (Fig. 1) in late Holocene times.

The moderately well-to-well sorted medium grained sand (median values average 1.45-1.80ϕ) that forms the present foreshore and dune deposits of Santa Rosa Island, bear a close textural resemblance to sands of the Gulfport Formation as well as to Holocene deposits in Santa Rosa Sound. Silty-clay and clayey sand deposits locally occur in the Sound, but the sands were derived mostly from Recent island and Gulfport deposits on the mainland shore through wave erosion, wind transport and rare hurricane-overwash events. Wave- and tide-induced currents were probably responsible for formation of triangular-shaped, large cuspate spits east of Navarre on the mainland and island shores of central Santa Rosa Sound, similar to those on Nantucket Harbor, Massachusetts, shores (Rosen, 1975).

SANTA ROSA ISLAND AND THE GENETIC BARRIER ISLAND CATEGORIES

Genetically, Santa Rosa is a secondary, "composite" barrier island; that is, an island that contains a shallow pre-Holocene core, extending near or above present sea level and veneered by Holocene shoreface, beach, and dune deposits. The core formed a topographic high on the pre-transgression land surface. This island development pattern essentially was identical to that of eastern Dauphin Island (Otvos, 1976; 1979) and a number of South Carolina, Georgia and northern Florida islands (e.g., Hilton Head, Sapelo, Ossabaw, St. Catherines and Wassaw Islands). Fenneman (1938, p. 44), Zeigler (1959) and Tanner (1960) were among the first to identify these barrier types in the Georgia-Florida area. Some important differences do exist between Santa Rosa and Dauphin Islands and the South Carolina-Florida composite barrier islands. The surface areas of Pleistocene cores on the south Atlantic composite barrier islands often are more extensive than the regressive Holocene beach ridge segments attached to them. Their Holocene dune cover, if present at all, is not substantial. Beach ridge-strandplains are absent from Dauphin and Santa Rosa Islands. Texel, with a large Pleistocene core, is another example of the composite island category in the West Frisian island chain of the Netherlands (van Staalduinen, 1977; Map Supplement No. 4-West).

Santa Rosa Island evolved during marine transgression around a high island core, but contrary to the previously cited islands, its Pleistocene core apparently never extended above present sea level. The distinction is clear between Santa Rosa and primary-aggradational barrier islands (Otvos, 1981a). The latter emerged from subtidal, nearshore bottoms, formed by shallow underwater Pleistocene sediment or rock ledges (e.g., Tampa-area islands, Florida; Riggs and O'Connor, 1974) during the late Holocene. While Holocene eolian dunes certainly, and beach-foreshore deposits possibly covered Santa Rosa Island in its early development stage, no Holocene sediments with microfossils were found in the drillholes. This indicates that during the transgression the Pleistocene core-summit became submerged and was overlain by nearshore-shoreface deposits. The composite origin allowed much faster stabilization and further seaward-and longshore progradation of the island. This origin contrasts with barrier island types that develop through vertical aggradation from shallow sea bottoms.

ACKNOWLEDGMENTS

Wayne D. Bock identified the foraminifer fauna. Wade E. Howat supervised the drilling activities and sediment analysis. The U.S. Army Corps of Engineers, Pensacola Testing Laboratory, and other engineering firms donated additional core material. Radiocarbon dating was performed by the Center for Applied Isotope Studies, University of Georgia under the supervision of Betty Lee Brandau. Eglin Air Force Base and the U.S. National Park Service gave persmission for drilling on Santa Rosa Island. In addition to the overall support by the Gulf Coast Research Laboratory, the Park Service provided funds for drilling the last four coreholes. The thorough critical review of the manuscript by Thomas F. Moslow has been sincerely appreciated.

REFERENCES CITED

Bernard, H.A., Major, C.F., Jr. and Parrott, B.S., 1959, The Galveston barrier island and environs; a model for predicting reservoir occurence and trend: Gulf Coast Assoc. Geol. Soc. Trans., v. 9, p. 221-224.

Cooley, N.R., 1978, An inventory of the estuarine fauna in the vicinity of Pensacola, Florida: Florida Dept. Natl. Resources Marine Research Publications, No. 31, 119p.

Fenneman, N.W., 1938, Physiography of eastern United States: McGraw-Hill, New York and London, 714 p.

Fish, H.N., 1959, Padre Island and Laguna Madre mud flats, south coastal Texas: Louisiana State Univ. Coastal Studies Inst., 2nd Coastal Geogr. Conf., p. 103-151.

Gallagher, R.M., 1971, Preliminary report on the hydrography of the Pensacola Bay estuary, Florida: Florida Dept. Natl. Resouces Marine Res. Lab. Spec. Scient. Report. No. 29.

Kraft, J.C., 1976, Radiocarbon dates in the Delaware Coastal Zone (eastern Atlantic Coast of North America): Delaware Sea Grant Techn. Report DEL-SG-19-76, 20 p.

Marsh, O.T., 1966, Geology of Escambia and Santa Rosa Counties, Western Florida Panhandle: Bull. Florida Geol. Survey. No. 46, 140 p.

Nelson, H.F. and Bray, E.E., 1970, Stratigraphy and history of the Holocene sediments in the Sabine-High Island area, Gulf of Mexico, p. 48-77: Deltaic sedimentation, modern and ancient (J.P. Morgan, Ed.), SEPM Special Publ. No. 15, 312 p.

Oertel, G.F., 1979, Barrier island development during the Holocene recession, southeastern United States, p. 273-290, in S. P. Leatherman, Ed., Barrier Islands 325 p.: Academic Press. New York, N.Y.

Otvos, E.G., 1972, Mississippi Gulf Coast Pleistocene beach barriers and the age problem of the Atlantic-Gulf Coast "Pamlico"-"Ingleside" beach ridge system: Southeasten Geol., v. 14, p. 241-250.

Otvos, E.G., 1975a, Late Pleistocene transgressive unit (Biloxi Formation), northern Gulf Coast: Bull. Amer. Assoc. Petr. Geologists . v. 59:148-154.

Otvos, E.G., 1975b, Inverse beach sand texture-coastal energy relationship along the Mississippi Coast barrier islands: Jour. Mississippi Acad. Sci., v. 19, p. 96-101.

Otvos, E.G., 1976, Holocene barrier island development over pre-existing Pleistocene high ground: Dauphin Island, Alabama: Geol. Soc. America Southeastern Sec. 25th Mtng.:76.

Otvos, E.G., 1979, Barrier island evolution and history of migration, north central Gulf Coast. p. 291-319, in S. P. Leatherman, Ed. Barrier Islands 325 p.: Academic Press, New York, N.Y.

Otvos, E.G., 1981a, Barrier island formation through nearshore aggradation-stratigraphic and field evidence: Marine Geol. v. 43, p. 195-243

Otovs, E.G., 1981b, Tectonic lineaments of Pliocene and Quaternary shorelines, northeast Gulf Coast:Geology, v. 9, p. 398-404.

Redfield, A.C., 1967, Postglacial change in sea level in the western North Atlantic Ocean:Science, v. 157, p. 687-692.

Riggs, S.R. and O'Connor, M.P., 1974, Relict sediment deposits in a major transgressive system. Univ. of North Carolina Sea Grant Publ. UNC-SG-74-04, 37p.

Rosen, P.S., 1975, Origin and processes of cuspate spit shorelines, in: Estuarine Research (L.E. Cronin, Editor), v. 2, p. 77-92, Academic Press, 587 p.

Schnable, J.E., 1966, The evolution and development of part of the northwest Florida coast: Ph.D. Dissertation, Florida State University, 231 p.

Shepard, F.P. and Moore, D.G., 1955, Central Texas coast sedimentation: Amer. Assoc. Petrol. Geol. Bull., v. 39, p. 1463-1593.

Staalduinen, C.J. van, 1977, Geologisch onderzoek van het Nederlandse Waddengebied: Rijks Geologische Dienst (Geological Survey of The Netherlands), 77 p + map supplements.

Stapor, F.W., Jr., 1975, Shoreline changes between Phillips Inlet and Pensacola Inlet, northwest Florida coast: Transactions GCAGS. v. 25, p. 373-378.

Tanner, W.F., 1960, "Perched" barrier islands, east Florida coast. Southeastern Geol. v. 2, p. 133-135.
Zeigler, J.M., 1959, Origin of the sea islands of the southeastern United States: Geograph. Rev., v. 49, p. 222-237.

PLUTONIC EVENTS IN THE PIEDMONT OF VIRGINIA

By

Douglas G. Mose and M.S. Nagel
Department of Chemistry and Geology
George Mason University
Fairfax, Virginia 22030

ABSTRACT

The Virginia Piedmont contains the regionally significant Chopawamsic Formation and the Arvonia-Quantico slate. Rb-Sr whole-rock data from plutons which intruded the Chopawamsic Formation and which were unconformably overlain by the slate yield isochron ages corresponding to Early Ordovician time. These isochron ages are compatible with an Ordovician age for the slate (based on fossils) and a Cambrian age for the Chopawamsic (based on U-Pb data). However, the Rb-Sr ages for the plutons do not agree with published U-Pb ages for the plutons. It is likely that the plutons contain xenocrystic zircons.

INTRODUCTION

The Piedmont surface in Virginia is composed mainly of deformed and metamorphosed rocks. Although unweathered exposures of these rocks are relatively rare due to the thick development of saprolite produced by chemical decomposition of the rocks, stream valleys often contain outcrops with which to develop an understanding of Piedmont Province geology. This paper discusses the crystalline rocks exposed along the Occoquan River and James River in Virginia.

Several geological field studies over the past few years have yielded our present picture of the general Piedmont structure, and several geological models for the formation of this structure are now under consideration (Hatcher, 1972a, 1972b; Butler, 1972; Odom and Fullagar, 1973; Hatcher, 1978; Long, 1979). In general, the Piedmont is composed of Late Precambrian to Late Paleozoic rocks (about 300 to 700 million years old). On the east, the Piedmont is covered by the Coastal Plain, and it is bounded on the west by the Blue Ridge.

There are some extensively studied rock units exposed in the western part of the Piedmont, and these rock units have proven useful because they extend from northern Virginia to as far south as south-central Virginia, having been preserved in the Quantico, Columbia and Arvonia synclines (Fig. 1). These rock units are called Chopawamsic Formation, the Arvonia Slate and the Quantico Slate and they are now exposed in the valley systems of the Occoquan River and James River.

Many geologists have contributed to our understanding of these rock units (Brown, 1979, 1970b; Pavlides, 1974, 1980; Higgins, 1972; Higgins and others, 1977; Southwick and others, 1971; Conley, 1980). The Chopawamsic Formation consists of metamorphosed mafic and felsic volcanic rocks and lesser amounts of metasedimentary rocks. The Chopawamsic is considered contemporaneous with the James Run Formation in eastern Maryland, and the Chopawamsic is known to extend from the Quantico syncline southward to the Arvonia syncline. The Chopawamsic and James Run formations have the same rock composition, and both have yielded zircons which have U-Pb age determinations (Figure 2) that correspond to Cambrian time (Higgins, 1976; Higgins and others, 1977).

The Quantico slate exposed in the Quantico syncline is a sulfidic and carbonaceous slate and siltstone (Pavlides, 1980). The contact between the Quantico slate and the underlying Chopawamsic Formtion has been described as gradational (Southwick and others, 1971; Seiders and other, 1975), but it is now believed that the contact is an unconformity (Pavlides and others, 1974; Pavlides, 1973, 1976, 1980). Late Odovician fossils have been found in the Quantico slate (Watson and Powell, 1911;

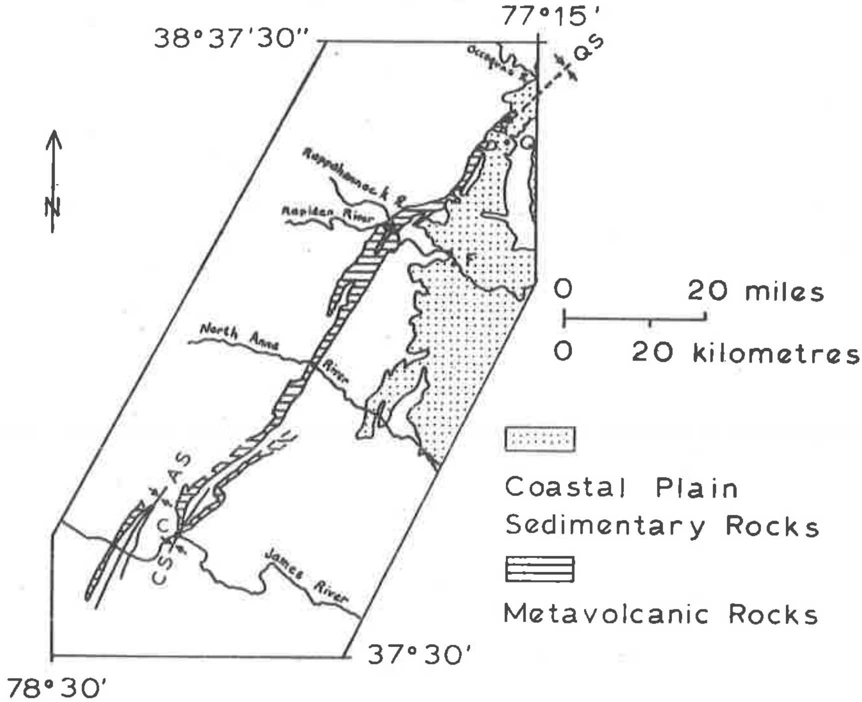

Figure 1. Generalized map of north-central Virginia showing the location of the towns of Quantico (Q), Fredericksburg (F), and Columbia (C), the Quantico syncline (QS), Columbia syncline (CS), and Arvonia syncline (AS) and the location of the Chopawamsic and related volcanics (modified from Higgins and others, 1977).

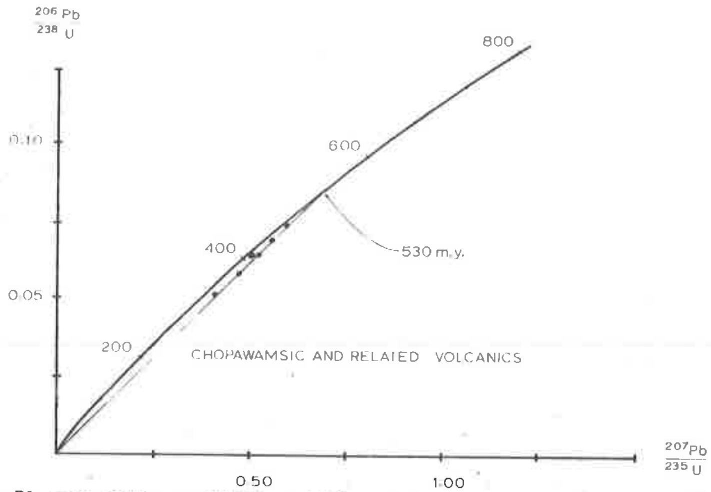

Figure 2. U-Pb concordia diagram showing data from the Chopawamsic and related volcanic rocks (modified from Higgins and others, 1977). The best-fit chord has an upper intercept of about 530 m.y.

Pavlides and thers, 1980).

The Quantico slate has been correlated with the Arvonia slate in the Arvonia and Columbia synclines in central Virginia and Late Ordovician fossils have been found in the Arvonia slate (Tillman, 1970; Higgins, 1972; Higgins and others, 1977; Brown, 1979; Pavlides, 1980). The Arvonia slate is mainly a graphitic slate which unconformably overlies the Chopawamsic Formation, and the Chopawamsic Formation along with the

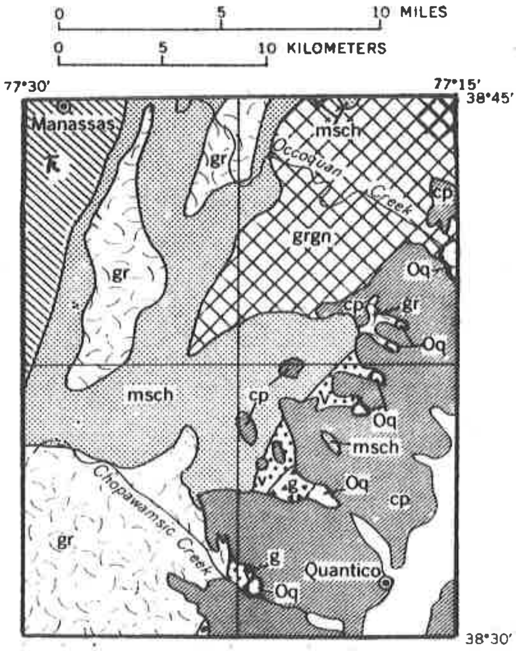

Figure 3. Generalized map of the Quantico area (modified from Pavlides, 1974). Key to symbols: grgn = Occoquan granite gneiss, gr = unnamed granite, msch = schist, v = metamorphosed volcanic and sedimentary rocks of the Chopawamsic Formation, Oq = Quantico slate, g = greenstone volcanics, Tr = Triassic rocks, cp = undivided Coastal Plain sedimentary rocks.

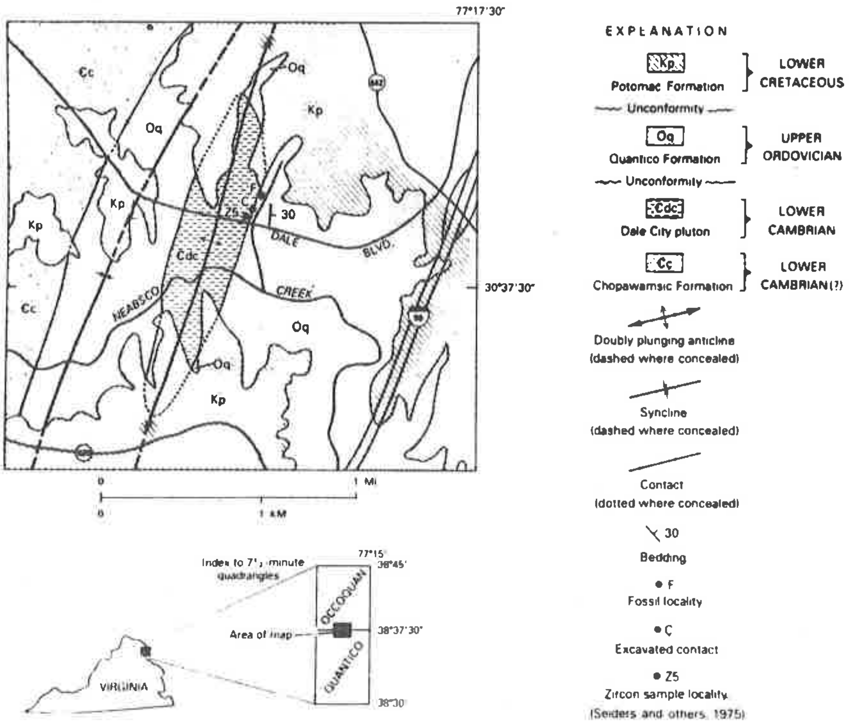

Figure 4. Generalized map of the Dale City area (Pavlides and others, 1980).

PLUTONIC ROCKS

Critical exposures of plutonic rocks have been located along the Occoquan River (Quantico area) and the James River (Columbia area) in that the plutonic rocks bear information about the time interval between deposition of the Chopawamsic volcanics and the Quantico-Arvonia sediments. In the Quantico area (Figure 3), the Occoquan pluton (granite, granodiorite, tonalite, quartz granitoid) intruded the upper part of the wissahickon Formation (diamictite facies) and the Chopawamsic Formation (Southwick and others, 1971; Seiders and others, 1975). There is no exposed contact between the Occoquan pluton and the Quantico slate, but a nearby pluton called the Dale City pluton (quartz diorite, quartz monzonite) intruded the Chopawamsic Formation and is unconformably below the Quantico slate (Higgins, 1976; Pavlides and others, 1980) (Figure 4).

In the Columbia area (Figure 5), the Arvonia slate unconformably overlies the Columbia pluton (granite, granodiorite, tonalite) and the pluton is seen to have intruded the Chopawamsic Formation (Brown, 1969, 1970b, 1979; Conley, 1978). It has been noted that while the Columbia pluton intruded the low-grade Chopawamsic metavolcanics along the western side of the Columbia syncline, the pluton also intruded high-grade rocks which are probably part of the Chopawamsic Formation along the eastern side of the syncline. It has been proposed (Conley and Johnson, 1975; Conley, 1978) that since the more highly metamorphosed Chopawamsic rocks merge into a migmatite around the Columbia pluton (part of the Hatcher Complex of Brown, 1969), the pluton and the volcanics are probably about the same age. The radiometric data discussed below suggests that the migmatite was produced when the pluton inruded the volcanic rock, and that the volcanics are about 100 m.y. older than the pluton.

PREVIOUS AGE DETERMINATIONS

Radiometric dating in the Appalachians has been instrumental to our understanding of the complex metamorphic and igneous events which occurred in the Paleozoic Era. The radiometric studies relevant to the rocks in the Quantico and Columbia areas include both U-Pb and Rb-Sr age determinations.

As mentioned earlier, the Chopawamsic volcanics in the Quantico and Columbia

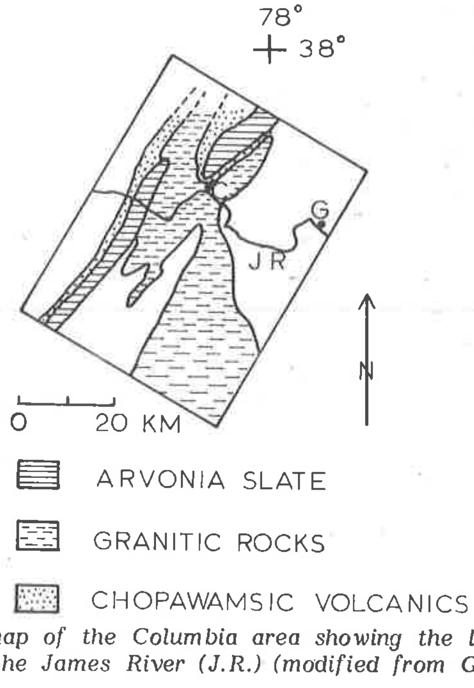

Figure 5. Sketch map of the Columbia area showing the location of Columbia (C), Goochland (G) and the James River (J.R.) (modified from Glover and Read, 1979).

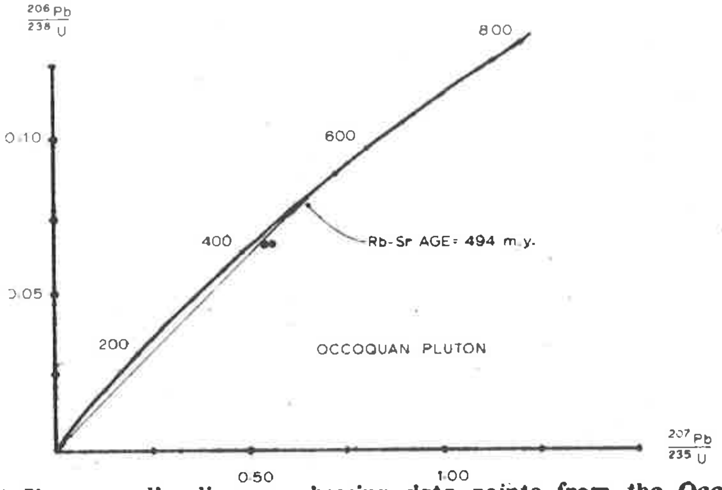

Figure 6. U-Pb concordia diagram showing data points from the Occoquan pluton (modified from Higgins and others, 1977). A chord with an upper intercept corresponding to the Rb-Sr age of 454 ± 14 m.y. is shown for reference.

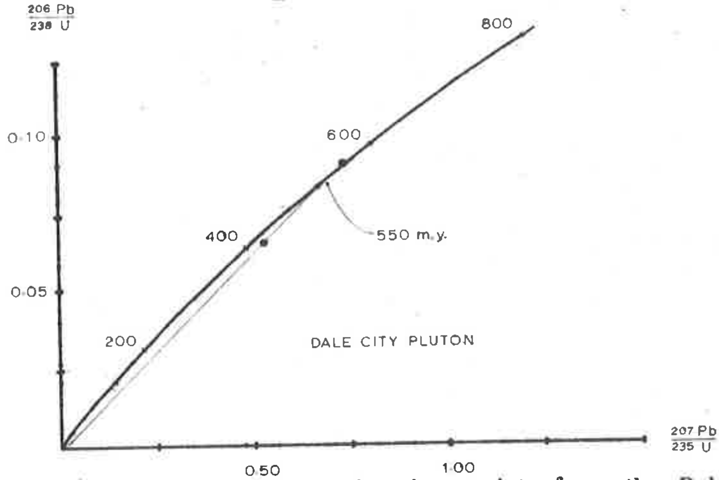

Figure 7. U-Pb concordia diagram showing data points from the Dale City pluton (modified from Higgins and others, 1977). A chord with an upper intercept of 500 m.y. is shown for reference.

areas yield a Cambrian age. In this case, the U-Pb data yield a relatively linear array on a concordia diagram (Figure 2); the lower chord intercept is slightly to the right of the origin and the upper intercept is at about 530 m.y. (Higgins and others, 1977). An age of about 530 m.y. appears reasonable when compared to the age of the overlying Quantico-Arvonia Slate that yields a fossil age of Late Ordovician (440 to 460 m.y.).

U-Pb data from the Occoquan pluton were originally thought to fall on a chord whose lower intercept is to the right of the origin on a concordia diagram, and whose upper intercept is at about 500 m.y. (Seiders and others, 1975; Higgins and othres, 1977). However, as noted by Higgins (1976), point no. 1 on Seider's diagram is analytically poor and unusable. The remaining two points (Figure 6) do not yield a chord whose upper end intersects the concordia. U-Pb data from the Dale City pluton yield a two-point chord whose upper intersection with the concorida is about 500 m.y. (Figure 7) but one data point lies above the concordia curve and the lower end of the chord falls to the right of the concordia origin (Seiders and others, 1975; Higgins, 1976; Higgins and othrs, 1977). U-Pb data from zircons which yield chords that miss intersection with the concordia origin and chords whose upper end does not intersect the concordia curve are thought to be characteristic of zircons that have inherited

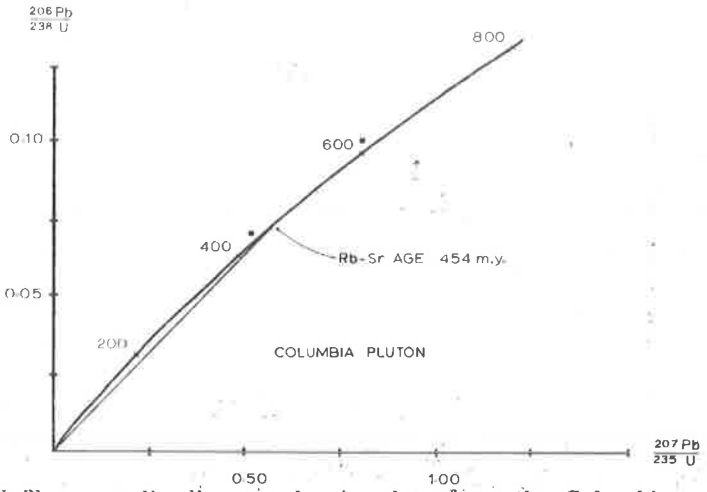

Figure 8. U-Pb concordia diagram showing data from the Columbia pluton (modified from Higgins and others, 1977). A chord with an upper intercept corresponding to the Rb-Sr age of 454 ± 9 m.y. is shown for reference.

radiogenic lead, probably in the form of seed crystals (Higgins, 1976; Higgins and others, 1977). Although Seiders (1978) pointed out that there is no analytical data in Higgins and others (1977) which clearly reveal the presence of inherited radiogenic lead, and that there is no textural evidence for xenocrystic zircons in the Occoquan and Dale City plutons, Zartman (1978) noted that in areas of older sialic basement (such as the appalachians), younger igneous rocks may contain zircon seed crystals derived from the old basement, and that zircon morphology studies do not always reveal the presence of inherited radiogenic lead.

A similar problem exists for U-Pb data from the Columbia pluton, since the U-Pb data fall on a chord which intersects neither the origin of the concordia nor the curve (Figure 8); U-Pb data from the Columbia pluton generate a two-point chord that is tangential to the concordia curve (Higgins and others, 1977); Seiders, 1978).

Several problems clearly remain unsolved. First, although U-Pb data from Seiders and others (1977) at first suggested that the Occoquan and Dale City plutons both are about 500 m.y. old, comments by Higgins (1976), Higgins and others (1977) and Zartman (1978) suggest that the U-Pb data probably do not yield a meaningful age. Secondly, U-Pb data from the Columbia pluton also do not yield an estimate of age. Thirdly, although Higgins (1976) and Zartman (1978) suggested that the Occoquan intrusion has passed through (or has been derived from) older sialic rocks and incorporated radiogenic lead, the closet basement rocks of distinctly older age are in the Grenville gneiss domes around Baltimore, the Blue Ridge Grenville rocks to the west, and the recently discovered State Farm gneiss dome near Richmond (Poland and others, 1979). All of these areas are at least 70 km distant.

Since the U-Pb technique has not yielded definitive results, we have applied the Rb-Sr whole-rock isochron technique to these Virginia plutons.

Rb-Sr TECHNIQUE OF AGE DETERMINATION

The Rb-Sr method of age determination is based on the radioactive decay of ^{87}Rb to ^{87}Sr by beta-emission. The half-life for the decay is now estimated to be about 4.89 x 10^{10} years, and the decay constant is 1.42 x 10^{-11} $years^{-1}$ (Steiger and Jager, 1977). For this study of Virginia plutons, samples of about 10 kg each were collected, crushed and split to a 10 g portion which was subsequently powdered, and about 0.3 g of each sample was isotopically analyzed. Each analysis was done using ^{84}Sr and ^{87}Rb spikes, ultrapure Hf, $HClO_4$ and HCl. The solutions were brought to dryness in Teflon beakers, dissolved in dilute HCl, and the solutions were passed through cation exchange columns to obtain Rb and Sr fractions.

The Sr analyses were made using a Nier-type, 6-inch radius, single filament mass spectrometer with a programmable automatic data acquisition system at the Department of Terrestrial Magnetism of the Carnegie Institution in Washington, D.C.. The Rb isotopic analyses were made using a 12-inch radius mass spectrometer at Florida State University. All the strontium isotopic compositions were calculated from analyses of sample plus spike mixtures. The $^{85}Rb/^{87}Rb$ ratio was taken to be 2.593 (Steiger and Jager, 1977).

The Rb-Sr age and initial $^{87}Sr/^{86}$ ratio on the isochron diagrams were calculated using the regression treatment described in York (1966). The one-standard-deviation experimental error in $^{87}Rb/^{86}$ was calculated to be 2 percent; the one-standard-deviation experimental error in $^{87}Sr/^{86}Sr$ was calculated to be 0.05 percent. These error estimates were derived from an examination of duplicate analyses done over the past six years, and these estimates include sample splitting errors. The estimate of one standard deviation experimental errors which do not include an error increment related to sample splitting are 1 percent for $^{87}Rb/^{86}Sr$ and 0.02 percent for $^{87}Sr/^{86}Sr$. The isotopic data are listed in Appendix 1. The errors assigned to the reported ages and initial $^{87}Sr/^{86}Sr$ ratio are given at the 68 percent confidence level (1 sigma). Visual examinations of the fit of the Rb-Sr data to isochron lines are provided by Figures 9 to 12; the data on these diagrams are presented as 2 sigma error boxes (4 percent by 0.10 percent).

Four analyses of National Bureau of Standards 70a standard K-feldpsar were performed over the course of this study (Appendix 2). The data are in close agreement with the data for this standard that have been reported by others, indicating that there are no significant systematic errors in the isotope tracer calibrations used in this study. The whole-rock isotopic analyses reported in this study were obtained in 1978 and 1979. Analyses of the Eimer and Amend strontium standard determined during this interval (Appendix 2) are in agreement with the certified value of this standard, indicating that there is no significant systematic eror in the mass spectrometer calibration.

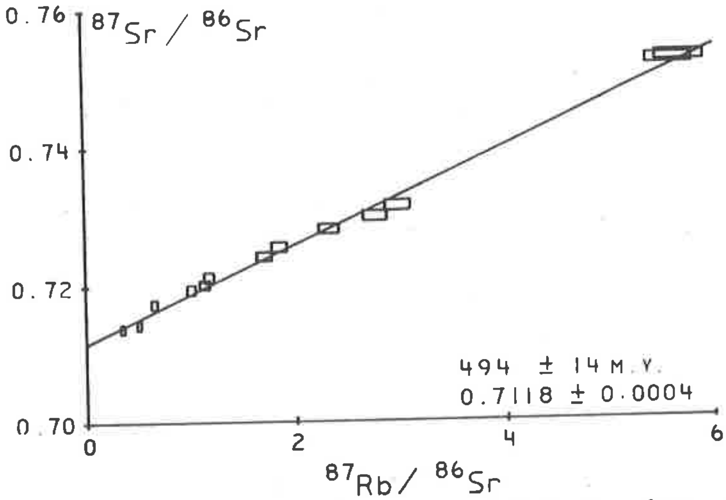

Figure 9. Rb-Sr isochron diagram showing whole-rock data from samples of the Occoquan pluton.

WHOLE-ROCK Rb-Sr AGE DETERMINATION

Whole-rock samples of the Occoquan pluton and Dale City pluton were collected in the Occoquan River area and analyzed for their Rb and Sr isotopic composition, as were two sets of samples from the Columbia pluton along the James River area. The first set of Columbia pluton samples came from the Cowherd quarry east of the town of Columbia, and the second set came from sites west of Columbia. Sample sites are reported in Appendix 3 and modal analyses are shown in Appendix 4. The Rb-Sr isochron age of the Occoquan pluton is 494 + 14 m.y. and the initial $^{87}Sr/^{86}Sr$ ratio in the pluton as 0.7118 + 0.0004 (Figure 9). The Dale City pluton samples did not yield

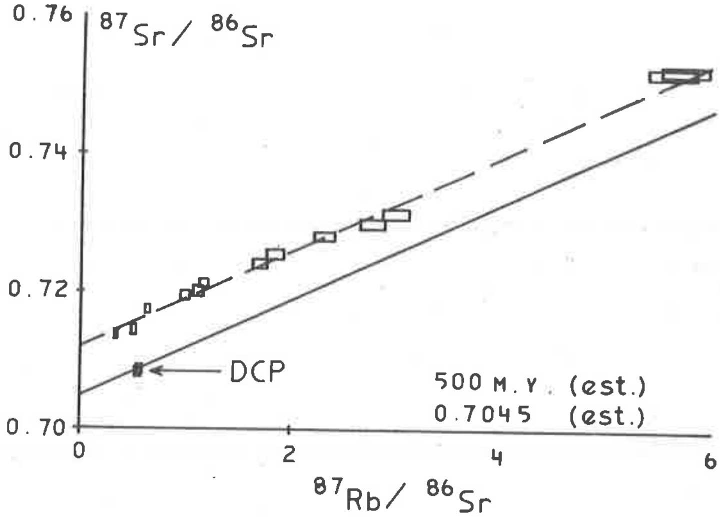

Figure 10. Rb-Sr isochron diagram showing whole-rock data from samples of the Dale City pluton (DCP). A reference isochron (dashed line) generated by samples from the Occoquan pluton is shown for reference.

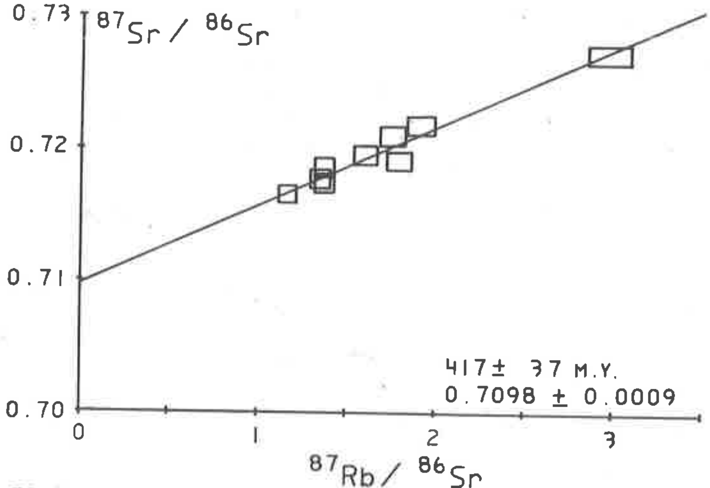

Figure 11. Rb-Sr isochron diagram showing whole-rock data from samples of the Columbia pluton, east of Columbia.

an isochron, but if the pluton is about 500 m.y. old, its initial $^{87}Sr/^{86}Sr$ ratio was about 0.7045 (Figure 10). The Columbia pluton from the Cowherd quarry site east of Columbia yields an age of 417 ± 37 m.y. Figure 11); the Columbia pluton from west of Columbia yields a better defined age of 454 ± 9 m.y. and an initial $^{87}Sr/^{86}Sr$ ratio of 0.7059 ± 0.0003 (Figure 12).

METAMORPHISM OF THE COLUMBIA PLUTON

As discussed earlier, the Columbia pluton intruded between the Charlotte Belt of high-grade metamorphic rocks and the James River belt, an area of low-grade metavolcanic and metasedimentary rocks. The first collection of samples was made on the east side of the town of Columbia, in an area of high-grade metamorphism known as the Cowherd quarry. The rocks from the quarry tend to be finer grained than the rocks in the larger outcrop area to the west, probably because this quarry is located in the axial region of a syncline where the folding could cause more extensive

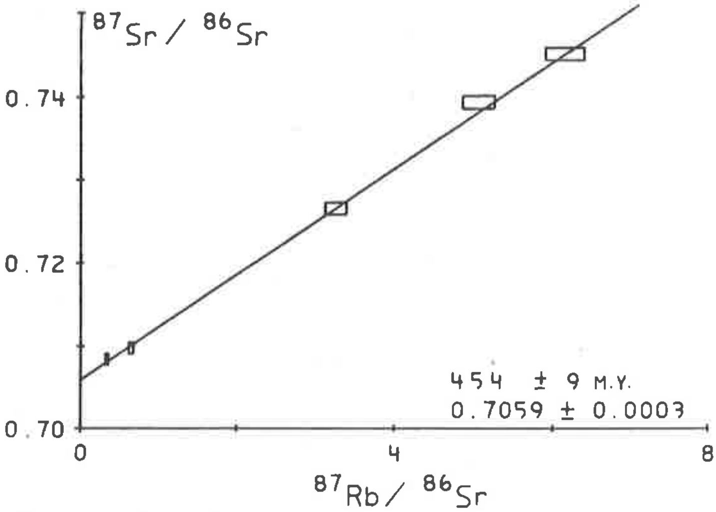

Figure 12. Rb-Sr isochron diagram showing whole-rock data from samples of the Columbia pluton, west of Columbia.

recrystallization. The second sample set from the Columbia pluton came from the northwest end of the pluton, in an area where the pluton and the country rocks were subjected to only low-grade metamorphism (Brown, 1979).

This difference in metamorphic grade could be reflected in the mineral-plus whole-rock isochron ages which were generated from these rocks, but all the isochron ages are the same with analytical error (errors for two-point isochron ages are assumed to be ± 10 percent):

Sample	*Rb-Sr Age*	*Initial $^{87}Sr/^{86}Sr$ Ratio*
East of Columbia		
B-2a	278 ± 28 m.y.	0.7120 (Whole-rock plus muscovite)
West Columbia		
F-1	305 ± 31 m.y.	0.7069 (whole-rock plus biotite)
F-4	304 ± 30 m.y.	0.7175 (whole-rock plus muscovite)
F-4	347 ± 35 m.y.	0.7144 (whole-rock plus biotite)

It is generally thought that if a pluton is metamorphosed at some time after it crystallized, a Rb-Sr whole-rock isochron will yield the time of crystallization, and a whole-rock plus mica isochron will yield a time during regional uplift and cooling after metamorphism. This is because micas such as muscovite and biotite lose radiogenic ^{87}Sr (and radiogenic ^{40}Ar) until the rock in which the mica formed has cooled to about 300°C. The metamorphic rocks around Columbia evidently cooled below about 300°C at about 300 m.y. go, and were not heated above this temperature since that time.

COMPOSITION OF PLUTONIC ROCKS

The plutonic rocks examined in this study are relatively rich in quartz. Many modal analyses (Appendix 4) plot on the quartz side of the Streckheisen (1973) quartz-alkali feldspar-plagioclase feldspar diagram (Figure 13). Higgins (1972) pointed out that most magmatic rocks have less than 50 percent quartz, while most clastic sedimentary rocks have more than 50 percent quartz, and suggested that rocks like the Occoquan pluton and the Columbia pluton may be, at least in part, of sedimentary origin. Seiders and others (1975) and Seiders (1976) point out that there are many metamorphosed plutonic and volcanic rocks which contain more than 50 percent quartz (although

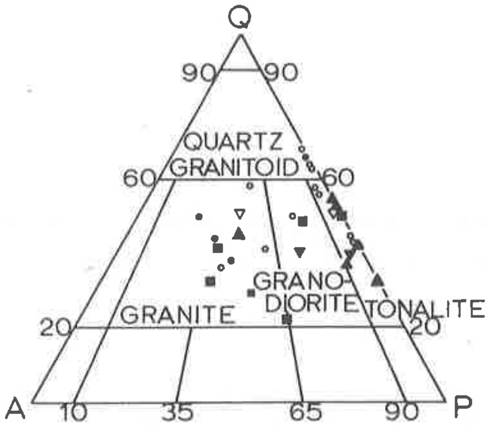

Figure 13. Modal analyses of samples from the Dale City, Occoquan and Columbia plutons. The symbols on the Quartz (Q) - Alkali Feldspar (A)-Plagioclase Feldspar (P) diagram present normalized modal analyses from the following:

- ▼ *Dale City Pluton (Seiders and thers, 1975)*
- ▽ *Dale City Pluton (New data, Appendix 3)*
- ∘ *Occoquan Pluton (Seiders and others, 1975)*
- • *Occoquan Pluton (New data, Apendix 3)*
- ▲ *Columbia Pluton, west side of Columbia (Brown, 1969)*
- ■ *Columbia Pluton, east side of Columbia (Bourland and Glover, 1979)*

unaltered magmatic rocks do tend to have less than 50 percent quartz). In short, the Strekheisen diagram is useful for assigning a name to a rock, but it cannot be used to determine if a relatively quartz-rich rock is of sedimentary or magmatic origin.

However, the Occoquan pluton clearly shows that what appear to be intrusive relationships with its country rock, and it contains what appear to be xenoliths and it shows a texture commonly associated with magmatic rocks (Seiders and others, 1976; Seiders, 1976). The same may be said for the Columbia pluton (Bourland and Glover, 1979; Brown, 1979). It thus may be said that these bodies are probably plutons, but it is not possible to know how they came to be relatively rich in quartz. The high initial $^{87}Sr^{86}Sr$ ratio of the Occoquan pluton suggests that the Occoquan pluton incorporated older country rock from which quartz-rich solutions may have entered the magma. However, the Columbia pluton and the Dale City pluton have low initial $^{87}Sr/^{86}Sr$ and therefore appear to have incorporated less country rock, yet the Columbia pluton is as enriched in quartz as the Occoquan pluton. Further studies may solve this problem.

DISCUSSION AND CONCLUSIONS

Recent studies in the Northern Virginia Piedmont have centered around the Chopawamsic Formation which is composed mainly of volcanic rocks, the Quantico and Arvonia Slate unit which unconformably overlies the Chopawamsic Formation, and the Occoquan, Dale City and Columbia plutons which intruded the Chopawamsic Formation but which were exposed by uplift and erosion prior to being covered by the Quantico-Arvonia Slate.

U-Pb dating of the Occoquan pluton (Seiders and others, 1975) suggested a Cambrian age for this pluton (about 550 m.y.), but Higgins (1976), Higgins and other (1977) and Zartman (1978) suggested that the U-Pb age is probably erroneous due to an incorporation of older zircons into the pluton. The lack of agreement between the U-Pb age and the Rb-Sr age of 494 $\pm$ 14 m.y. reported in this paper is interpreted to be due to inherited lead in zircons. The presence of older rocks which could have provided the radiogenic lead is suggested by the relatively high $(^{87}Sr/^{86}Sr)_0$ ratio of the Occoquan pluton, at 0.7118 $\pm$ 0.0004. Early Paleozoic plutons in the southern Appalachians, in areas generally thought to be devoid of greatly older sialic rocks, generally have $(^{87}Sr/^{86}Sr)_0$ ratios of less than 0.706 (Fullagar, 1971). The high initial ratio in the Occoquan pluton suggests that the magma which formed this pluton incorporated a sizable amount of older country rock, some of which may have contributed xeoncrystic zircons.

The isotopic data from the Dale City pluton are not sufficient to define the age of the pluton. However, the data fall below the isochron for the Occoquan pluton, indicating either that the plutons are not comagmatic or that the Dale City pluton incorporated less country rock. Assuming that the Dale City pluton is about 500 m.y. old, its $(^{87}Sr/^{86}Sr)_0$ ratio would have been about 0.7045.

U-Pb dating of the Columbia pluton did not yield a meaningful age. Rb-Sr analyses yield ages of 417 ± 37 and 454 ± 9 m.y., the later of which is taken to be more significant. Since the overlying Arvonia slate is estimated to be Late Ordovician (440 to 460 m.y.) based on its fossil content, it appears that there was an interval of relatively rapid uplift which exposed the pluton prior to deposition of the Arvonia sediments.

The radiometric work on the plutons along the Occoquan and James Rivers presented in this study have served to place a minimum age of 494 ± 14 m.y. on the regionally significant Chopawamsic Formation and a maximum age of 454 ± 9 m.y. on the Arvonia Slate which can be correlated with the Quantico Slate in northern Virginia. The Rb-Sr data support the fossil age of Late Ordovician for the Arvonia and Quantico slates, and they are compatible with the Cambrian age for the Chopawamsic Formation which was determined by U-Pb data.

The Rb-Sr ages also support the contention of Pavlides (1973, 1976, 1980) that an interval of erosion occurred between the deposition of the Chopawamsic Formation and the subsequent deposition of the Quantico-Arvonia Slate. Assuming that the Dale City pluton and the nearby Occoquan pluton are coeval, the Rb-Sr ages suggest that this erosional interval occupied at least about 20 m.y. in the early part of the Ordovician period.

At the present time, relatively few plutonic rocks in the Appalachians have been studied using both the U-Pb and Rb-Sr techniques. This study of plutons in the Virginia Piedmont suggests that the Rb-Sr technique may be the more reliable technique in some cases, and that more detailed U-Pb studies may show that Appalachian plutonic rocks often contain a mixed population of zircons (part of which are derived from the host rock) that produce U-Pb chords whose interpretation is difficult. The presence of xenocrystic zircons has been proposed in other parts of the Appalachians to explain a significant difference between Rb-Sr ages (Odom and Fullagar, 1971; Eckelmann and Mose, 1981; Mose, 1981; Smith and others, 1981) and U-Pb ages (Rankin and others, 1969; Lukert, 1973; Davis, 1974) for Late Precambrian plutonic rocks. Higgins and others (1977) were clearly correct in suggesting that U-Pb ages from polymetamorphic terranes such as the Appalachians should be used with caution.

REFERENCES CITED

Bourland, W.C., and Glover, L., 1979, The Columbia metagranite, *in* Guides to Field Trips 1-3, Southeastern Meeting, Geol. Soc. of America, Blacksburg, Virginia, p. 14-16.

Brown, W.R., 1969, Geology of the dillwyn quadrangle, Virginia: Virginia Division of Mineral Resources Report of Investigations 10, 77 p.

Brown, W.R., 1970[a], Superposed folding in the Arvonia Slate district, Virginia: Geol. Soc. America Abstracts with Programs, v. 2, p. 198.

Brown, W.R., 1970[b], Investigations of sedimentary record in the Piedmont and Blue Ridge of Virginia, *in* Fisher, G.W., Pettijohn, F.J., Reed, J.C., Jr., and Weaver, K.N., eds., Studies of Appalachian Geology-Central and Southern: New York, Interscience Publishers, p. 335-349.

Brown, W.R., 1979, Field Guide to the Arvonia-Schuyler district, *in* Guides to Field Trips 1-3, Southeastern Section, Geol. Soc. of America Ann. Mtng., Blacksburg, Virginia, p. 24-41.

Butler, J.R., 1972, Age of Paleozoic regional metamorphism in the Carolinas, Georgia, and Tennessee, southern Appalachians: American Journal Sci., v. 272, p. 319-333.

Compston, W., Chappel, B.W., Arriens, P.A., and Vernon, J.J., 1969. On the feasibility of NBS 70aK-feldspar as Rb-Sr age reference sample: Geochimica et Cosmochmica Acta, v. 33, p. 753-757.

Conley, J.F. 1978, Geology of the Piedmont of Virginia-Interpretations and problems, *in* Contributions to Virginia geology III: Virginia Division of Mineral Resources Publication 7, p. 115-149.

Conley, J.R., and Johnson, S.S., 1975, Road log of the geology from Madison to Cumberland counties in the Piedmont, central Virginia: Virginia Minerals, v. 21, no. 4, p. 29-38.

Davis, R.G., 1974, Pre-Grenville ages of basement rocks in central Virginia-A model for interpretation of zircon ages: M.S. thesis, Virginia Polytechnic Institute and State University, 46 p.

DeLaeter, J.R., and Abercrombie, I.D., 1970, Mass spectrometric isotope dilution analyses of rubidium and strontium in standard rocks: Earth and Planetary Science Letters, v. 9, p. 327-330.

Eckelmann, F.D., and Mose, D.G., 1981, Search for xenocrystic zircons in latest Precambrian plutonic rocks in the Blue Ridge: Geol. Soc. America Abstracts with Programs, v. 13, no. 1, p. 7.

Fullagar, P.D., 1971, Age and origin of plutonic intrusions in the Piedmont of the southern Appalachians: Geol. Soc. America bull., v. 82, p. 2845-2862.

Fullagar, P.D., and Butler, J.R., 1976, Petrochemical and geochronologic studies of plutonic rocks in the southern Appalachians, II, the Sparta Complex, Georgia: Geol. Soc. of America Bulletin, v. 87, p. 53-56.

Glover, L. and Read, J.F., 1979, Virginia Piedmont geology along the James River from Richmond to the Blue Ridge: Guides to Field Trips 1-3, Southeastern Section Meeting, Geol. Soc. America Annual Meeting, p. 2-3.

Hatcher, R.D., 1972a, Developmental model for he southern Appalachians: Geol. Soc. America Bull., V. 83, p. 2735-2760.

Hatcher, R.D., 1972b, Recent trends in thought and research on southern Appalachian tectonics: Southeastern Geology, V. 14, p. 131-151.

Hatcher, R.D., 1978, Tectonics of the western Piedmont and Blue Ridge, southern Appalachians: Review and speculation: American Jour. Sci., v. 278, p. 276-304.

Higgins, M.W., 1972, Age, origin, regional relations, and nomenclature of the Glenarm Series, central Appalachian Piedmont: A reinterpetation: Geol. Soc. America Bull., v. 83, p. 989-1026.

Higgins, M.W., 1976, Age, origin, regional relations, and nomenclature of the Glenarm Series, central Appalachian Piedmont: A reinterpretation: Reply: Geol. Soc. America bull., v. 87, p. 1523-1528.

Higgins, M.W., Sinha, A.K., Zartman, R.E., and Kirk, W.S., 1977, U-Pb zircon dates from central Appalachian Piedmont: A possible case of inherited radiogenic lead: Geol. Soc. America Bull., v. 88, p. 124-132.

Long, L.T., 1979, The Carolina slate belt-evidence of a continental rift zone: Geology, v. 7, p. 180-184.

Lukert, M.T., 1973, The petrology and geochronology of the Madison area, Virginia: Ph.D. thesis, Case Western University, 218 p.

Mose, D.G., 1981, Cambrian age for the Catoctin and Chopawamsic Formations in Virginia: Geol. Soc. America Abstracts with Programs, V. 13, no. 1, p. 31.

Odom, A.L., and Fullagar, P.D., 1971, A major discordancy between U-Pb zircon ages and Rb-Srwhole rock ages of Late Precambrian granites in the Blue Ridge Province: Geol. Soc. America Abstracts with Programs, v. 3, no. 7, p. 663.

Odom, A.L., and Fullagar, P.D., 1973, Geochronologic and tectonic relationships between the Inner Piedmont, Brevard Zone and Blue Ridge belts, North Carolina: American Jour. Sci., v. 273-A, p. 133-149.

Pavlides, L., 1973, Stratigraphic relationships and metamorphism in the Fredricksburg area, Virginia, *in* Geological Survey Research 1973: U.S. Geological Survey Prof. Paper 850, p. 37-38.

Pavlides, L., 1974, Age, origin, regional relations, and nomenclature of the Glenarm series, central Appalachian Piedmont, A reinterpretation: Discussion: Geol. Soc. America Bull., v. 85, p. 153-155.
Pavlides, L., 1976, Piedmont geology of the Fredricksburg, Virginia, area and vicinity: Geological Society of American Northeast-Southeast Section Meeting, Guidebook for Field Trip 1 and 4, 44 p.
Pavlides, L., 1980, Revised nomenclature and stratigraphic relationships of the Fredricksburg complex and the Quantico Formation of the Virginia Piedmont: U.S. Geological Survey, Prof. Paper1146, 29 p.
Pavlides, L., Pojeta, J., Gordon, M., Parsley R.L., and Bobyarchick, A.R., 1980, New evidence for the age of the Quantico Formation in Virginia: Geology, v. 8, p. 286-290.
Pavlides, L., Sylvester, K.A., Daniels, D.L., and Bates, R.G., 1974, Correlation between geophysical data and rock types in the Piedmont and Coastal Plain of northeast Virginia and related areas: Jour. Research U.S. Geol. Survey, v. 2, p. 569-580.
Poland, R.B., Glover, L., and Mose, D.G., 1979, The geology of rocks along the James River between Sabot and Cedar Point, Virginia, *in* Guides to Field Trips 1-3, Southeastern Section, Geol. Soc. America Annual Meeting, p. 11-14.
Rankin, D.W., Stern, T.W., Reed, J.C., and Newel, M.F., 1969, Zircon ages of felsic volcanic rocks in the upper Precambrian of the Blue Ridge, Appalachian Mountains: Science, v. 66, p. 741-744.
Seiders, V.M., Mixon, R.B., Stern, T.W., Newell, M.F., and Thomas, C.B., 1975, Age of plutonism and tectonism and a new minimum age limit on the Glenarm series in the northeast Virginia Piedmont near Occoquan: American Journal Science, v. 275, p. 481-511.
Seiders, V.M., 1978, U-Pb zircon dates from the central Appalachian Piedmont: A possible case of inherited radiogenic lead: Discussion: Geol. Soc. America Bull., V. 89, p. 1115-1116.
Seiders, V.M., 1976, Age, origin, regional relations, and nomenclature of the Glenarm series, central Appalachian Piedmont: A reinterpretation: Discussion and Reply: Geol. Soc. American Bull., v. 87, p. 1519-1528.
Smith, S.F., Frye, K., Mose, D.G., and Nagel, M.S., 1981, A latest Precambrian-cambrian granite in the Virginia Blue Ridge: Geol. Soc. America Abstracts with Programs, v. 13, no. 1, p. 35.
Southwick, D.L., Reed, J.C., and Mixon, R.B., 1971, The Chopawamsic Formation-a new stratigraphic unit in the Piedmont of northeastern Virgnia: U.S. Geol. Survey, Bull., v. 1324-D, p. D1-D11.
Streckeisen, A.L., 1973, Plutonic rocks: Classification and nomenclature recommended by the IUGS Subcommission on the systematics of igneous rocks: Geotimes, v. 18, no. 10, p. 26-30.
Steiger, R.H., and Jager, E., 1977, Subcommission on geochronology: convention on the use of decay constants in geo- and cosmochronology: Earth and Planetary Science Letters, v. 36, p. 359-363.
Tillman, C.G., 1970, Metamorphosed trilobites from Arvonia, Virginia: Geol. Soc. American Bull., v. 81, p. 1189-1200.
Van Schumus, W.R., 1971, Rb-Sr age of middle Keweenawan rocks, Mamainse Point and vicinity, Ontario, Canada: Geo. Soc. of America, v. 82, p. 3221-3226.
Watson, T.L., and Powell, S.L., 1911, Fossil evidence of the Age of the Virginia Piedmont slates: American Jour. Sci., 4th ser., v. 31, p. 33-344.
York, D., 1966, Least-squares fitting of a straight line: Canadian Jour. Physics, v. 44, p. 1079-1086.
Zartman, R.E., 1978, U-Pb zircon dates from the central Appalachian Piedmont: A possible case of inherited radiogenic lead: Reply: Geol. Soc. America Bull., v. 89, p. 1116-1117.

Appendix 1. Rb-Sr isotopic analyses of whole-rocks and minerals.

ROCK UNIT	NUMBER	$(^{87}Rb/^{86}Sr)p$	$(^{87}Sr/^{86}Sr)p$	^{86}Sr ppm	^{87}Rb ppm
Occoquan Pluton	S-1	1.709	0.7240	15.80	27.32
	S-2	2.986	0.7314	11.36	34.30
	S-3	1.857	0.7254	14.71	27.64
	S-4	2.324	0.7280	14.07	33.06
	S-5	0.354	0.7138	30.78	11.03
	S-6	1.180	0.7211	9.23	11.02
	S-9	2.764	0.7298	13.01	36.36
	S-10	1.137	0.7200	16.48	18.96
	S-12	5.581	0.7520	7.55	42.60
	S-13	0.656	0.7174	21.64	14.36
	S-14	5.686	0.7524	8.00	46.04
	S-15	1.008	0.7193	19.65	20.040
	S-16	0.514	0.7143	20.98	10.91
Dale City Pluton	S-20	0.557	0.7084	46.15	26.02
	S-21	0.575	0.7087	44.76	26.02
Columbia Pluton	F-1	0.664	0.7098	45.15	30.32
West of Columbia	F-2	0.356	0.7085	60.16	21.68
	F-3	6.133	0.7450	6.29	39.02
	F-4	5.041	0.7393	7.56	38.53
	F-5	3.235	0.7265	16.63	54.41
Columbia Pluton	B-1a	1.371	0.7174	8.25	11.44
East of Columbia	B-1b	1.348	0.7177	9.18	12.52
	B-2a	1.163	0.7166	14.31	16.84
	B-2b	1.604	0.7195	9.70	15.73
	B-44	1.792	0.7191	10.74	19.47
	B-5	1.371	0.7186	10.92	15.14
	SB-1	2.974	0.7272	7.46	22.43
	SB-2	1.755	0.7210	8.35	14.82
	SB-3	1.913	0.7218	6.57	12.71
B-2a muscovite		7.723	0.7425	5.70	44.51
F-1 biotite		27.526	0.8264	5.12	142.65
F-4 muscovite		47.742	0.9237	2.52	121.47
F-4 biotite		161.178	1.5107	1.56	253.95

Appendix 2a. Analyses of the National Bureau of Standards 70a Standard K-feldspar (interlaboratory concentration standard)

^{87}Rb (ppm)	^{86}Sr (ppm)	$^{87}Rb/^{86}Sr$	Analysis
149.5	5.983	24.70	1
150.7	6.059	24.59	2
149.7	6.026	24.56	3
149.5	5.992	24.67	4
150	6.01	24.7	Compston and others (1969)
148	6.13	23.9	DeLaeter and Abercrombie (1970)
150	6.03	24.5	Van Schmus (1971)
149	5.95	24.8	Fullagar and Butler (1976)

Appendix 2b. Analyses of Eimer and Amend standard strontium (interlaboratory isotopic standard).

Year	Number of Analyses	Average	Standard Deviation
1976	8	0.70790	0.00005
1977	15	0.70790	0.00004
1978	6	0.70793	0.00004
1979	8	0.70789	0.00006
1980	20	0.70796	0.00009

Appendix 3. Sample sites of granite collected for Rb-Sr isotopic analysis.

ROCK UNIT	NUMBER	7 1/2' QUADRANGLE	COORDINATES ON THE 1000 METER UNIVERSAL TRAVERSE MERCATOR GRID, ZONE 18
Occoquan pluton	S-1	Occoquan	42 84 190 N, 302 980 E
	S-2	Occoquan	42 84 240 N, 302 890 E
	S-3	Occoquan	42 88 130 N, 299-970 E
	S-4	Occoquan	42 83 660 N, 300 995 E
	S-5	Independent Hill	42 90 250 N, 292 700 E
	S-6	Occoquan	42 88 270 N, 296 570 E
	S-9	Occoquan	42 87 880 N, 297 370 E
	S-10	Occoquan	42 86 950 N, 298 320 E
	S-12	Occoquan	42 84 680 N, 303 590 E
	S-13	Occoquan	42 84 310 N, 303 260 E (rock quarry)
	S-14	Occoquan	same
	S-15	Occoquan	same
	S-16	Occoquan	same
Dale City pluton			
	S-20	Occoquan	42 77 930 N, 299 080 E
	S-21	Occoquan	42 78 150 N, 298 950 E
Columbia pluton West of Columbia			
	F-1	Columbia	41 85 300 N, 747 000 E
	F-2	Columbia	same
	F-3	Lakeside Village	41 77 900 N, 744 200 E
	F-4	Lakeside Village	same
	F-5	Lakeside Village	41 79 000 N, 745 250 E
Columbia pluton East of Columbia			
	B-1a	Lakeside Village	41 81 700 N, 750 500 E
	B-1b	Lakeside Village	same
	B-2a	Lakeside Village	41 81 700 N, 750 600 E
	B-2b	Lakeside Village	same
	B-44	Lakeside Village	41 81 700 N, 750 700 E
	B-5	Lakeside Village	41 81 700 N, 750 800 E
	SB-1	Lakeside Village	41 81 700 N, 750 750 E
	SB-2	Lakeside Village	41 81 700 N, 750 700 E
	Sb-3	Lakeside Village	41 81 700 N, 750 650 E

Appendix 4. Modal analyses of the whole-rocks used in the Rb-Sr study.

ROCK UNIT	SAMPLE NUMBER	PERCENTAGE QUARTZ	PERCENTAGE ALKALI FELDSPAR	PERCENTAGE PLAGIOCLASE FELDSPAR	PERCENTAGE MICA	REFERENCE
Dale City pluton	5	12	1	20	25	Seiders and others (1975)
	6	17	7	19	20	
Dale City pluton	S-20	41	0	38	16	(new data)
	S-21	31	12	13	22	
Occoquan pluton	1	45	3	21	19	Seiders and others (1975)
	2	29	25	22	18	
	3	39	30	19	9	
	4	42	24	17	16	
Occoquan pluton	S-1	31	0	38	31	(new data)
	S-2	42	13	30	14	
	S-3	28	3	18	33	
	S-4	42	2	31	13	
	S-5	20	21	15	20	
	S-6	40	0	47	12	
	S-9	45	0	24	28	
	S-10	52	0	24	21	
	S-12	33	25	27	12	
	S-13	50	0	23	26	
	S-14	52	0	32	16	
	S-15	44	0	25	28	
	S-16	33	11	15	26	
Columbia pluton in its western area	1	40	0	45	8	Brown (1969)
	2	49	0	43	4	
	4	35	23	21	33	
	5	42	0	57	0	
	7	33	5	51	10	
	9	28	0	60	0	
Columbia pluton in its eastern area	5-14	36	8	29	22	Bourland and Glover (1976)
	5-14	40	0	40	12	
	5-23	25	18	42	15	
	5-44	19	25	44	11	
	5-213	30	39	26	5	
	5-253	18	29	36	16	
	6-37c	36	1	49	1	

URANIUM AND THORIUM VARIATIONS IN PLUTONIC ROCKS OF THE GEORGIA PIEDMONT

Paul A. Mueller, Michael, P. Davis*, and Frank N. Blanchard
Department of Geology
University of Florida
Gainesville, Florida 32611

ABSTRACT

Samples from four major Paleozoic intrusive complexes (Danburg, Sparta, Elberton and Siloam) of the outer Piedmont and several smaller bodies of the inner Piedmont, including the Stone Mountain granite, were analyzed chemically and petrographically. The results, in conjunction with available U and Th abundance data, seem to show a poorly defined but rather unusual trend of decreasing Th/U ratios with increasing differentiation. This variation is apparently the result of higher U contents and relatively constant Th contents in the more felsic rocks. This condition may result from varying degress of hydrous melting that would favor high U and low Th contents in the more silicic early melts or from the higher bonding energy of Th^{+4}-O vs. U^{+4}-O.

INTRODUCTION

Uranium and thorium contents, together with Th/U ratios, in igneous intrusions are important in helping to delineate the magmatic processes involved in the evolution of the magmas. Th/U ratios have been used to indicate the extent of oxidative processes during magmatic differentiation (Whitfield, Rogers, and Adams, 1959). These ratios may then be used to indicate whether crystal fractionation or partial melting was the dominant process in controlling the U and Th distribution because direct mantle derivatives tend to have lower Th/U ratios than their differentiated products (Rogers *et al.*, 1978). In addition, the growing world reliance on nuclear power has led to increased interest in the distribution of U in all rocks, particularly granites.

In this study we report major element, Rb, Sr, U and Th values for samples from four major intrusive complexes of the Georgia Piedmont: the Sparta, Danburg, Elberton, and Siloam granitic complexes (Fig. 1). In addition, values for several samples from smaller granitic intrusives of the Inner Piedmont of Georgia and South Carolina, including the Stone Mountain Granite, are included (Fig. 1). The samples were originally described by Garvey (1975) and were part of a regional study of heat flow and U and Th abundances of the southern Appalachians (Smith, *et al.*, 1980). This particular investigation was initiated in the hope of explaining a rather unusual negative correlation of Th/U and K (Whitfield, Rogers and Adams, 1959) in the data of Garvey (1975).

GENERAL GEOLOGY

The intrusive rocks of the southeastern Piedmont were classified by Butler and Ragland (1969) into three main groups according to their age relative to the last major episode of metamorphism. Pre-, syn-, and post-metamorphic groups of intrusions are recognized. The post-metamorphic intrusions (younger than 350-380 myb.p.) are generally granitic in composition and are most abundant in the Charlotte Belt and less common in the remaining belts of the outer Piedmont and in the inner Piedmont. These intrusions, some of which are of batholitic dimensions, consist of rocks in which biotite typically is the main accessory mineral and in which hornblende is important only locally. Sphene is ubiquitous, as are muscovite and epidote minerals (Butler and Ragland, 1969).

Fullagar (1971) and Fullagar and Butler (1976) recognized the post-metamorphic

*Present address: U.S. Bureau of Mines
Pittsburg, Pennsylvania

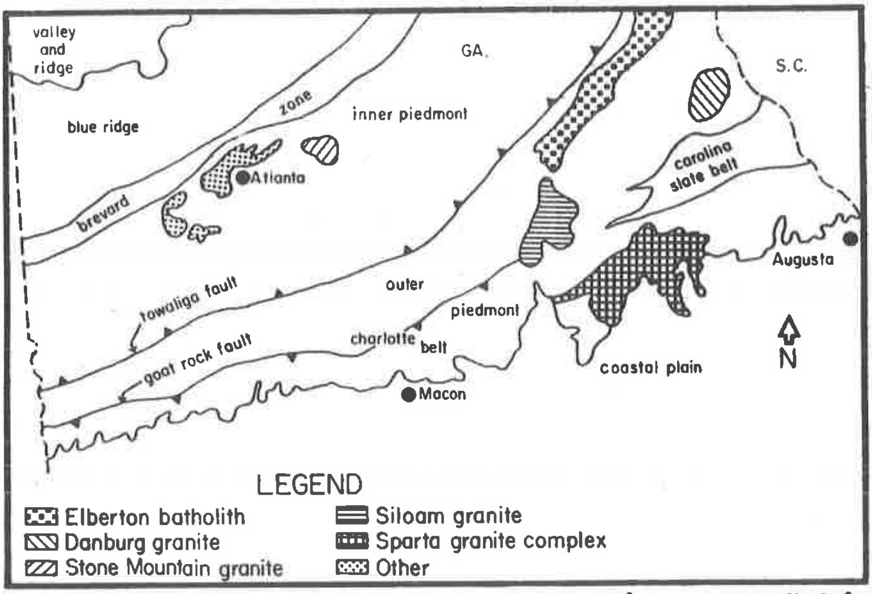

Figure 1: Location map showing general outcrop areas of plutons studied for this

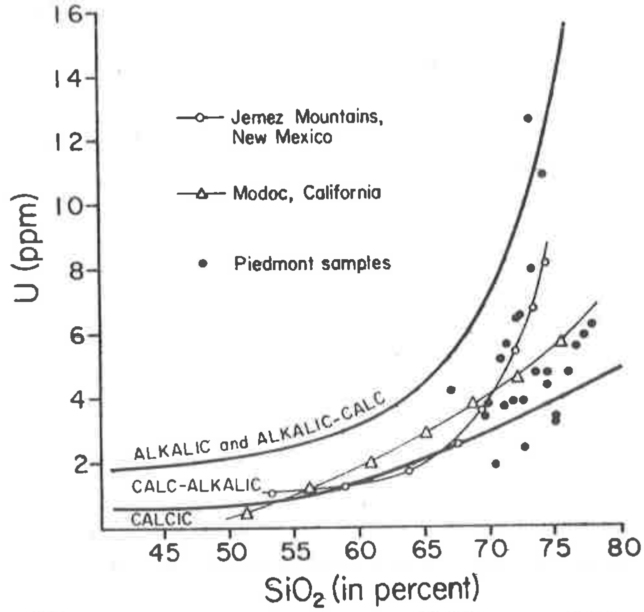

Figure 2: U vs. SiO_2 for samples analyzed in this study with general trends from the Jemez Mountains and Modoc series for reference (after Tilling and Gottfried, 1969).

intrusions of Butler and Ragland (1969) as a "300 my plutonic belt" in South Carolina and Georgia and indicated that several igneous plutons (Fig. 2) located in the outer Piedmont of Georgia can be considered as the southwestern extension of the belt of post-metamorphic intrusives recognized by Butler and Ragland (1969). All of the major plutons discussed in this report are considered part of this suite of post-metamorphic plutons (Butler and Ragland, 1969; Jones and Walker, 1973; Fullagar and Butler, 1976; and Whitney, *et al.*, 1976). Although these rocks all appear to have been generated at about the same time, it is not our intention to suggest that they are comagmatic. Their age, Sr isotopic compositions, and structural/tectonic position, however, do seem to indicate a probable common source.

Table 1: Average elemental abundances for major rock groups and average or representative modal compositions. "Other" represents a variety of rocks from the Piedmont of west central Georgia and South Carolina.

SiO_2	73.10	72.40	73.10	73.00	74.60	71.40
TiO_2	0.29	0.45	0.24	0.26	0.12	0.48
Al_2O_3*	13.70	13.40	13.50	13.90	14.20	14.20
Fe_2O_3*	1.90	2.70	2.80	1.70	1.00	2.90
MgO	0.35	0.69	0.60	0.36	0.17	0.80
CaO	1.20	1.50	1.60	1.10	0.80	2.00
Na_2O	3.80	3.40	3.70	3.80	3.70	3.70
K_2O	5.10	4.80	3.90	5.00	4.80	4.12
Σ	98.24	99.34	99.44	99.13	99.39	99.60
Rb (ppm)	207	185	145	232	258	100
Sr (ppm)	162	295	230	252	126	344
U (ppm)	6.8	6.8	3.6	4.5	7.4	4.0
Th (ppm)	51.6	38.4	16.4	34.6	6.4	28.8
Th/U	7.6	5.6	4.6	7.7	0.9	6.2
Larsen Index	31.8	24.2	23.6	26.3	27.8	22.5
			MODAL PERCENTAGE			
Quartz	31	30	25	24	30	28
Plagioclase (An)	31(12)	32(25)	40(14)	29(11)	30(10)	38(10)
K-spar	29	32	25	39	29	24
Biotite	5	5	8.7	4.2	1	7
Muscovite	1.5	0.2	0.1	0.2	10	1
Chlorite	tr	0.6	0.1	tr	tr	-
Epidote	tr	tr	tr	-	tr	0.2
Allanite	tr	-	-	-	-	-
Sphene	tr	-	0.1	0.7	-	0.4
Zircon	tr	tr	0.1	-	tr	0.1
Opaques	0.1	0.4	0.5	1.0	-	0.5
Hornblende	-	-	-	-	-	-
Apatite	tr	-	tr	tr	tr	tr

ANALYTICAL METHODS

Whole rock samples taken from quarries or other exposures of fresh rock were crushed, and representative splits were taken for analyses. Major elements were determined by X-ray Fluorescence (Si, Al, Ti, Fe, Ca, and K), atomic absorption spectrometry (Na, Mg, Rb, and Sr), or both (Si, Fe, Ca and K). Comparison of duplicate analyses suggests all major elements are accurate to within 3%; those determined by both A. A. and XRF may be slightly better. The U and Th values are from Garvey (1975), and were obtained by γ-ray spectrometry on coarsely crushed whole rock samples. Modal analyses were made from point counts of thin sections (700-1000 counts per section).

RESULTS

The samples analyzed in this study show a relatively high degree of differentiation. The silica content varies from 67 to 78 percent, and all intrusives studied are peraluminous (weight % $Al_2O_3 > CaO + Na_2O + K_2O$). Average elemental abundances are given in Table 1.

Modal compositions derived from petrographic analyses were recalculated to quartz + alkali feldspar + plagioclase = 100 percent and are displayed on the Q-A-P diagram (Fig. 2). Most of the samples lie within the granite region which contains the granite, granodiorite and quartz monzonite divisions of several other classifications. Four samples are classified as granodiorite and there are one each of alkali-feldspar granite and quartz monzonite. The textures of the rocks vary from fine to coarse grained, and from equigranular to porphyritic. Most of the rocks appear to be predominantly hypidiomorphic-granular, but several show allotriomorphic-granular tex-

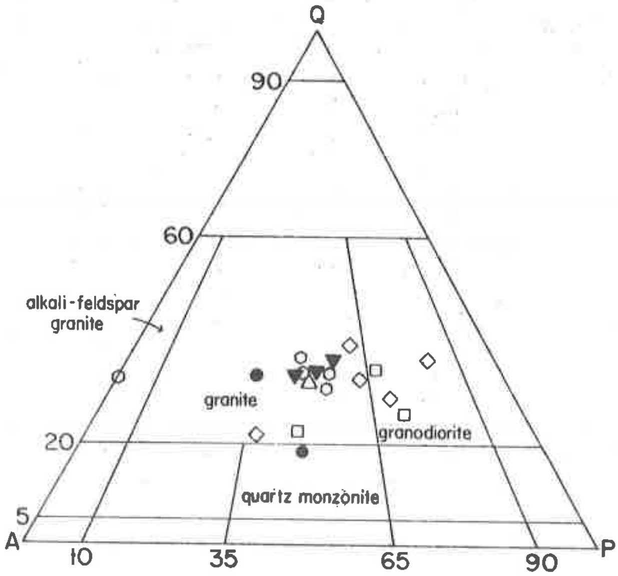

Figure 3: Modal classification diagram with fields according to I.U.G.S. recommendation (Streckeisen, 1973). Symbols represent sample groups, Elberton (○), Siloam (△), Sparta (□), Danburg (●), Stone Mountain (▼) and other (◇).

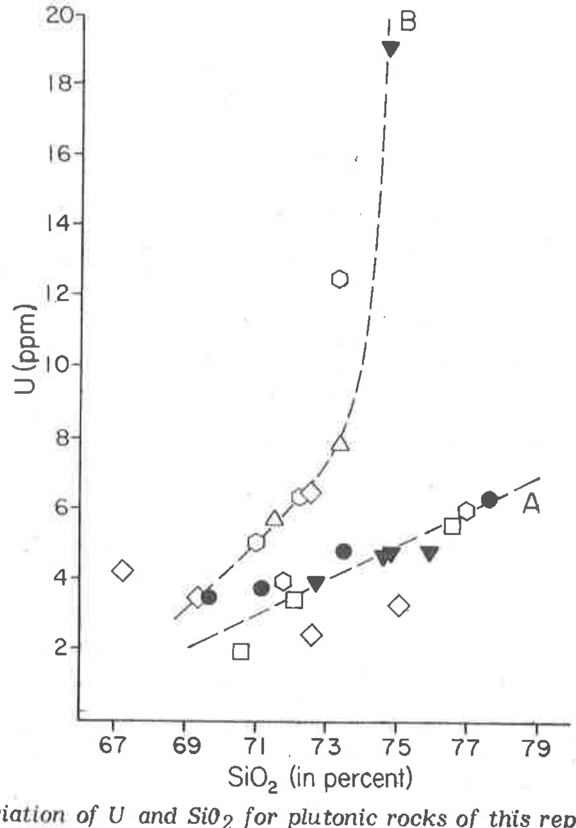

Figure 4: Covariation of U and SiO_2 for plutonic rocks of this report. Lines for trends A and B are for reference only, symbols same as Figure 3.

ture. Average modal compositions are given in Table 1.

In an effort to best understand the variation in U and Th abundances, comparisons of the modal and chemical data with U and Th abundances were made. Co-variations between U, Th and Th/U ratios for all common modal and chemcial differentiation indicators, as well as accessory mineral content, were examined. Despite the variety of relationships plotted, the common SiO_2 vs U, Th and Th/U (e.g. Tilling and Gottfried, 1969) proved to be the most useful.

The rocks studied generally show a U-SiO_2 variation pattern typical of calc-alkaline suites of rocks (Figs. 2 and 4). Curves for two reference calc-alkaline suites, the Modoc suite of California and the Jemez Mountain suite of New Mexico, show a progressive increase of U with increasing silica content which is typical of calc-alkaline rocks. Points representing igneous samples from the Piedmont tend to form two trends, each approximating the slope of a reference-suite curve.

Two separate subtrends seem evident in Fig. 4 (A and B). Trend A contains points representing the Danburg granite, the Sparta granite, and the Stone Mountain granite. An approximately regular increase of U with silica content is apparent for the samples representing these three intrusive units. A least-squares line constructed through the points representing four samples of the Danburg granite, for example, has a slope of 0.370 and a correlation coefficient of 0.997, while four samples from the Stone Mountain granite yield a line with a slope of 0.347 and a correlation coefficient of 0.974. Samples from three unnamed plutons from west-central Georgia also are included on the lower trend.

The upper trend represents samples from several different areas, one from Stone Mountain, two from the Siloam granite, three from the Elberton batholith and one from an unnamed intrusive in South Carolina. These samples yield a best-fit line with a slope of 0.531 and a correlation coefficient of 0.934.

The origin of the two trends is not readily apparent. They are not as obvious on other diagrams, e.g., U vs. CaO, K_2O or Rb. This suggests that the trends do not relate directly to differentiation. Rather, they are more likely the result of redistribution during the latter stages of emplacement. The fact that samples from several plutons plotted on both the A and B trends is strong evidence in support of a late stage mobilization that probably involved deuteric fluids or, more generally, hydrothermal fluids.

The relationship of SiO_2 to Th abundances shown in Fig. 5 is vaguely reminiscent of the U vs. SiO_2 plot. The two groups (C and D) are broadly coincident, in terms of samples, with groups A and B. The relative lack of definition in the Th vs. SiO_2 relative to the U vs. SiO_2 plot can be taken to support the concept of a late stage magmatic process being responsible for the U vs. SiO_2 relation. In this case, the more regular nature of the U vs. SiO_2 relation would reflect the greater mobility of hexavalent U relative to Th. Late stage, water rich, oxidizing fluids could preferentially relocate U and SiO_2 relative to Th and allow more pronounced and regular U vs. SiO_2 relations to be generated. Tetravalent Th would, then, be immobile relative to both Si and U.

The variation of Th/U vs. SiO_2 is shown in Fig. 6. Although scattered, the data seem to suggest a decrease in Th/U with increasing SiO_2. In gross terms, this relation is a function of the relatively constant but scattered Th, and the more coherent increase of U with SiO_2. In detail, most individual plutons show a decrease in Th/U ratio with increasing SiO_2 content (Danburg, Stone Mountain, Sparta, and Elberton), while a combination of samples from the Siloam granite and the South Carolina Piedmont show an increase. Although not unequivocal, it appears that a general decrease of Th/U with increasing SiO_2 is characteristic of this suite of post-metamorphic plutonic rocks.

DISCUSSION

This study has revealed an apparent trend of decreasing Th/U ratios with increasing degrees of petrogenetic evolution as marked by such parameters as SiO_2 content. This relationship appears to be distinctly atypical in the light of several previous studies (Whitfield, et al., 1959; Larsen and Gottfried, 1960; Rogers and

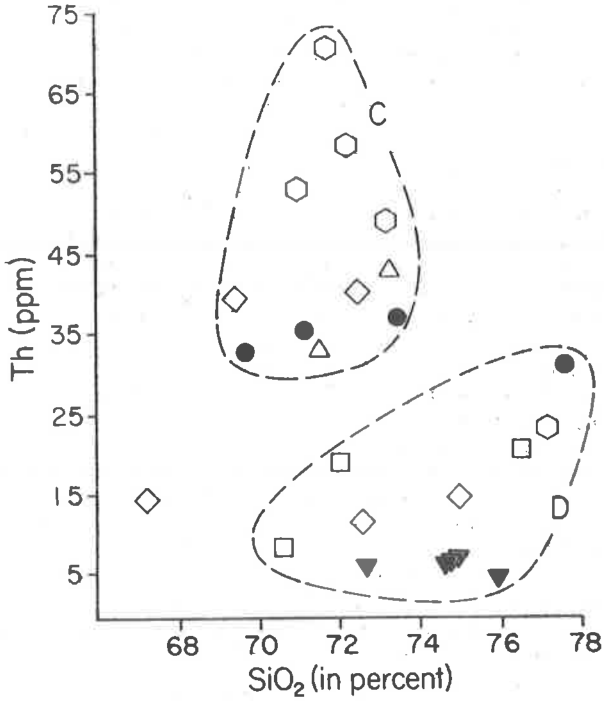

Figure 5: Covariation of Th and SiO_2 for plutonic rocks of this report, symbols same as Figure 3.

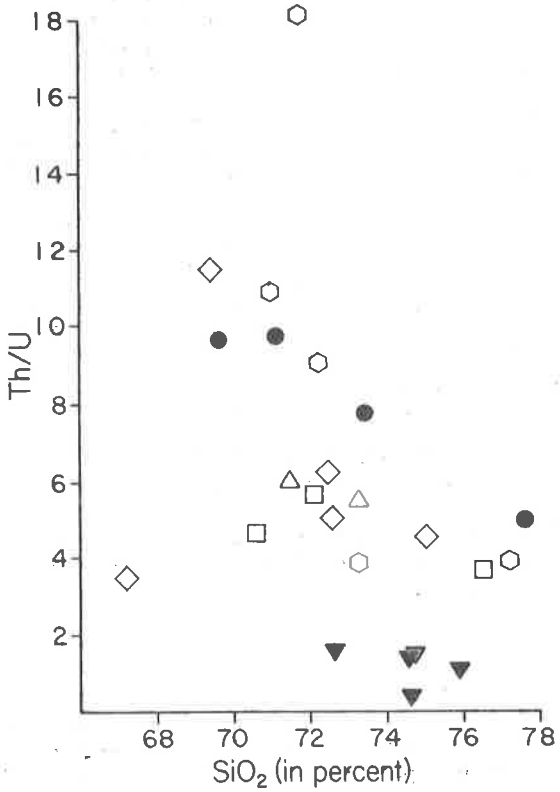

Figure 6: Th/U vs. SiO_2 for plutonic rocks of this report, symbols same as Figure 3.

Ragland, 1961; and Lyons, 1964). These authors all reported either an increasing Th/U ratio or a Th/U ratio which remained relatively constant with increasing degrees of differentiation.

In an attempt to understand the significance of this rather atypical behavior in which U displays a greater and more regular increase than Th with increasing differentiation, the possibility that chemical weathering has affected the distribution of U and Th should not be overlooked, particularly in Piedmont rocks. Although most samples were taken from quarries and roadcuts and appear fresh in hand specimen, petrographic study has revealed varying degrees of weathering in almost all of the samples. It is generally accepted that Th is less mobile than U in most weathering environments (e.g., Gableman, 1977); consequently, the relatively strong correlation between U and various differentiation indices and the decreasing Th/U ratio tend to discount any major redistribution of U and Th resulting from weathering. It would appear, then, that an explanation should be sought which involves the origin and history of these magmas.

Two major differentiation mechanisms capable of producing granitic rocks of this type are crystal fractionation and partial melting. Crystal fractionation would tend to favor the enrichment of both U and Th in the liquid throughout most of the crystallization sequence. This enrichment would result from the exclusion of these elements in the crystal structure of most common igneous minerals. The increased concentration of U and Th in the magma during the last stages of differentiation allows these elements to be scavenged by the accessory minerals, held along grain boundaries, or redistributed by late stage fluids in the more differentiated rocks. There is no evidence that any minerals capable of fractionating U from Th (e.g. monazite) were present throughout the differentiation history of these plutons. Although other associated processes, such as the repeated oxidation of U from +4 to +6 and the subsequent loss of the +6 U to the fluid phase during differentiation (Whitfield, *et al.*, 1959), may alter the Th/U ratio, they tend to produce an increase in Th/U ratios with differentiation. This argument, in conjunction with the observation that many individual plutons are represented on both trends, would appear to suggest that crystal fractionation is not a satisfactory explanation of the relative variations in the U and Th abundances of these Piedmont rocks. In addition, the relative overall differences in rock composition and texture do not suggest a common crystal fractionation history for the plutons.

A preferable explanation of the unusual behavior of Th relative to U probably lies with processes operating in the source regions of the magmas. Green and Ringwood (1968) concluded that partial melting of mafic or ultramafic rocks with eclogitic or amphibolitic mineralogy may give rise to calc-alkaline suites of rocks which, when formed under wet-melting conditions, would produce compositions as silicic as granodiorite or adamellite. If the magmas under discussion were generated by wet melting of a mafic or ultramafic source, it is enticing to consider that higher oxygen fugacities in the earlier stages of melting could lead to a preferential migration of U, as U^{+6}, into the liquid. As melting proceeded, then, oxygen fugacities would be reduced as a result of the consumption of oxygen by oxidative processes and the U would not be oxidized and separated from the Th so readily. This would result in a pattern of decreasing Th/U ratios in more SiO_2 rich rocks. Unfortunately, no experimental data are available to quantitatively justify this model. Such data are essential if the relative effects of oxidation and reduction by dissociated H are to be realisticially evaluated.

Alternatively, quantitative data do exist with regard to the relative bond energy of Th-O vs. U-O bonds. Rogers *et. al.*, (1978) present calculations which suggest that the bonding energy of U^{+4} and oxygen is 320 K cal/mole and 394 K cal/mole for Th^{+4} and oxygen; a difference of almost 25% of the U^{+4}-O bond energy. If, in fact, the relative release of U and Th during partial melting is controlled by Th and U to oxygen bond strengths, then a ready explanation of low Th/U ratios in the more silicic, early formed melts is available. Such a model would call upon depletion of the U during the early stages of melting to produce the observed variation in the Th/U ratios. If the depletion were severe enough, then later melts might show higher Th/U ratios resulting from a lack of available U. This model must also be taken with caution because our understanding of the behavior of incompatible trace elements during partial melting is still quite incomplete.

Although both models seem plausible, neither can be substantiated with experimental evidence. It would seem certain, though, that partial melting, rather than crystal fractionation processes, is responsible for the Th/U variations. None of the major rock forming minerals contain sufficient U or Th to effectively alter their ratio by fractionation, and no correlations betwen Th or U and any of the accessory minerals were detected. This would seem to indicate that one, or perhaps both, of the aforementioned processes was responsible for the rather unique Th-U relationship observed in these plutons.

CONCLUSION

A limited study of samples of late Paleozoic granitic rocks from the Piedmont of Georgia and South Carolina suggests that more differentiated rocks have higher U, similar Th and lower Th/U values than less differentiated ones, regardless of the index of differentiation. This relation is best seen when Th/U is compared to SiO_2. This variation is atypical and most likely is related to the conditions of partial melting which generated the parent magmas. Either a hydrous melting model involving oxidation and preferential partitioning of U into the liquid or a melting model relying solely on the lower U-O bond energy relative to Th, or some combination of these models, seems necessary to account for the unusual behavior of the Th/U ratios observed in these plutons.

ACKNOWLEDGMENTS

The authors would like to thank D.L. Smith for his partial support of this project under U.S.G.S. grant no. 14-08-001-G-199. In addition, the helpful reviews of D.L. Smith, P.C. Ragland, J.J.W. Rogers and V. Price are appreciated.

REFERENCES CITED

Butler, J.R., and Ragland, P.C. 1969, A petrochemical survey of plutonic intrusions in the Piedmont, southeastern Appalachians, U.S.A.: Contr. Mineralogy and Petrology, v. 24, pp. 164-190.

Fullagar, P.D., 1971, Age and origin of plutonic intrusions in the Piedmont of the southeastern Appalachians: Geol. Soc. America Bull., v, 82, pp. 2845-2862.

Fullagar, P.D., and Butler, J.R., 1976, Petrochemical and geochronologic studies of plutonic rocks in the southern Appalachians: II, The Sparta granite complex, Georgia: Geol. Soc. America Bull., v. 87, pp. 53-56.

Gabelman, J.W., 1977, Migration of Uranium and Thorium--Exploration significance: A.A.P.G.Studies of Geology No. 3, p. 54.

Garvey, M.J., 1975, Uranium, Thorium, and Potassium abundances in rocks of the Piedmont of Georgia: Unpublished master's thesis, University of Florida, 94 p.

Green, T.H., and Ringwood, A.E., 1968, Genesis of the calc-alkaline igneous rock suite: Contr. Mineralogy and Petrology, v. 18, pp. 105-162.

Jones, L.M., and Walker, R.L., 1973, Rb-Sr whole-rock age of the Siloam granite, Georgia: A Permian intrusive in the southern Appalachians: Geol. Soc. America Bull., v. 84, pp. 3653-3658.

Larsen, E.S., and Gottfried, D., 1960, Uranium and thorium in selected suites of igneous rocks: American Jour. Sci., v. 258-A, pp. 151-169.

Lyons, J.B., 1964, Distribution of thorium and uranium in three Paleozoic plutonic series of New Hampshire: U.S.G.S. Bull. 1147-F, pp. 1-41.

Rogers, J.J.W., and Ragland, P.C., 1961, Variation of thorium and uranium in selected granitic rocks: Geochim. et Cosmochim. Acta, v. 25, pp. 99-109.

Rogers, J.J.W., Ragland, P.C., Nishimori, R.K., Greenberg, J.K. and Haucks, S.A., 1978, Varieties of granitic uranium deposits and favorable exploration areas in the Eastern United States: Econ. Geol. v. 73, pp. 1539-1555.

Smith, D.L., Gregory, R.G., and Emhof, J.W., Geothermal Measurements in the Southern Appalachian Mountains and Southeastern Coastal Plains: Amer. Jour. Sci., in press, 1980.

Strekeisen, A.L., 1973, Plutonic rocks-Classification in nonmenclature recommended by the I.U.G.S. Subcommission on the Systematics of Igneous Rocks: Geotimes, v. 18, no. 10, pp. 26-30.

Tilling, R.I., and Gottfried, D., 1969, Distribution of thorium, uranium, and potassium in igneous rocks of the Boulder batholith region, Montana: U.S.G.S. Prof. Paper 614-E, 29 p.

Whitfield, J.M., Rogers, J.J.W., and Adams, J.A.S., 1959, The relationship between the petrology and the thorium and uranium contents of some granitic rocks: Geochim, et Chosmochim, acta, v. 17, pp. 248-271.

Whitney, J.A., Jones, L.M., nd Walker, R.L., 1976, The age and origin of the Stone Mountain granite, Lithonia district, Geogia: Geol. Soc. Amer. Bull., v. 87, pp. 1067-1077.

THE "DEPOSIT NO. 9" DUNITE, MACON COUNTY, NORTH CAROLINA

BY

J.R. Dribus**, R.A. Heimlich and D.F. Palmer
Department of Geology
Kent State University
Kent, Ohio 44242

ABSTRACT

The dunite occurs as a semi-elliptical, composite body with plan dimensions of 350 by 520 meters. Its long axis is oriented east-west at an angle to the east-northeast striking foliation in the country rock which is primarily quartz-oligoclase-biotite-almandine gneiss (middle amphibolite facies).

Primary dunite mineralogy consists of magnesian olivine (Fo 91), chromite, and pyrrhotite. Two distinct alteration suites are present. Scattered in occurence throughout the dunite, the first consists of talc, kammererite, clinochlore, tremolite, and chrysotile. The other suite consists of antigorite, anthophyllite, penninite, talc, vermiculite, hematite, and chalcedony confined to an alteration envelope which encloses and divides the ultramafic massinto two separate bodies.

Deformational features, characterized by flaser olivine, elongate strained prophyroclasts, undulatory extinction, and elongate grains of chromite are common in the dunite and most pronounced at the margins of the body. Toward the interior, textures are dominated by equant polygonal olivine grains displaying triple-point junctions typical of recrystallized materials.

Olivine shows a strong preferred orientation in the three samples of the dunite analyzed. None of the preferred orientations show a consistent relationship to the plan shape of the body nor to the attitude of the foliation in the country rock.

The composite body consists of two juxtaposed masses of dunite derived from the upper mantle. The dunite underwent syntectonic recrystallization in the mantle source region and was later deformed by shear during tectonic emplacement into saturated eugeosynclinal sediments. In addition it was subjected to two intervals of hydrous alteration: an earlier (dominantly) progressive carbonation event and a later episode which resulted in new generations of chlorite and talc, as well as formation of vermiculite and anthophyllite.

INTRODUCTION

Considerdable controversy exists regarding the origin of ultramafic bodies associated with folded orogenic belts. Major aspects of this controversy focus on mode of emplacement, physical state of the material during emplacement, and timing of serpentinization typically associated with such rocks. Recent research on alphine ultramafic masses in the northern Appalachian Mountains of Newfoundland suggests two distinct emplacement mechanisms have operated in this area: lateral obduction of ophiolite and vertical emplacement of mantle-derived fragments above a subduction zone (Church and Stevens, 1971; Williams, 1971; Dewey and Baird, 1971; Stevens, Strong and Kean, 1974; Malpas and Strong, 1975). Both modes of emplacement involve the introduction of ultramafic rocks into orogenic terrains as cold, solid, allochthonous masses.

Investigations of the ultramafic belt in the southern Appalachians, especially in western North Carolina, have been limited in scope and until quite recently have not

*Contribution No. 201, Department of Geology, Kent State University, Kent, Ohio
**Present address: Bendix Field Engineering Corporation, Casper Regional Office P.O. Box 1937, Casper, Wyoming 82602

dealt with the origin-emplacement problem (Misra and Keller, 1978). Stevens, Strong and Kean (1974) believe the southern Appalachian ultramafites to be the vertically-emplaced type assocated with subduction. Detailed studies of individual bodies (Greenberg, 1976; Hahn and Heimlich, 1977) support this view. Several workers (Carpenter and Phyfer, 1969; Hearn, Heron, Schumaker, and Swanson, 1977) have revived an earlier concept that many of these ultramafic plutons were emplaced as serpentinites which were later dehydrated to an olivine-talc (relict)-chromite assemblage during metamorphism. Petrofabric analyses of several bodies (Astwood, Carpenter, and Sharp, 1972) indicate random olivine grain orientations consistent with *in situ* formation of the olivine as suggested by Carpenter and Phyfer (1969).

The subject of the present investigation is the ultramafic body known as the "Deposit No. 9" dunite (Hunter, 1941). It occurs within a zone of typically small (less than 0.5 km. diameter) ultramafic bodies which trends northeast-southwest across North Carolina and Georgia. For the most part, this zone is restricted to the Blue Ridge province of the southern Appalachians. The Deposit No. 9 dunite is located just east of County Highway 1001 in Macon County, approximately 9 km. east of Franklin and 78 km. southwest of Asheville (Fig. 1).

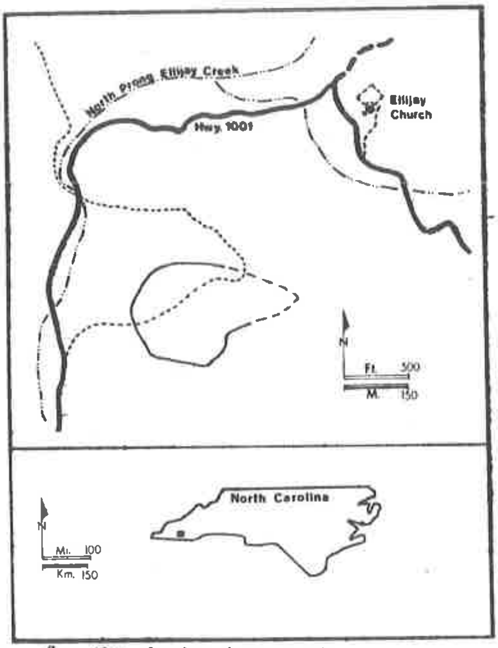

Figure 1. Location map for the dunite (stippled).

METHODS OF INVESTIGATION

In general, all outcrops including roadcuts and prospect pits were sampled (Fig. 2). Where outcrop is extensive, dunite samples were collected at roughly 6 m. intervals. Veins and lenses of accessory and alteration minerals were sampled also. Country rock was collected where exposed along roadcuts and creek banks. An outcrop map was constructed in the field on enlarged sections (one inch equals 200 feet) of the North Carolina Corbin Knob Quadrangle (U.S.T.V.A. 1968, 7.5-minute) topographic map utilizing pace and compass techniques. U.S. Department of Agriculture areal photographs (1963) were also utilized, but due to their age and resolution, they were helpful only or general location purposes.

The composition of plagioclase in the country rock was determined by the use of extinction angles of albite twins in thin sections perpendicular to (010) and the appropriate determinative chart in Kerr (1959). Modal analyses conducted on 40 ultramafic and 12 country rock samples are based on a minimum of 1400 points per thin section counted along a traverse grid system designed to cover maximum area and

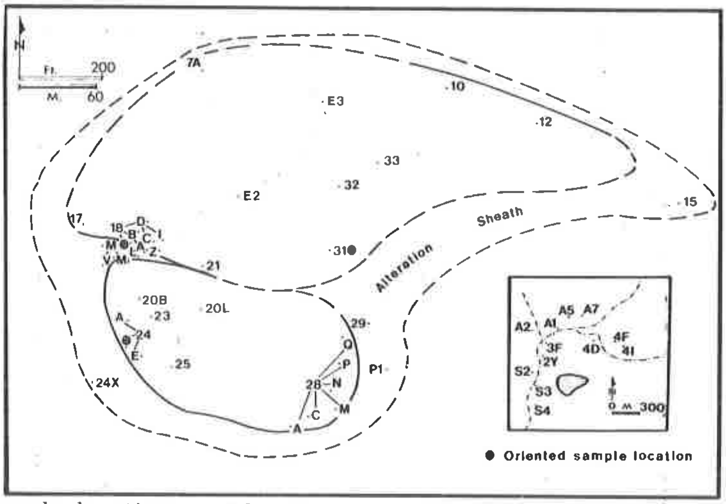

Figure 2. Sample location map for the dunite and the country rock.

minimize analytical error to below two percent (Chayes, 1956).

Initial X-ray determination of olivine composition by the method of Yoder and Sahama (1957) demonstrated that special care was necessary to reduce experimental error introduced by accessory mineral contaminants, especially talc and vermiculite. When present in quantities exceeding roughly 5 percent, these minerals tend to interfere with and obscure the comparison peaks of the internal standard. To eliminate this problem and reduce experimental error to below 4 percent, samples were specially prepared in the following manner. Two fractions were extracted from each sample, disaggregated by mortar and pestle and subjected to dry mechanial sieving. Magnetic separation was performed with a Frantz Isodynamic Separator at .35 and .90 ampere intervals on the fractions falling between .02 inch and .015 inch diameter to remove expected opaques and micas. Additional contaminants were removed by hand brusing under a binocular microscope. The resulting cleaned olivine fractions were reduced to a fine powder in a pica mill and analyzed by X-ray diffraction (Yoder and Sahama, 1957). Precision, based on duplicate samples was within 1 percent of the relative mean.

Alteration minerals were analyzed by X-ray diffraction methods suggested by R.W. Manus (personal communication, 1976) using Cukα radiation with a nickel filter and pure alpha quartz as an internal standard. The optical identification of selected opaque minerals was also confirmed by X-ray diffraction.

Chemical analysis was conducted on whole rocks, olivine separates, and talc separates. Sample powders were fused with lithium metaborate, following the procedure outlined by Ingamells (1970), and dissolved in five percent nitric acid (5% lanthanum oxide in 25% hydrochloric acid was added for CaO analysis). Analysis was performed using Perkin Elmer Model 403 atomic absorption spectrophotometer for major elements and nickel. Standards were prepared from Spex Industries chemically pure metals, and the U.S.G.S. PCC-1 and DTS-1 ultramafic rock standards were used as calibration and reference standards. The coefficient of variation is less than 2% based on these standards. Precision, based on duplicate samples, was within 2% of the relative mean for whole rock analyses and within 1% for the olivine analyses.

GEOLOGIC SETTING

The Deposit No. 9 dunite is one of many alpine ultramafic bodies which occur within the Blue Ridge province of the southern Appalachians of western North Carolina. In this area, the Blue Ridge province is dominated by two Precambrian metamorphic rock units, a hornblende gneiss and mica gneiss (Stuckey and Conrad, 1958), also referred to as the "Roan Gneiss" and "Carolina Gneiss" (Keith, 1903), respectively. the Roan Gneiss is recognized as the most common rock enclosing the ultramafic bodies,

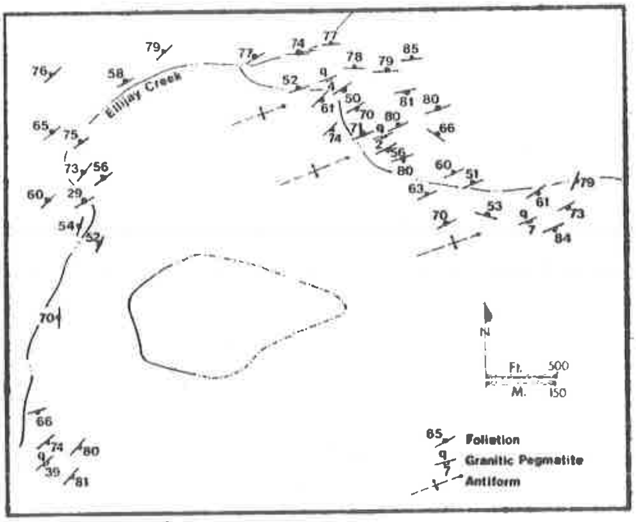

Figure 3. Geologic setting of the dunite.

Table 1. Modes of the country rock.

Sample Number	AI	A2	A5	A7	2Y	3F	4DI	4F	4I	S2A	S3	S4
Plagioclase	18.4	10.6	13.5				29.0	10.8	15.1	22.0	14.8	9.0
Quartz	47.7	10.6	58.3	27.1	33.8	18.4	46.7	43.9	46.6	52.1	63.3	43.6
K-Feldspar	5.6									2.7	0.6	
Almandine	1.7						6.4	4.4	4.0	2.7	2.0	4.3
Epidote	4.8	0.3	0.6	59.3	55.8	49.8				0.7	0.3	0.1
Sphene	0.1	tr	0.4	1.3	tr							
Leucoxene	tr			0.1	0.8	0.5						
Apatite	0.3	tr	tr	tr			tr	tr	tr			
Hornblende		77.8		8.9	tr	27.2						
Allanite			tr	1.0						tr		
Muscovite	1.1		5.7				2.1	17.4	13.9	0.9	tr	10.4
Biotite	8.3		21.1	0.2			16.3	18.7	17.3	17.4	17.7	28.1
Vermiculite	0.5									0.4	tr	
Magnetite	0.6		0.4				1.1	2.4	2.3	0.7	1.3	4.3
Hematite	0.5	0.7		2.0	9.6	4.1	0.2	2.3	0.5	0.4	tr	0.2
Topaz	0.4			0.1			0.2				tr	
Zircon	tr	tr	tr	tr	tr	tr	tr	0.1	tr	tr	tr	
Staurolite							0.5		0.3			

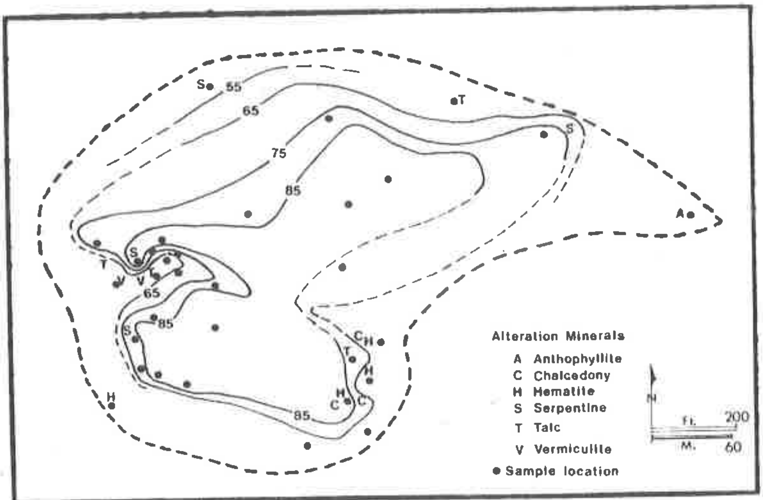

Figure 4. Map showing variation in olivine content (contours) and distribution of dominant alteration minerals.

although a biotite-rich variety of the Carolina Gneiss (Hunter, 1941) is also associated with many of them.

The structural features of the Blue Ridge province metamorphic rocks are complex and only generally understood. The gneisses have a well-developed foliation which displays a regional northeast-southwest strike and general dip to the southeast at steep angles. At least two, and possibly three metamorphic episodes (Butler, 1973) have affected these rocks.

COUNTRY ROCK

Examination of the country rock enclosing the dunite reveals a complex structural picture in the Ellijay Creek area (Fig. 3). A regional northeast-southwest strike is dominant with dips of foliation defining a local antiform plunging to the northeast. The dunite is positioned discordantly along the southern flank of this structure. Northeast of the dunite, the plunging nose of the antiform consists of a series of accordian-like shear folds commonly cut by small faults along their axes. Several of these axial faults have been intruded by granitic pegmatitie.

The local Carolina Gneiss consists of light-colored, resistant plagioclase-quartz-mica gneiss commonly interlayered with weaker, red-weathering garnet schist and orange-weathering biotite schist. Although abundant in the Blue Ridge Province, Roan Gneiss is generally uncommon in this area. It occurs typically in areas adjacent to the ultramafic bodies.

The Roan Gneiss is uniform in texture and conformable with the associated gneisses. In the Ellijay Creek area, petrographic study reveals that quartz-oligoclase-biotite-(almandine) gneiss is the dominant type but that hornblende-oligoclase-quartz gneiss and epidote-quartz-hornblende gneiss are also present (Table 1).

Plagioclase is conspicuously absent from the epidote-quartz-hornblende gneiss, but ranges from 9 to 29 percent in the other two varieties of gneiss. In the hornblende-rich gneiss (Sample A2), plagioclase is characterized by a biaxial positive optic sign, general absence of twinning, and a composition of An 18. The other gneisses contain plagioclase which is characterized by a biaxial negative optic sign, wavy albite-pericline twinning, and a composition of An 21. Uncommon in the gneisses, K-feldspar occurs as large, commonly untwinned grains rarely containing quartz inclusions. In addition to its occurrence in local granitic pegmatite bodies, quartz occurs in all the gneisses as layers of segmented grains containing rare zircon inclusions, as pod-like aggregates, and as veins and interstitial fillings.

Abundant near the dunite, epidote is characterized by irregular, granular aggregates arranged in parallel layers. Many crystals are rimmed by allanite. Commonly associated with epidote, sphene typically separates epidote from quartz. The crystals display characteristic rhombic cross-sections, and are partly to completely altered to leucoxene.

Almandine garnet is common, particularly within muscovite-rich horizons in gneisses that are poor in epidote and hornblende. The dark red, irregularly shaped crystals contain numerous vermiculite-filled fractures, and are commonly rimmed by hematite. Iron-rich biotite, commonly associated with muscovite or epidote, is partially altered to chlorite along cleavage traces.

Hornblende occurs in epidote-quartz-hornblende gneiss as irregularly shaped, strongly pleochroic (X=pale green, Y=dark green, Z=brown) aligned crystals. In hornblende-oligooclase-quartz gneiss, it displays pseudohexagonal outlines and well-developed prismatic cleavage. The crystals are commonly associated with euhedral apatite and contain numerous fractures filled with hematite.

Rare topaz is present as granular aggregates associated with irregular masses of magnetite. Staurolite is uncommon and restricted to the quartz-oligoclase-biotite-almandine gneiss. The irregularly shaped crystals are pale yellow in color and commonly contain quartz inclusions.

The gneisses containing garnet and micas are characterized by almandine porphyroblasts which displace layers of muscovite and biotite. Where almandine is absent, mica-bearing gneisses are characterized by lepidoblastic texture. Blasto-psephitic textures are represented by pod-like "aggregates" of quartz grains. Quartz layers alternating with epidote-rich and mica-rich layers are interpreted as interbeds of original arenaceous, calcareous and argillaceous sediments.

The abundance and variety of calcium-bearing minerals (epidote, hornblende, and sphene) and the presence of staurolite support the textural evidence indicating a largely argillaceous-calcareous sedimentary parentage for these gneisses.

FIELD OCCURRENCE OF THE DUNITE

The Deposit No. 9 dunite is semi-elliptical in plan view and measures roughly 350 meters by 520 meters in maximum dimensions. Its long axis is oriented east-west at a distinct angle to the strike of foliation in the enclosing gneisses (Fig. 3). Many of is field characteristics are common to southern Appalachian alpine ultramafic bodies. Inherent from its homogeneity, it is more resistant than the enclosing well-foliated gneisses, and occurs as a prominent topographic high. The dunite is rimmed by a weak, heavily eroded hydrous alteration zone which is the locus of gullies and small streams.

Streams expose the body along the northwestern and southwestern margins, and across the center parallel to its long axis, where the rock is primarily talc schist. The existence of a zone of alteration transecting the ultramafic mass strongly suggests that two separate bodies are present; such zones of intense alteration are typically confined to the periphery of dunites in this region. The two bodies are surrounded by and separated from each other by the hydrous alteration zone (Fig. 2). North of the east-west trending talc-rich zone, the minerals talc, serpentine, and anthophyllite are the dominant alteration zone constituents. South of it, hematite and hematitic chalcedony are the prominent secondary minerals (Fig. 4). This contrast in alteration assemblages is further suggestive that the Deposit No. 9 dunite consists of two separate dunite masses juxtaposed.

At the southeastern corner of the body, the dunite is exposed by an abandoned open-cut, the former Higdon chromite prospect developed in 1917. Along the eastern wall of this cut, several thick (2-5 cm.) layers of chromite strike roughly northeast-southwest and dip gently southeast. These layers may be remnants of the large chromite lens reported by Hunter, Murdock and MacCarthy (1942). Throughout the dunite there are subtle, generally horizontal chromite stringers which define a lineation that trends typically northeast-southwest. Other internal structures, such as joints, are notably lacking in the duntite.

MINERALOGY

The relatively unaltered core of the body consists of the primary dunite minerals and accompanying minor amounts of platy talc, chrysotile, tremolite, clinochlore, and kammererite. The peripheral alteration sheath (Fig 2) consists of antigorite, anthophyllite, penninite, clinochlore, talc, vermiculite and, in the southern section, hematite and chalcedony. Magnesite, magnetite and pyrite occur in small amounts indiscriminately throughout the entire body. The core is progressively more altered toward its periphery (less than 10% to more than 55%). Beyond this point is the intensely altered peripheral sheath. The contact between the moderately altered dunite core and the highly altered sheath is sharp (Fig. 2) and clearly deformational as evidenced by shear features observed in thin section.

Primary Mineralogy of the Core

The primary mineral assemblage of the dunite core is olivine, chromite and pyrrhotite (Table 2). Because of its occurrence as minute inclusions, pyrrhotite was not counted in the modes. Orthopyroxene, a common primary accessory mineral in southern Appalachian alpine ultramafic bodies (Misra and Keller, 1978), is absent.

As the dominant primary mineral, olivine ranges in abundance from greater than 90 percent at the interior of the pluton to less than 50 percent at the dunite-alteration sheath contact. Modal olivine contours display a "pinch" consistent with the idea that

Table 2. Modes and olivine composition for the dunite.

Sample Number	7A	10	12	15	17	18B	18C	18D	18I	18L	18	18V	18Z	20B	20L	21
Olivine	49.0	14.5	79.8		80.8	83.9	30.3	86.6	67.8	37.9	89.4		67.7	81.2	90.8	76.8
Chromite	0.9	0.9	1.3	1.1	3.3	2.5	1.7	0.8	0.3	0.9	1.2		0.5	1.7	0.7	0.9
Chlorite	2.0	1.4	1.6		11.1	9.9	5.5	1.1	3.4	4.3	0.8		3.8	1.8	0.6	0.6
Tremolite	4.1	14.9					15.4			2.7	0.5		3.8			
Serpentine	34.0	0.5	11.0		2.8	3.5	3.9	5.3	12.1	4.7	7.3		3.2	10.3	7.8	10.0
Talc	0.8	46.1	6.3		0.1	0.2	43.2	6.1	16.0	49.5	0.4		21.0	4.9	0.1	8.1
Anthophyllite	tr	9.5		72.4												2.2
Vermiculite		2.3		18.7								100	tr			tr
Magnesite	0.3				1.9				0.4		0.4					1.4
Magnetite		2.7						0.1				tr				
Hematite	8.9	7.2		7.8										0.1		
Chalcedony																
Olivine Fo%	91.8		90.9		89.7	90.0			90.5						94.4	91.2

Sample Number	24A	24E	24	24X	25	28A	28M	28N	28P	28Q	29	31	32	33	E2	E3
Olivine	84.5	88.5	83.5		86.5			88.2	52.0	83.7		83.9	86.9	89.8	78.9	80.3
Chromite	1.5	1.2	3.2	tr	1.2	0.6	1.4	4.2	0.9	1.4	0.6	1.9	1.2	0.9	2.2	1.8
Chlorite	1.8	1.5	3.3	6.4	0.6	0.8	0.2	0.8	10.3	5.4	1.0	3.3	4.1	0.3	0.8	0.3
Tremolite			0.3	2.1					0.1			0.6				
Serpentine	11.5	5.5	5.9	1.2	9.5	0.4		6.2	3.3	6.0	0.4	5.2	6.4	7.4	17.9	15.3
Talc	0.6	3.3	3.0	21.0	0.3	2.7	4.5	0.5	30.2	3.2	3.8	2.5	1.4	0.6	0.2	2.3
Anthophyllite																
Vermiculite			0.8				0.4		tr		1.5					
Magnesite					0.1	tr		0.1		0.3						
Magnetite														0.2		
Hematite				42.2	1.8	14.0	25.5		2.9		36.8	2.6		0.7		
Chalcedony				27.0		81.5	68.0		0.3		55.9					
Olivine Fo%	91.5				90.9	91.8		90.9		91.1		86.6	90.3	90.3	90.9	92.6

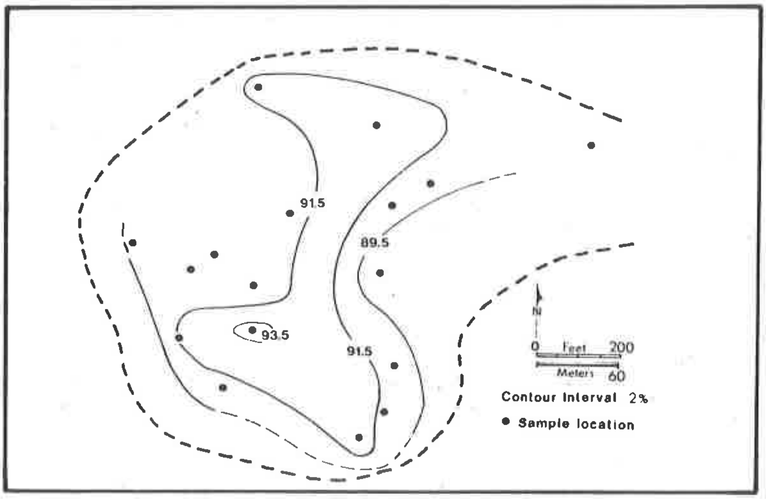

Figure 5. Variation in olivine composition (Fo content) within the dunite.

the body consists of two discrete masses of dunite (Fig. 4). Most commonly, olivine occurs as anhedral, colorless grains showing well-developed parting parallel to (010). Grain shape and size vary depending on location within the pluton and textural category of the grain. Most grains are altered to some degree, typically along parting and grain boundaries. Twinning is rare, and inclusions of chromite and pyrrhotite are common.

X-ray analysis of 17 olivine separates (Table 2) shows a narrow spread of Fo values (86-94 percent, mean 91 percent), consistent with results for other North Carolina ultramafites (Misra and Keller, 1978). A plot of this data (Fig. 5) suggests that the olivine is slightly more magnesian toward the center of each of the two portions of the dunite. This trend is confirmed by chemical analysis of selected olivine samples.

Chromite is represented by three distinct species. The first, observed in polished section, is characterized by minute, euhedral octahedra which occur exclusively as inclusions in unstrained olivine grains. The most common chromite occurs as grains situated between olivine grains. This species displays a range in grain size, euhedrism, mode of occurrence, and alteration characteristics (Table 3), and commonly shows impingement cracks on adjacent grains of mosaic olivine. Such chromite from the center of the body is characterized by euhedral disseminated grains commonly altered

Table 3. Characteristics of the primary interstitial chromite.

Typical Grain Size (mm.)	0.5	1.0	15
Euhedrism	Euhedral	Subhedral	Anhedral
Occurrence	Disseminated	Subtle Bands	Layers
Alteration Product(s)	Kammererite	Kammererite	Kammererite Magnetite
Alteration Form	Internal along octahedral parting	Irregular internal and external	Irregular external
Nature of Enclosing Olivine	Unstrained	Undulose extinction	Multi-strain banded

to Fe-rich chlorite (kammererite). Internal alteration of these grains follows octahedral parting and forms a striking lattice grid pattern. Externally, the kammererite blades have grown with cleavage traces parallel to the crystal faces of the altered chromite grain. Toward the periphery, the chromite grains increase in size (1.0 mm.) and tend to form subtle bands of subhedral crystals. Alteration to kammererite is common though quite irregular and is no longer governed by parting. Enclosing olivine demonstrates strain in the form of undulose extinction and occasional grains with two or three strain bands. Near the periphery of the body chromite is represented by large (15 mm.) anhedral grains which occur in layers and as elongate stringers. Alteration to kammererite and magnetite is irregular, and the enclosing olivine consists of multistrain-banded grains. In the peripheral alteration zone, chromite occurs as disrupted elongate masses. The third species of chromite is represented by anhedral masses which fill interstices between polygonal olivine neoblasts. Identified by polished section techniques, this chromite is clearly a product of remobilization following recrystallization.

As the third primary mineral of the dunite, pyrrhotite occurs exclusively and sparingly as minute, euhedral, generally equant grains. The pyrrhotite is present only as inclusions within polygonal olivine grains; none occurs at olivine grain boundaries or within the alteration minerals.

Secondary Mineralogy of the Core

The secondary mineral assemblage of the dunite core comprises from 10 to 40 percent of the rock (Table 2). Kammererite occurs as colorless, nonpleochroic flakes associated with irregular masses of magnetite. Both of the minerals are restricted to chromite grains wherein they typically follow parting planes and other zones of weakness. X-ray analysis of several altered chromite separates verified the identification of kammererite and magnetite based on optical properties. Locally, flakes of kammererite, extending from chromite grains, are sheathed by light green clinochlore, indicating at least two episodes of chloritization.

Colorless clinochlore occurs typically as discrete elongate flakes interstitial to and transecting adjacent olivine grains along parting. These flakes are nonpleochroic and commonly show wavy cleavage traces. Many clinochlore flakes display overgrowths of a second generation of clinochlore corresponding to the overprints on kammererite. Typically, first generation clinochlore is of a darker color under crossed nicols. Both generations show partial to complete transformation to flaky talc.

Also typically altered to talc, tremolite occurs as acicular crystals and radiating fibrous aggregates which transect olivine grains. The crystals are characterized by inclined extintion (13-18^{o}) and prismatic cleavage.

Serpentine is represented by chrysotile slip-fiber veins occupying the interstices between olivine grains. Commonly these veins are partially to completely replaced by talc, and rarely by magnesite. Polished section examination disclosed dusty, anhedral magnetite to be a common associate of the chrysotile.

In addition to the above occurrences in the dunite core, talc is present as veins following major fractures through olivine grains and across chrysotile, chlorite, and talc pseudomorphs, suggesting at least two episodes of steatitization.

Uncommon in the dunite core, magnesite occurs along partings in chromite and along olivine grain boundaries where it replaces talc. Rare pyrite occurs as bright yellow masses associated with magnetite, along parting in chromite grains, and with secondary chromite.

Mineralogy of the Peripheral Alteration Zone

As indicated earlier, the peripheral alteration sheath consists of two mineral assemblages. X-ray analysis of samples from the southern alteration zone indicates the major constituents to be chalcedony, hematitie, and talc. Chalcedony occurs as granular, dusty masses replacing polygonal olivine grains and as granular aggregates replacing interstitial chrysotile, thus preserving the mosaic morphology of the primary assemblage. Chromite grains, partially altered to kammererite, are commonly preserved within the chalcedony mosaic network.

Hematite occurs in association with interstitial chalcedony, and commonly fills cracks and fractures in the silica-rich rock. Locally, hematite development exceeds silicification resulting in hematite pseudomorphs after polygonal olivine. As a minor constituent of the silica-hematite rock, talc occurs as irregular shreds comprising rare veins which cut the silica-hematite replacement network.

The northern alteration zone is dominated by hydrous minerals including patchy aggregates of antigorite, typically associated with talc, and containing numerous minute, elongate grains of anhedral magnetite. Anthophyllite, present as acicular crystals and radiating aggregates, occurs locally intergrown with vermiculite forming knots and lenses of fibrous anthophyllite-vermiculite rock. The vermiculite is moderately pleochroic (light green to brown), has a flaky habit, and lacks bird's-eye mottling. Additionally, it commonly displays polysynthetic twinning and shows characteristic anomalous "Prussian blue" interference colors. Chlorite is represented by clinochlore, which occurs as discrete flakes in association with antigorite, and by penninite which occurs exclusively as flaky aggregates associated with talc.

In the northern alteration zone much of the talc appears to be fine-grained and massive. In the east-west alteration zone between the two dunite masses (Figs. 2 and 4) this talc-rich rock shows evidence of intense deformation in the form of microfolds and shears. A second variety of talc (identified by X-ray diffraction analysis) occurs as thick (3 cm.) veins of subhedral, tabular crystals (roughly 3 cm. x 0.5 cm. 0.1 cm.). These veins cut olivine, massive talc, serpentine, and anthophyllite, indicating a later episode of talc alteration.

Chemical analysis suggests that the bladed vein talc (18Z) is chemically purer than the massive variety (23), the higher iron content of the latter due to the presence of hematite. Chemical data for these talc samples compares closely with analyses of talc from other localities (Table 4).

TEXTURE

Characteristic deformational textures are ubiquitous in the dunite and in the enclosing alteration sheath. At the dunite-steatite contact, tear drop-shaded flaser pods of anhedral olivine occur typically enclosed in fine-grained granulated olivine, and occasionally within masses of sheared and disrupted talc and antigorite. Ranging in length from 1 cm. to 5 cm. with long axis aligned parallel to the strike of the contact, the pods are characterized by a blunt convex nose which tapers to a ragged splintered tail.

Other textural features comon to the peripheral area of the dunite are elongate, anhedral grains of olivine surrounded by small (.05 mm.) subrounded equigranular olivines. The elongate grains range in size from 6 mm. x 0.5 mm. to 5 mm. x 2 mm. and have typical length/width ratios on the order of 12. These grains are aligned with long axes parallel to the strike of the contact, and are frequently splintered and fractured. The smaller equigranular olivines represent abraded material trapped and ground between the larger grains during deformation. Peripheral chromite occurs as elongate hackly grains which have been disrupted and drawn out parallel to olivine elongation by pencil shear.

Table 4. Chemical analyses of talc.

Sample	SiO_2	Fe_2O_3*	MgO	CaO	MnO	Total
18Z	61.70	1.02	32.48	0.14	0.08	95.42
23	60.20	4.53	32.36	0.24	0.18	97.31
T1	62.61	2.46	30.22		0.01	
T2	60.06	1.74	30.83	0.40		

*Total Fe as Fe_2O_3 except for T1 and T2 (total Fe as FeO).

18Z Vein talc from Deposit No. 9 dunite
23 Massive talc from Deposit No. 9 dunite
T1 Talc from altered peridotite in Sweden (Du Rietz, 1935).
T2 Talc from serpentinite in Italy (Repossi, 1942).

Toward the center of the body, deformational textures are less pronounced. Chromite grains tend to be equidimensional and olivine occurs as polygonal subhedral grains and locally as large, anhedral porphyroclasts. The porphyroclasts display length/width ratios on the order of 6 with average dimensions of 3 mm. x 0.5 mm. They are characterized by strain-induced kink bands attributed to nonelastic response during plastic deformation and subsequent intracrystalline gliding (Nicolas, Bouchez, Boudier, and Mercier, 1971). The frequency of porphyroclasts as well as the number of kink bands per grain increases with distance towards the periphery of the pluton. Locally, near the periphery, porphyroclasts constitute greater than 80 percent of the olivine population and show a striking alignment of their kink bands parallel to the predominant strike of the country rock. The polygonal olivines or neoblasts surrounding the porphyroclasts are characterized by length/width ratios of 1 with maximum dimensions less than 1 mm. They display curved grain boundaries, triple-point junctions, and boundary angles of 110^o to 135^o. Euhedral to subhedral chromite grains occur typically at the center of olivine triple-point junctions. The neoblasts may display undulatory extinction, and a few contain two or three strain bands. At the boundaries between neoblasts and porphyroclasts, the smaller polygonal grains commonly make angular projections into strained grains with points exactly at junctions between kink bands, a phenomenon noted by Ragan (1969) in New Zealand peridotites.

CHEMICAL DATA

Fourteen dunite samples were analyzed by atomic absorption spectrophotometry

Table 5. Chemical analyses of dunite.

Sample	SiO_2	Fe_2O_3*	MgO	CaO	MnO	Total	Ni(ppm)
7A	41.90	8.92	42.92	0.20	0.20	94.14	2290
12	41.60	9.75	45.67	0.17	0.14	97.33	2260
17	41.20	9.63	46.69	0.17	0.14	97.83	2270
18A	41.10	9.34	46.70	0.15	0.16	97.45	2300
20L	39.90	8.49	47.30	0.14	0.14	95.97	2270
21	41.60	7.84	46.68	0.14	0.13	96.39	2350
24A	42.10	8.47	46.85	0.12	0.14	97.68	2330
25	42.70	8.95	46.53	0.17	0.15	98.50	2290
28C	43.80	9.59	47.25	0.20	0.15	99.99	2310
28Q	43.40	9.97	47.06	0.14	0.15	100.72	2290
31	43.50	10.42	45.76	0.23	0.15	100.06	2260
33	44.20	10.05	44.65	0.11	0.15	99.16	2220
E2	41.90	8.80	46.99	0.13	0.14	97.96	2270
E3	43.20	8.81	47.29	0.14	0.15	99.59	2260

*Total Fe as Fe_2O_3

for major oxides (SiO_2, MgO, CaO, MnO and total Fe as Fe_2O_3) and nickel (Table 5). Although sample 7A contains less than 50 percent olivine, the remaining 13 samples contain in excess of 75 percent. The results show no significant geographic trends in oxide distribution, except for CaO which increases slightly toward the periphery with increase in alteration minerals, including calcium-bearng amphibole.

Chemical analyses were made for olivine concentrates from six samples (Table 6) and compared with those for olivines from several sources including metamorphic forsterite, peridotitic olivine, and olivine from ultramafic inclusions in basalt. The three olivines of suspected mantle origin show similar values for the major oxides, which contrast sharply with the values for metamorphic forsterite, especially in total Fe oxide, MnO, and MgO. The data obtained for the Deposit No. 9 olivines shows a closer correlation with the mantle-derived olivines than with metamorphic forsterite.

PETROFABRIC DATA

Petrofabric data were obtained for three oriented samples, two of which were extracted from dunite in direct contact with the peripheral alteration zone of the body. Sample 24 was obtained from an inward dipping wall of relatively unaltered dunite at the southwestern margin, and sample 18 from a vertical wall of fresh dunite adjacent to the east-west alteration zone (Fig. 2). Sample 31 is also relatively fresh dunite collected some 15 meters inward from the core-alteration sheath contact. Each specimen is characterized by a mosaic of small (.05 mm. - .5 mm.), polygonal, strain-free olivine grains which enclose occasional large (.7 mm. - 2.8 mm.), elongate, strain-banded porphyroclasts.

Thin sections were cut along the horizontal plane of each sample and the orientations of olivine crystallographic axes for 100 to 150 grains were measured in each section, using a modified version of the standard universal stage method (Emmons, 1943). Two areas in each thin section were selected at random and all of the grains within the field of the microscrope were measured to minimize bias. The complete range of grain size and both strained and unstrained grains were measured without exception. Raw data was plotted on an equal area stereographic projection (lower hemisphere) and contoured at levels of 1,2,3,5,7, and 9 percent per 1 percent area. The trend of the horizontal chromite lineation was plotted as well (Fig. 6).

The data for sampes 18 and 31, both from the northern of the two portions of the dunite, show strong α point maxima nearly normal to the chromite lineation (L) which is oriented northeast-southwest. In these samples a strong preferred orientation is also exhibited by the β and γ axes. The degree of preferred orientation in sample 24, from the southern portion of the dunite, is less pronounced than that in samples 18 and 31. However, there is again a distinct α maximum nearly normal to the chromite lineation which, in this sample, is oriented northwest-southeast, essentially normal to the lineation in samples 18 and 31. Sample 24 also exhibits a strong preferred orientation of β and γ axes.

The preferred orientation of the samples shows no consistent relationship to the plan shape of the body nor to the attitude of foliation in the country rock. Moreover, the chromite lineation lacks parallelism with the strike of country rock foliation and is substantially different in orientation between the two portions of the dunite.

DISCUSSION AND CONCLUSIONS

Based on its highly magnesian olivine, characteristic recrystallization textures, relict porphyroclasts, tectonite fabric, and similarities with mantle-derived peridotite nodules in basalts (Mercier and Nicolas, 1975; Jackson and Thayer, 1972), we conclude that this dunite originated in the upper mantle and then was transported essentially intact to its present crustal position.

If the body had been emplaced as serpentinite and later dehydrated to dunite, we would expect it to exhibit at least some of the features characteristic of the "deserpentinization" peridotites in the Cascade Mountains. In these rocks, Vance and Dungan (1977) described and documented several modes ofoccurrence of the olivine

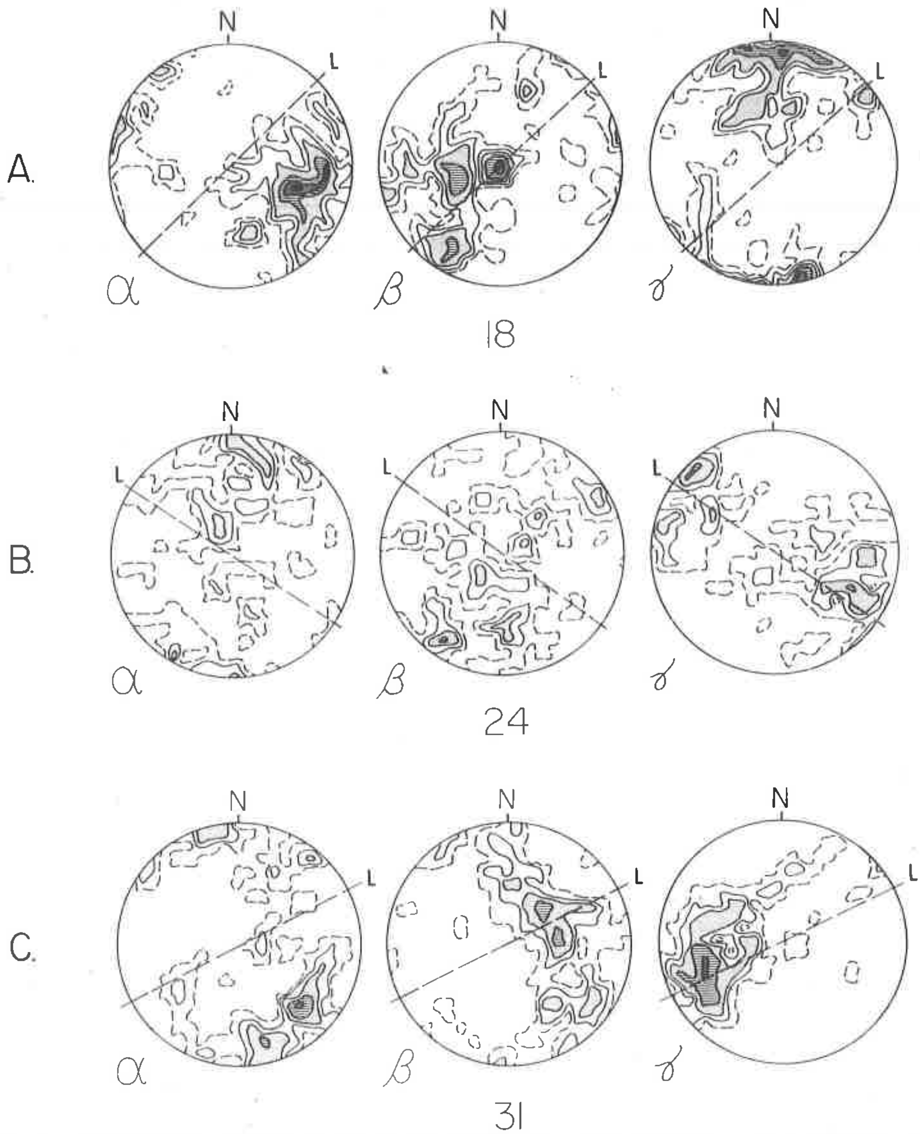

Figure 6. Petrofabric diagrams for three dunite samples (Contours at 1,2,3,5,7, and 9 percent). L = chromite lineation.

which indicate clearly that it formed later and at the expense of serpentine with which it is associated. Critical textures of this young olivine include olivine veinlets which transect serpentine, olivine overgrowths, and subhedral to euhedral olivine porphyroblasts. Such textures are totally lacking in the Deposit No. 9 dunite which shows all degrees of alteration of olivine to serpentine and to other hydrous minerals as well as a concentration of alteration minerals along its rim, features difficult to explain by the dehydration hypothesis. Whereas ragged grains of sulfides, interpreted as relics from a serpentine precursor (Vance and Dungan, 1977),occur in the Cascade Mountains peridotites in which they replace chromite rims and appear to replace olivine, pyrrhotite is present as sub-equant inclusions within polygonal olivine of the Deposit No. 9 dunite.

There are also distinct chemical contrasts. For example, the composition of olivine in the Cascade Mountains "deserpentinization" peridotites is highly variable (Fo 85-98 in contrast with the narrow range (Fo 88-93) for upper-mantle tectonite

Table 6. Chemical analyses of olivine.

Sample	SiO_2	Fe_2O_3*	MgO	CaO	MnO	Total	Ni(ppm)
17	42.10	8.98	48.38	0.13	0.18	99.77	2130
25	43.10	8.43	48.59	0.13	0.16	100.41	2110
28N	41.80	9.30	48.41	0.13	0.19	99.83	2130
21	41.50	8.18	48.46	0.13	0.17	98.44	2210
E2	42.20	7.89	49.18	0.12	0.16	99.55	2130
31	42.80	9.97	48.22	0.13	0.20	101.32	2130
Average	42.25	8.79	48.54	0.13	0.18	99.89	2140
1**	40.96	7.86	50.45	0.15	0.13	99.55	
2	40.84	8.18	50.27		0.17	99.45	
3	40.30	10.26	48.60	0.07	0.09	99.32	
4	41.72	1.11	57.83			100.66	

*Total Fe as Fe_2O_3 except for 1-4 (Fe as FeO)

** Analyses 1-4 from Deer, Howie, and Zussman (1966).

1. Olivine from dunite, Dun Mountain, New Zealand
2. Olivine from dunite, Little Castle Creek, California
3. Olivine from nodules in basalt, Japan.
4. Forsterite from crystalline limestone, Burma.

peridotites (Vance and Dungan, 1977). Olivine composition for the Deposit No. 9 dunite (Fo 87-94) matches closely that for the latter group, an argument against a deserpentinization origin for the dunite studied here. Moreover, Vance and Dungan (1977) note the anomalously high MnO content (up to 1.5%) of the Cascades peridotite olivines, arguing that such values are consistent with conversation of serpentine to olivine but incompatible with the idea that the olivine is a relic which survived serpentinization of peridotite. As shown in Table 6, olivines from the Deposit No. 9 dunite are uniform and extremely low in MnO content (maximum 0.20%), suggesting that these olivines were not formed by dehydration of serpentine.

Consistent with solid-state emplacement of the Deposit No. 9 dunite is the strong preferred orientation of its olivine, a feature which we believe was established prior to final emplacement of the body and independent of the regional deformation responsible for the mapped foliation in the country rock (Fig. 3). This conclusion is supported by the fact that the olivine orientation lacks a consistent relationship to the plan shape of the body and the attitude of foliation in the gneiss; the dunite mass itself transects the strike of this foliation. We interpret the dunite fabric as the result of syntectonic recrystallization in the upper mantle (Ave'Lallement and Carter, 1970).

The mineralogy of the country rock is indicative of middle amphibolite facies metamorphism, suggesting temperatures on the order of 500-600°C. (Turner, 1968). Because olivine cannot recrystallize below 1050°C. (Carter and Ave'Lallement, 1970), we conclude that this dunite, with its dominant polygonal recrystallization texture (Ragan, 1969; Talbot *et al.*, 1963), underwent recrystallization in the upper mantle and possibly during the early stages of ascent. Although olivine can form from serpentine during metamorphism below 600°C. (Vance and Dungan, 1977), we see no evidence in the Deposit No. 9 dunite for such a dehydration event to have actually occurred here.

Chidester and Cady (1972) propose that alpine ultramafites are portions of the upper mantle that have been "nipped off and kneaded through the crust" to their present positions above subduction zones. Some such vertical emplacement process may have operated relative to this dunite rather than its emplacement laterally as ophiolite (Coleman, 1977). Although ophiolite is well-documented in the northern part of the Appalachian belt in Newfoundland (Dewey and Bird, 1971; Church and Stevens, 1971; Williams, 1971), in Quebec (Laurent, 1977), and recently in Connecticut (Merguerian, 1979), typical ophiolite stratigraphic units are not associated with the Deposit No. 9 dunite. If they are present in the region, this dunite is part of a highly dismembered ophiolite.

Whether a single mass (which later broke into two) was detached from the mantle or if two bodies were emplaced from the start, the petrofabric data support field and mineralogic data in suggesting that, at the present erosion level, two separate and contiguous masses were involved. The contrast in olivine crystallographic and chromite lineation orientations between samples 18 and 24, both from the periphery of the dunite, would be expected if the two samples are from separately emplaced portions, as shown in Figure 2. These differences may be explained by assuming that, during emplacement, the smaller more nearly equidimensional southern portion of the dunite rotated in relation to the elongate and more geometrically stable northern portion. The contrast in several olivine crystallographic orientations between samples 18 and 31, both from the northern dunite portion, relate undoubtedly to their different structural locations. We believe that sample 18 was affected by peripheral stresses during emplacement whereas sample 31, further toward the interior, was effectively shielded from them.

During ascent, the periphery of both portions of the dunite was shattered and deformed by shear, as suggested by the nature and prevalence of deformational features in the rim. Upon encountering saturated eugeosynclinal sediments, the shattered and exposed dunite periphery reacted with fliuds from the enclosing wallrock (the amount of alteration minerals decreases gradually inward as shown in Fig. 4) to form an envelope of serpentine (Riodon, 1955) which facilitated emplacement by reducing friction and localizing movement at the periphery. Deformation of the interior was minimized by reduction of friction at the contact (Ragan, 1963).

While serpentine was forming along the margins, other reactions produced the alteration suite within the interior of the body. Although no orthopyroxene relics occur in the dunite, this mineral may have been present in minor amounts originally, serving as a probable source for the scattered secondary tremolite in the body. Calcium and aluminum were probably supplied by the altering fluids to facilitate the formation of tremolite as well as chlorite (Bennington, 1956). Based on mineral assemblages and textural relationships observed in thin-section, olivine and chromite reacted with the fluids to produce magnetite, magnesite, and kammererite. As the influx of (carbon dioxide-bearing) fluid continued, progressive carbonation of the serpentine envelope produced a talc-magnesite assemblage which eventually reacted with additional carbon dioxide to produce a chalcedony-magnesite assemblage.

This progressive carbonation sequence accounts for the silica-rich envelope encasing the southern portion of the dunite. The northern portion lacks a silica-rich envelope, suggesting that the dunite here was not exposed to the carbon dioxide-bearing fluid for as long a time as was the dunite to the south. It appears that the end product of the alteration process may be related directly to the amount of time the rock is exposed to the agents of carbonation. This might explain the presence of orthopyroxene in an ultramafic mass located within three kilometers of this one (Hahn and Heimlich, 1977). If emplaced later than the Deposit No. 9 dunite and exposed to the fluids for a shorter time, orthopyroxene would not have had sufficient time to convert completely to tremolite. Hematitization must have occurred prior to emplacement of the northern dunite as indicated by its absence in this dunite and abundance in the southern dunite. Soon after emplacement and alteration of the northern dunite to talc, carbonation was terminated (before alteration of the northern talc-rich envelope could progress to a silica-rich assemblage).

We believe that following the major emplacement and progressive carbonation of the body (both portions), the dunite was altered again, resulting in the second episode of chloritization and steatitizaton and the late development of vermiculite and anthophyllite. The interpretation of two intervals of alteration is based on the presence of several types of chlorite and talc, mineral alteration relationships, and cross-cutting associations of minerals as observed in thin-section.

The dunite was subjected to an initial deformational episode in the upper mantle source region where it experienced high temperature flow, plastic creep (Carter and Ave'Lallemant, 1970) and syntectonic recrystallizaiton which annealed all but a trace of the strained grains (Capedri, 1973). These traces, or porphyroclasts, occur disseminated throughout the recrystallized mosaic network. A second deformation occurred during detachment from the mantle and ascent into the crust. Most of the deformational imprint from ascent was localized at the periphery of the body where frictional contact and drag were greatest. During progressive carbonation most of the evidence of this peripheral deformation was erased with conversion of the original olivine to a secondary mineral assemblage.

ACKNOWLEDGMENTS

We are pleased to acknowledge the Society of the Sigma Xi and the Division of Earth Resources of the North Carolina Department of Natural Resources & Community Development. Both organizations provided financial assistance for this investigation. We especially thank K.R. Hahn, for field assistance, and Ted Higdon and Harley Stewart for their friendly cooperation and permission to work on their properties. Finally, Virginia Dribus provided unfaltering encouragement and understanding throughout the study.

REFERENCES CITED

Astwood, P.M., Carpenter, J.R., and Sharp, W.E., 1972, A petrofabric study of the Dark Ridge and Balsam Gap dunites, Jackson County, North Carolina Southeast. Geol., v. 14, p. 181-194.

Ave'Lallemant, H.G., and Carter, N.L., 1970, Syntectonic recrystallization and modes of flow in the uppermantle: Geol. Soc. America Bull., v. 81, p. 2203-2220.

Bennington, K.O., 1956, Role of shearing stress and pressure in differentiation as illustrated by some mineral reactions in the system $MgO-SiO-H_2O$: Jour. Geol., v. 64, p. 558-577.

Brobst, D.A., 1962, Geology of the Spruce Pine District, Avery, Mitchell, and Yancey Counties, North Carolina: U.S. Geol. Survey Bull. 1122-A, 26 p.

Capedri, S.S., 1974, Genesis and evolution of a typical alpine-type peridotite mass under deep-seated conditions (Central Euboea, Greece): Boll. Soc. Geol. It., v. 93, p. 81-114.

Carpenter, J.R., and Phyfer, D.W., 1969, Proposed origin for the alpine type ultramafics of the Appalachians: Geol. Soc. America Abs. Prog., v. 7, p. 261-263.

Carr, D.R., and Kulp, J.L., 1957: Potassium-argon method of geochemistry: Geol. Soc. America Bull., v. 68, p. 763-784.

Carter, N.L., and Ave'Lallemant, H.G., 1970, High temperature flow of dunite and peridotite: Geol. Soc. America Bull., v. 81, p. 2181-2202.

Chayes, F., 1956, Petrographic modal analysis: John Wiley & Sons, Inc., New York. 113 p.

Chidester, A.H., and Cady, W.M., 1972, Origin and emplacement of alpine-type ultramafic rocks: Nat. Phys. Sci., v. 240, p. 27-31.

Church, W.R., and Stevens, R.K., 1971, Early Paleozoic complexes of Newfoundland Appalachians as mantle-ocean crust sequences:Jour. Geophys. Res., v. 76, p. 1460-1466.

Coleman, R.G. 1971, Plate tectonic emplacement of upper mantle peridotites along continental edges: Jour. Geophys. Res., v. 76, p. 1212-1222.

Condle, K.C., and Madison, J.A., 1969, Compositional and volume changes accompanying progressive sepentinization of dunites from the Webster-Addie ultramafic body, North Carolina: Am. Mineral, v. 54, p. 1173-1179.

Conrad, S.G., Wilson, W.F., Allen, E.P. and Wright, T.J., 1963, Anthophyllite asbestos in North Carolina: North Carolina Depart. Cons. Devel. Bull. 77, 61 p.

Dallmeyer, R.D. 1974, Eclogite inclusions in an alpine peridotite, sill, Georgia-North Carolina: Their chemistry and petrogenetic evolution: American Jour. Sci. v. 274, p. 356-377.

Deer, W.A., Howie, R.A., and Zussman, J., 1966, An introduction to the rock-forming minerals: John Wiley & Sons, Inc., New York, 528 p.

Dewey, J.F., and Bird, J.M., 1971, Origin and emplacement of the ophiolite suite: Appalachian ophiolites in Newfoundland: Jour. Geophys. Res., v. 76, p. 3179-3207.

Du Rietz, T., 1935, Peridotites, serpentines, and soapstones of northern Sweden with special reference to some occurrences in northern Jamtland: Geol. For. Forh. Stockholm, v. 57, 133 p.

Eckelmann, F.D., and Kulp, J.L., 1956, The sedimentary origin and stratigraphic equivalence of the so-called Cranberry and Henderson granites in western North Carolina: American Jour. Sci., v. 254, p. 288-315.

Greenberg, J.L., 1976, The alpine ultramafic problem in the southern Appalachians: The Webster-Addie dunite (Abs.): Geol. Soc. America Abst. Prog., v. 8, p. 185.

Hahn, K.R., and Heimlich, R.A., 1977, Petrology of the dunite exposed at the Mincey Mine, Macon County, North Carolina. Southeast. Geol., v. 19, p. 39-53.

Hearn, F., Heron, S.D. III, Schumaker, D., and Swanson, S.E., 1977, Petrology of the Rich Mountain alpine ultramafic, Watauga County, North Carolina (Abs.): Geol. Soc. America Abst. Prog., v. 9, p. 146.

Hunter, C.E., 1941, Forsterite olivine deposits of North Carolina and Georgia: North Carolina Dept. Cons. Devel. Bull. 41, 117 p.

Hunter, C.E., Murdock, T.G., and MacCarthy, G.R., 1942, Chromite deposits of North Carolina: North Carolina Dept. Cons. Devel. Bull. 42, 39 p.

Ingamells, C.O., 1970, Lithium metaborate flux in silicate analysis: Analyt. Chim. Acta, v. 52, p. 323-334.

Jackson, E.D., and Thayer, T.P., 1972, Criteria for distinguishing between stratiform, concentric, and alpine type peridotite-gabbro complexes: 24th Int. Geol. Congr. Proc., v, 2, p. 289-296.

Keith, A., 1903, Cranberry folio: U.S. Geol. Survey Geol. Atlas No. 90, 9 p.

Kerr, P.G., 1959, Optical Mineralogy: McGraw-Hill Book Co., New York, 442 p.

Kesler, T.L., 1944, Correlation of some metamorphic rocks of the Central Carolina Piedmont: Geol. Soc. America Bull., v. 55, p. 755-782.

Kesler, T.L., 1955, The Kings Mountain area *in* Russell, R.J., ed., Guides to Southeastern Geology: Geol. Soc. America, p. 374-387.

Kingsbury, R.H., and Heimlich, R.A., 1978, Petrology of an ultramafic body near Micaville, Yancey County, North Carolina: Southeast. Geol., v. 20, p. 33-46.

Malpas, J., and Strong, D.F., 1975, A comparison of chrome-spinels in ophiolites and mantle diapirs of Newfoundland: Geochem. Cosmochim Acta, v. 30, p. 1015-1060.

Mercier, J.C., and Nicholas, A., 1975, Textures and fabrics of upper-mantle peridotites as illustrated by xenoliths from basalts: Jour. Pet., v. 16, p. 454-487.

Misra, K.C., and Keller, F.B., 1978, Ultramafic bodies in the southern Appalachians: A review: American Jour. Science, v. 278, p. 389-418.

Moores, E.M., 1973, Geotectonic significance of ultramafic rocks: Earth-Science Rev., v. 9, p. 241-258.

Nicholas, A., Bouchez, J.L., Boudier, F., and Mercier, J.C., 1971, Textures, structures and fabrics due to solid state flow in some European lherzolites: Tectonophysics, v. 12, p. 55-86.

Odom, A.L., and Fullagar, P.D., 1973, Geochronologic and tectonic relationships between the Inner Piedmont, Brevard zone, and Blue Ridge belts, North Carolina: American Jour. Sci., Cooper Memorial Vol.

Overstreet, W.L., and Griffitts, W.R., 1955, Inner Piedmont belt *in* Russell, R.J., ed., Guides to southeastern geology: Geol. Soc. America Guidebook, p. 549-577.

Parker, J.M., III, 1952, Geology and structure of part of the Spruce Pine District, North Carolina: North Carolina Dept. Cons. Devel. Bull. 65, 26 p.

Pratt, J.H., and Lewis, J.V., 1905, Corundum and peridotites of western North Carolina: North Carolina Geol. Survey 1, 464 p.

Ragan, D.M., 1963, Emplacement of the Twin Sisters dunite, Washington: American Jour. Sci., v. 261, p. 549-565.

Ragan, D.M., 1969, Olivine recrystallization textures: Min. Mag., v. 37, p. 238-240.

Repossi, E., 1942, Il talco dell' Appennino parinense: Rend. Soc. Min. Ital., v. 2, p. 47.

Riodon, T.F., 1955, Asbestos in ultrabasics: Econ. Geol., v. 50, p. 67-79.

Stuckey, J.L., and Conrad, S.G., 1958, Explanatory text for geological map of North Carolina: North Carolina Dept. Cons. Devel. Bull. 71, 51 p.
Stevens, R.K., Strong, D.F., and Kean, B.F., 1974, Do some eastern Appalachian ultramafic rocks represent mantle diapirs produced above a subduction zone? Geology v. 2, p. 175-178.
Talbot, J.L., Hobbs, B.E., Wilshire, H.G., and Sweatman, T.R., 1963, Xenoliths and xenocrysts from the lavas of the Kerguelen Archipelago: American Min. v. 48, p. 159-179.
Turner, F.J., 1968, Metamorphnic petrology-mineralogical and field aspects: McGraw-Hill Book Co., New York, 403 p.
Turner, F.J., and Verhoogen, J., 1960, Igneous and metamorphic petrology: McGraw-Hill Book Co., 694 p.
Vance, J.A., and Dungan, M.A., 1977, Formation of peridotites by deserpentinization in the Darrington and Sultan areas, Cascade Mountains, Washington: Geol. Soc. America Bull., v. 88, p. 1497-1508.
Williams, H., 1971, Mafic-ultramafic complexes in western Newfoundland Appalachians and evidence for their transportation: A review and interim report: Geol. Assoc. Canada Proc., v. 24, p. 9-25.
Yoder, H.S., Jr., and Sahama, T.G., 1957, Olivine X-ray determinative curve: American Min., v. 42, p. 475-491.

ERRATUM FOR VOLUME 22, NO. 4

Clay Mineralogy of Weathering Profiles From the Carolina Piedmont

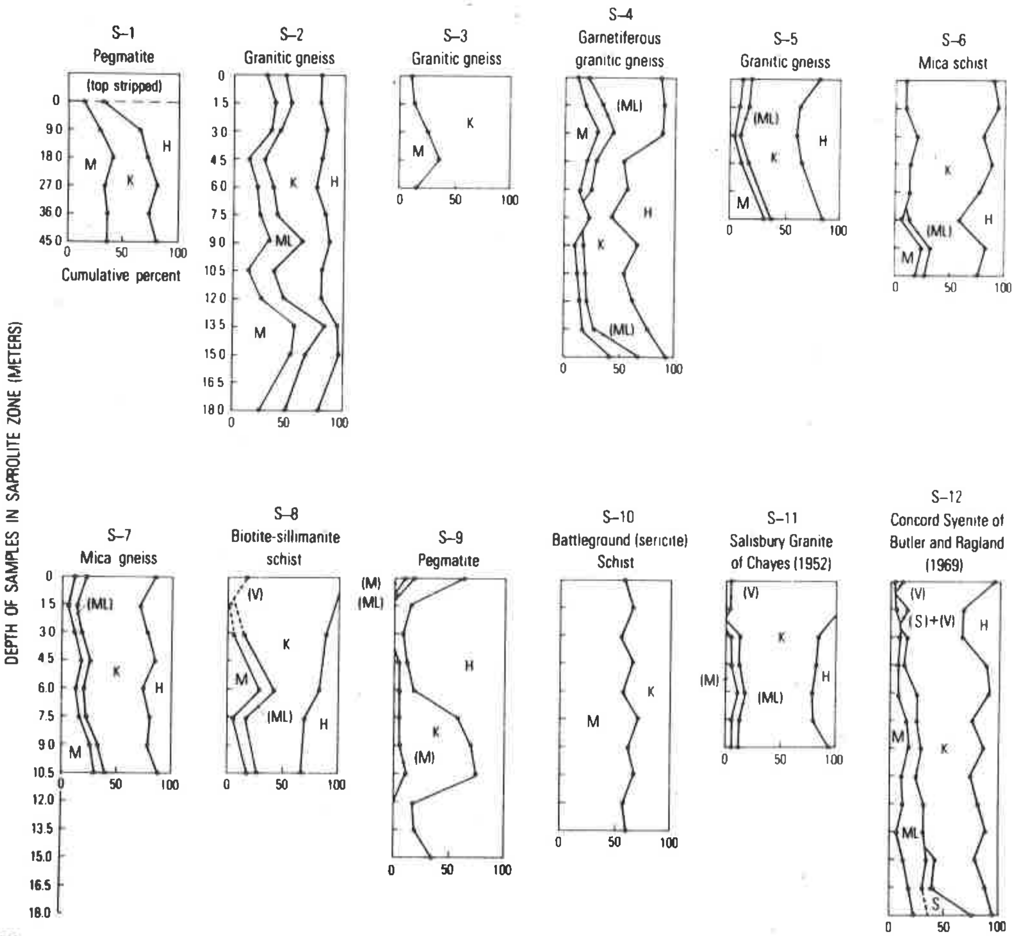

Figure 3. Graphs of the <2μm clay minerals in saprolite profiles. Dots represent data points for individual samples. Abbreviations used are: H = halloysite; K = kaolinite; M = mica; ML = mixed-layed clay; S = smectite; V = vermiculite.